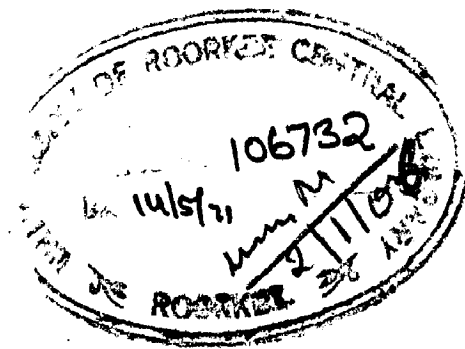
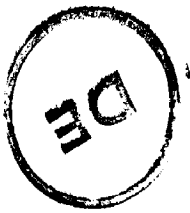


MEAN FLOW CHARACTERISTICS OF 16° CONICAL AND SQUARE DIFFUSERS

A Dissertation
submitted in partial fulfilment
of the requirements for the Degree
of
MASTER OF ENGINEERING
in
HYDRAULICS AND IRRIGATION ENGINEERING

By
H.S. DASS

RECEIVED
1970



✓
e82

DEPARTMENT OF CIVIL ENGINEERING
UNIVERSITY OF ROORKEE
ROORKEE
Nov, 1970


C E R T I F I C A T E

Certified that the thesis entitled 'MEAN FLOW CHARACTERISTICS OF 16° CONICAL AND SQUARE DIFFUSERS' which is being submitted by Sri H. S. Dass in partial fulfilment for the award of the Degree of Master of Engineering of University of Roorkee is a record of the student's own work carried out by him under my supervision and guidance. The matter embodied in this thesis has not been submitted for the award of any other Degree or Diploma.

This is further to certify that he has worked for a period of 10 months from January 1970 to November 1970 for preparing this thesis for Master of Engineering at the University.

Roorkee,

Dated November 10th 1970.


(P.V. Rao)
Reader,

Civil Engineering Deptt.
University of Roorkee, Roorkee.
U.P. India.

ACKNOWLEDGEMENTS

The author expresses his sincere gratitude to Dr. P.V. Rao, Reader in Civil Engineering Department, for his valuable and expert guidance at all levels while working on this problem.

The author would also like to express thanks to Dr. O.P.Jain, Professor and Head of the Civil Engineering Department for providing library and laboratory facilities.

Thanks are also due to Sri B.R.Sethi and other staff members of the Hydraulics Laboratory for their cooperation and assistance in preparing the apparatus.

SYNOPSIS

An accurate knowledge of the flow phenomena and the energy losses in diffusers is important in several engineering problems. An experimental study of these aspects in conical and square diffusers having a constant area ratio equal to 4 and an overall angle of divergence 16° is presented in this thesis. For both types, three boundary geometries were tested corresponding to the stream line of a potential flow, Gibson's profile and a plane profile. The Reynolds number was varied from 323000 to 738000 and its effect on the performance of diffusers is studied. Turbulent boundary layer is ensured in all cases by placing a proper stimulator at the entrance of the diffuser. Growth of the turbulent boundary layer along one side of the diffuser is traced by measuring the mean velocity profiles along it.

Air was used as the fluid. The diffuser section discharges into the square duct. Time-average values of total and static heads had been measured at the inlet and exit sections and also in the boundary layer along the centre line of one side of the diffuser. In the case of square diffusers, measurements were also taken at the corner at a distance of 1.5 cm. from the side wall at the entrance and the exit section. Dimensionless plots of the wall pressure for the square and circular diffusers at

different Reynolds numbers are given. The energy correction factors were obtained by graphical integration and the results are tabulated. The coefficient of energy loss as a function of Reynolds number for all the diffusers is presented on a log-log graph. The results indicate that the values of this coefficient are relatively high for the diffusers with straight geometries. The results also indicate that the effect of Reynolds number on the coefficient of energy loss is small. The plots of wall pressure distribution within the diffuser indicate that the pressure rises gradually except just at the entrance section.

Weightless fibers were attached in the diffuser to visualise the flow pattern near the wall. The motion of threads indicated flow asymmetry across the section. They indicated alternating flow at the top near the exit end though at the bottom they were aligned only in the forward direction. This alternating tendency of the separated flow is found to reduce with the increase in Reynolds number.

LIST OF SYMBOLS

- AR = area ratio,
- b = half length of impervious floor,
- C_c = convection of turbulence energy by mean motion,
- C_L = coefficient of head loss, $C_L = \frac{\Delta E}{\rho U_o^2 / 2}$
- C_p = coefficient of pressure rise, $C_p = \frac{p-p_o}{\rho U_o^2 / 2}$
- C_f = coefficient of skin friction,
- D_o = diameter of diffuser at inlet,
- D_d = diffusion of kinetic and potential energy across the flow,
- D = lateral dimension of conduit,
- D_s = Darcy coefficient in the equation $(1 - \frac{u}{u_1}) = D_s (1 - y/\delta)^{3/2}$
- ΔE = Energy loss,
- F = form parameter giving a measure of relative magnitude of pressure gradient and turbulent shear,
$$F = \frac{\delta^2}{u_1} \cdot \frac{du_1}{dx}$$
- g = Gravitational constant,
- G = constant,
- h = head causing flow,
- H = boundary layer form parameter, $H = \delta^*/\theta$.
- k = coefficient of permeability,
- L = length of the diffuser,
- L_a = length of the approach pipe to the diffuser,
- L_* = length parameter, $L_*^2 = \left(\frac{x}{R_o}\right)^2 \frac{R_o}{\theta_o}$,

- n = exponent in power law, $u/U_0 = (y/\delta)^n$
- p, p' = temporal mean pressure and fluctuating pressure at a point respectively,
- P = mean pressure at a section,
- R_0 = Reynolds number corresponding to inlet width or diameter,

$$R_0 = \frac{U_0 W}{\nu} \text{ or } \frac{U_0 D}{\nu}$$
- R_x = Reynolds number corresponding to an axial distance x ,
- r = radius of the conduit, radial coordinate.
- S = distance along the boundary of diffuser,
- u, v, w = temporal mean velocities in the three coordinate directions,
- u', v', w' = fluctuating velocity components in the three coordinate directions,
- U = free stream velocity,
- U_0 = average velocity at start of the diffuser,
- U_s = mean velocity at separation,
- u_1 = velocity outside the boundary layer,
- W = lateral dimension of square or rectangular conduit,
- x, y, z = distances measured in the three orthogonal coordinate directions with x measured in overall flow direction,
- X_0 = distance to the point of separation point from the start of diffuser,
- α = energy correction factor,
- β = total angle of divergence,
- ϕ_n = dimensionless potential function, $\phi_n = \frac{\phi R}{Kh}$
- ϕ = potential function,
- δ = nominal thickness of the boundary layer,

δ^* = displacement thickness of the boundary layer,

θ = momentum thickness of the boundary layer,

θ_3 = three dimensionally defined momentum thickness of the boundary layer,

ρ = mass density of the fluid

μ = dynamic viscosity of the fluid,

ν = Kinematic viscosity of the fluid,

ϵ = Eddy viscosity of the fluid,

η = efficiency of the diffuser,

η_e = energy efficiency, $\eta_e = \frac{(P - P_o + \rho \alpha U^2/2)}{\rho \alpha U_o^2/2}$

η_p = pressure efficiency, $\eta_p = \frac{C_p}{1 - (\frac{D}{D_o})^4}$

β = total divergence angle of the diffuser in Eq. (1)

Subscript

o = inlet section of the diffuser,

e = exit section of the diffuser.

LIST OF TABLES

1. Energy correction factor, α for conical and square diffusers.
2. Coefficient of head loss, $C_L = \frac{\Delta E}{\rho U_0^2 / 2}$ for all the diffusers.
3. Appendix I - Coordinates of diffuser geometries of conical diffusers.
4. Appendix II- Coordinates of diffuser geometries of square diffusers.

LIST OF FIGURES

<u>Figure No.</u>	<u>page</u>
1. Sketch of experimental set up	... 63
2. Compound elliptic transition for the inlet to the diffuser and square	... 64
3. Boundary geometries of axisymmetric and square diffusers.	... 65
4. Potential flow solution for square diffuser	... 66
5. Photographs	... 67
6. Head loss in straight tapered pipes by Gibson (conical diffusers)	... 68
7. Head loss in straight tapered pipes by Gibson (square diffusers)	... 69
8. Inlet velocity profiles for conical diffusers of straight Geometry for all the three Reynolds number	... 69
9. Inlet velocity profiles for conical diffusers of Gibson Geometry for all the three Reynolds number	... 70
10. Inlet velocity profiles for conical diffusers of Potential flow Geometry for all the three Reynolds number.	... 70
11. Exit velocity profiles for conical diffusers for all the three geometries and for all the three Reynolds number	... 71
12. Inlet velocity profiles for square diffusers of straight geometry for all the three Reynolds number both at centre and right corner.	... 72
13. Inlet velocity profiles for square diffusers of Gibson Geometry for all the three Reynolds number both at centre and right corner.	... 73
14. Inlet velocity profiles for square diffusers of Potential flow Geometry for all the three Reynolds number both at centre and right corner.	... 74

Figure No.**PAGE**

28. Boundary layer velocity profiles for Gibson model at the bottom of conical diffuser at $R_0 = 7.20 \times 10^5$... 88
29. Boundary layer velocity profiles for straight model at the bottom of conical diffuser at $R_0 = 3.89 \times 10^5$... 89
30. Boundary layer velocity profiles for straight model at the bottom of conical diffuser at $R_0 = 6.52 \times 10^5$... 90
31. Boundary layer velocity profiles for straight model at the bottom of conical diffuser at $R_0 = 7.38 \times 10^5$... 91
32. Boundary layer velocity profiles for potential flow model at the bottom of square diffuser at $R_0 = 3.23 \times 10^5$... 92
33. Boundary layer velocity profiles for potential flow model at the bottom of square diffuser at $R_0 = 5.73 \times 10^5$... 93
34. Boundary layer velocity profiles for potential flow model at the bottom of square diffuser at $R_0 = 6.28 \times 10^5$... 94
35. Boundary layer velocity profile for Gibson model at the bottom centre line of square diffuser at $R_0 = 3.24 \times 10^5$... 95
36. Boundary layer velocity profile for Gibson model at the bottom centre line of square diffuser at $R_0 = 5.82 \times 10^5$... 96
37. Boundary layer velocity profile for Gibson model at the bottom centre line of square diffuser at $R_0 = 6.40 \times 10^5$... 97
38. Boundary layer velocity profile for straight model at the bottom centre line of square diffuser at $R_0 = 3.30 \times 10^5$... 98
39. Boundary layer velocity profile for straight model at the bottom centre line of square diffuser at $R_0 = 5.72 \times 10^5$... 99
40. Boundary layer velocity profile for straight model at the bottom centre line of square diffuser at $R_0 = 6.09 \times 10^5$... 100

LIST OF FIGURES

<u>Figure No.</u>	<u>page</u>
1. Sketch of experimental set up	... 63
2. Compound elliptic transition for the inlet to the diffuser and square	... 64
3. Boundary geometries of axisymmetric and square diffusers.	... 65
4. Potential flow solution for square diffuser	... 66
5. Photographs	... 67
6. Head loss in straight tapered pipes by Gibson (conical diffusers)	... 68
7. Head loss in straight tapered pipes by Gibson (square diffusers)	... 69
8. Inlet velocity profiles for conical diffusers of straight Geometry for all the three Reynolds number	... 69
9. Inlet velocity profiles for conical diffusers of Gibson Geometry for all the three Reynolds number	... 70
10. Inlet velocity profiles for conical diffusers of Potential flow Geometry for all the three Reynolds number.	... 70
11. Exit velocity profiles for conical diffusers for all the three geometries and for all the three Reynolds number	... 71
12. Inlet velocity profiles for square diffusers of straight geometry for all the three Reynolds number both at centre and right corner.	... 72
13. Inlet velocity profiles for square diffusers of Gibson Geometry for all the three Reynolds number both at centre and right corner.	... 73
14. Inlet velocity profiles for square diffusers of Potential flow Geometry for all the three Reynolds number both at centre and right corner.	... 74

15. Exit velocity profiles for square diffusers for all the three geometries at the centre and for all the three Reynolds number. ... 75
16. Exit velocity profiles for square diffusers for all the three geometries at the corner and for all the three Reynolds number. ... 76
17. Wall pressure within the diffuser along the top centre line of conical diffusers.. 77
18. Wall pressure within the diffuser along the top centre line of square diffusers... 78
19. Wall pressure within the diffuser along the top right corner of square diffusers.. 79
20. Variation of coefficient of head loss with R_0 for conical diffusers. .. 80
21. Variation of coefficient of head loss with R_0 for square diffusers. ... 81
22. Contours of (u/v_0) at exit section of potential flow square geometry. ... 82
23. Boundary layer velocity profiles for potential flow model at the bottom of conical diffuser at $R_0 = 3.83 \times 10^5$... 83
24. Boundary layer velocity profiles for potential flow model at the bottom of a conical diffuser at $R_0 = 6.30 \times 10^5$... 84
25. Boundary layer velocity profiles for potential flow model at the bottom of a conical diffuser at $R_0 = 6.82 \times 10^5$... 85
26. Boundary layer velocity profiles for Gibson model at the bottom of conical diffuser at $R_0 = 3.58 \times 10^5$... 86
27. Boundary layer velocity profiles for Gibson model at the bottom of conical diffuser at $R_0 = 6.30 \times 10^5$... 87

Figure No.**PAGE**

28. Boundary layer velocity profiles for Gibson model at the bottom of conical diffuser at $R_0 = 7.20 \times 10^5$... 88
29. Boundary layer velocity profiles for straight model at the bottom of conical diffuser at $R_0 = 3.89 \times 10^5$... 89
30. Boundary layer velocity profiles for straight model at the bottom of conical diffuser at $R_0 = 6.52 \times 10^5$... 90
31. Boundary layer velocity profiles for straight model at the bottom of conical diffuser at $R_0 = 7.38 \times 10^5$... 91
32. Boundary layer velocity profiles for potential flow model at the bottom of square diffuser at $R_0 = 3.23 \times 10^5$... 92
33. Boundary layer velocity profiles for potential flow model at the bottom of square diffuser at $R_0 = 5.73 \times 10^5$... 93
34. Boundary layer velocity profiles for potential flow model at the bottom of square diffuser at $R_0 = 6.28 \times 10^5$... 94
35. Boundary layer velocity profile for Gibson model at the bottom centre line of square diffuser at $R_0 = 3.24 \times 10^5$... 95
36. Boundary layer velocity profile for Gibson model at the bottom centre line of square diffuser at $R_0 = 5.82 \times 10^5$... 96
37. Boundary layer velocity profile for Gibson model at the bottom centre line of square diffuser at $R_0 = 6.40 \times 10^5$... 97
38. Boundary layer velocity profile for straight model at the bottom centre line of square diffuser at $R_0 = 3.30 \times 10^5$... 98
39. Boundary layer velocity profile for straight model at the bottom centre line of square diffuser at $R_0 = 5.72 \times 10^5$... 99
40. Boundary layer velocity profile for straight model at the bottom centre line of square diffuser at $R_0 = 6.09 \times 10^5$... 100

C O N T E N T S

Chapter	page
CERTIFICATE	... (i)
ACKNOWLEDGEMENT	... (ii)
SYNOPSIS	... (iii)
LIST OF SYMBOLS	... (v)
LIST OF TABLES	... (viii)
LIST OF FIGURES	... (ix)
I	
INTRODUCTION	... 1-4
II	
REVIEW OF LITERATURE	... 5-30
1. Conversion of Kinetic Energy to Pressure Energy.	... 5
(a) Two-dimensional Diffusers.	... 6
(b) Axisymmetric diffusers	... 10
(c) Square Diffusers.	... 23
2. Turbulent Boundary Layer Growth and Separation under adverse pressure gradients.	... 23
III	
EXPERIMENTAL PROCEDURE	... 31-34
1. Apparatus	... 31
2. Measurement Technique	... 32
3. Procedure	... 34
IV	
DESIGN OF DIFFUSER GEOMETRY	... 35-40
1. Inlet Profile	... 35
2. Axisymmetric Diffusers	... 35
(a) Potential Flow Geometry	
(b) Gibson Geometry	
(c) Straight Geometry	
3. Square Diffusers	... 38
(a) Potential Flow Geometry	
(b) Gibson Geometry	
(c) Straight Geometry	

Chapter		Page
V	PRESENTATION OF RESULTS	... 41-44
	1. Wall Pressure Distributions	... 41
	2. Velocity Profiles in Boundary Layer	... 42
	3. Pressure and Velocity Profiles at inlet and outlet Sections	... 42
	4. Calculation of Energy Correction Factor	... 42
	5. Energy Loss Coefficient	... 43
VI	DISCUSSION OF RESULTS	... 45-50b
	1. Wall Pressure Distributions	... 45
	2. Flow Patterns in the Diffuser	... 47
	3. Energy-Loss in the Diffuser Section	... 48
	4. Boundary-layer Velocity Profiles in the Diffuser Section	... 50a
VII	CONCLUSIONS	... 51-53
	BIBLIOGRAPHY	... 54-58
	TABLES AND APPENDIX	... 59-62
	FIGURES AND PHOTOGRAPHS	... 63-100

CHAPTER I

INTRODUCTION

In the design of hydraulic pipe-lines, wind and water tunnels and the pipe outlets in a dam, it becomes often necessary to introduce a pipe or passage whose section shall increase gradually in the direction of flow, and thus converting part of the kinetic energy of flow into the more useful form of pressure energy. Such a pipe is known as diffuser. Flow in diffuser is of considerable practical importance in case of reservoir outlets, open channel expansions, draft-tubes and venturimeters etc. In all the above cases the efficiency of conversion process is of immediate interest since it affects the performance. Ideally, maximum pressure recovery and steady condition of discharge are wanted, combined with a satisfactory velocity distribution at exit. As in case of an abrupt expansion, a high energy loss takes place due to sudden changes in the flow characteristics, so a gradual expansion is needed. But a gradual expansion sometimes becomes inconvenient, expensive and also the saving in conversion loss is offset by the increase in friction loss along the wall. Therefore, the engineers in this field are trying to obtain an efficient diffuser geometry consistent with economy.

It is an observed fact that in an expanding flow region, the pressure increases continuously in the

downstream direction, with the result that flow has to take place in an adverse pressure gradient. In the case of very gradual expansions the forward velocities of the main flow overcome this gradient, but as the angle of expansion increases the adverse pressure gradient increases to such an extent that back flow occurs near the boundary resulting in separation. The reduction of mean flow energy occurs through turbulence and high shear along the separated stream line. The flow section is reduced resulting in poor recovery thus making the diffuser less efficient. Many researchers tried to avoid this separation by certain artifices such as splitter walls in the boundary layer flow. S. Kumar⁽²¹⁾ in his M.E. Thesis concluded that the use of splitter walls in open channels reduced the length of expansion transition from 10 to 50 percent and the efficiency of the transition was also improved. But at large flare angles the separation is unavoidable even with splitter walls.

It is believed that this separation is also affected by Reynolds number i.e. for the same boundary geometry, the diffuser performance is a function of Reynolds number. In the present study, the effect of boundary geometry and also that of Reynolds number on the performance of 16° conical and square diffusers, is observed. The total divergence angle of 16° is selected because the available studies on diffusers were for angles

diffusers these were the length of sides at outlet. The values of constant potential for getting the potential flow profile in the diffusers are assumed arbitrarily. ... observed.

Geometry and Reynolds number on the performance of these diffusers. They found the efficiency of potential flow model to be maximum but the effect of Reynolds number as observed by them was contradictory. Here also, three boundary geometries have been tested for each case.

For axisymmetric diffusers,

- (i) Geometry based on axisymmetric potential flow theory.
- (ii) Geometry given by Gibson's formula for circular diffusers.
- (iii) A straight geometry.

For square diffusers,

- (i) Profile by potential flow theory as applied to the two-dimensional confined seepage.
- (ii) Profile by Gibson's formula for rectangular diffusers.
- (iii) A straight boundary.

For all the diffusers, an overall divergence angle of 16° , area ratio 1:4 and length 54 cm. are used. For conical diffusers the inlet and outlet diameters were 15 cms. and 30 cms. respectively, whereas for square

downstream direction, with the result that flow has to take place in an adverse pressure gradient. In the case of very gradual expansions the forward velocities of the main flow overcome this gradient, but as the angle of expansion increases the adverse pressure gradient increases to such an extent that back flow occurs near the boundary resulting in separation. The reduction of mean flow energy occurs through turbulence and high shear along the separated stream line. The flow section is reduced resulting in poor recovery thus making the diffuser less efficient. Many researchers tried to avoid this separation by certain artifices such as splitter walls in the boundary layer flow. S. Kumar⁽²¹⁾ in his M.E. Thesis concluded that the use of splitter walls in open channels reduced the length of expansion transition from 10 to 50 percent and the efficiency of the transition was also improved. But at large flare angles the separation is unavoidable even with splitter walls.

It is believed that this separation is also affected by Reynolds number i.e. for the same boundary geometry, the diffuser performance is a function of Reynolds number. In the present study, the effect of boundary geometry and also that of Reynolds number on the performance of 16° conical and square diffusers, is observed. The total divergence angle of 16° is selected because the available studies on diffusers were for angles

greater than 30° , in which separation is always present. Also, the behaviour of smaller angle diffusers is not well known. Pullaiah (24) and Khan (16) tested 32° square and conical diffusers respectively and observed the effect of boundary geometry and Reynolds number on the performance of these diffusers. They found the efficiency of potential flow model to be maximum but the effect of Reynolds number as observed by them was contradictory. Here also, three boundary geometries have been tested for each case.

For axisymmetric diffusers,

- (i) Geometry based on axisymmetric potential flow theory.
- (ii) Geometry given by Gibson's formula for circular diffusers.
- (iii) A straight geometry.

For square diffusers,

- (i) Profile by potential flow theory as applied to the two-dimensional confined scope.
- (ii) Profile by Gibson's formula for rectangular diffusers.
- (iii) A straight boundary.

For all the diffusers, an overall divergence angle of 16° , area ratio 1:4 and length 54 cm. are used. For conical diffusers the inlet and outlet diameters were 15 cms. and 30 cms. respectively, whereas for square

diffusers these were the length of sides at inlet and outlet. The values of constant potential function for getting the potential flow profile in the case of square diffusers are assumed arbitrarily. Each diffuser geometry has been tested for three Reynolds numbers in the range 3.23×10^5 to 7.38×10^5 , obtained by operating the butterfly valve at the exit of the vertical exhaust duct. The inlets for both types of diffusers are compound elliptical transitions designed by the U.S. Corps of Engineers and tested by P.V. Rao⁽²⁵⁾.

The facility of a hot wire anemometer was at present not available and hence the present study is concerned with the time average values of total and static pressures as obtained by using a pitot tube. These values are used to find the reduction in the meanflow energy.

CHAPTER II

REVIEW OF LITERATURE

Flow in diffusers is of considerable practical importance in turbines, pumps, fans, compressors, and other rotodynamic machines. Therefore, civil, mechanical and aeronautical engineers generally come across such type of flows and they studied the effect, of inlet boundary layer, diffuser geometry, total angle of divergence, Reynolds number, on the diffuser performance. Since the head loss in diffusers is closely related to separation, so the growth of turbulent boundary layer and separation are also studied under adverse pressure gradient conditions. To have a clear view of the work done so far on diffusers the review is done under the following heads:-

I. Conversion of kinetic energy to pressure energy.

- (a) Two-dimensional diffusers.
- (b) Axisymmetric diffusers.
- (c) Square diffusers.

II. Turbulent boundary layer growth and separation under adverse pressure gradients.

I. Conversion of kinetic energy to pressure energy

The performance of all the three types of diffusers is effected by the following factors:-

- 1) Inlet conditions,
- ii) Diffuser Geometry and Reynolds number, and
- iii) Exit conditions.

(a) Two-dimensional Diffusers

(i) Effect of Inlet Conditions

Waitman, Reneau and Kline⁽³⁹⁾ studied the effect of inlet boundary layer thickness on diffusers of different divergence angles from 2.5 to 40 degrees and wall length to throat-width ratios of 8.0, 12.0 and 48.0, having varied the inlet boundary layer thickness from 0.08 in. to fully established flow. Different thicknesses of the inlet boundary layer were obtained by means of a bellmouth entry and by different approach lengths. Reduction in recovery occur as the inlet boundary layer is thickened. The coefficient of pressure rise, $C_p \left(= \frac{P - P_0}{\frac{\rho U_0^2}{2}} \right)$ is also a strong function of free stream turbulence intensity conditions at inlet, C_p increases with turbulence. Here P and P_0 are the pressures at any section and at inlet section respectively, ρ is the mass density and U_0 is the mean velocity at inlet. Upto 15° divergence angle, in long-walled diffusers of bellmouth entrance, the static pressure recovery remained constant.

(ii) Effect of Diffuser Geometry and Reynold's Number

A.H. Gibson^(9,10,11) tested the uniformly tapering rectangular pipes with one pair of parallel sides. The

ratio of final to initial areas ranged between 2.25 to 1 and 9 to 1. The flow during the test was a fully established flow and the head loss is expressed as a percentage of $(U_o - U_e)^2/2g$. He found the loss to be minimum when the divergence angle, β , is approx. 11° . It varies little with the size of the passage and with the ratio of enlargement, and is given with fair accuracy, for value of β between 10° and 35° , by the relationship,

$$\text{Loss} = 0.0072 \beta^{1.4} \left(\frac{U_o - U_e}{2g} \right)^2 \text{ feet.} \quad \dots (1)$$

The maximum loss is obtained when $\beta \approx 70^\circ$, while the critical value of β , above which the loss is greater than a sudden enlargement of section, varies from 32° to 40° . Loss of head was found highest for rectangular shape in comparison to the other shapes i.e. square and circular for the same area ratio. However, for pipes having boundaries curved so as to make respectively $\left(\frac{dy}{dt} = \text{constant}\right)$ and $\left(\frac{dy}{dx} = \text{constant}\right)$ showed that the loss was reduced respectively by 5.3 and 12.1 percent as compared to the straight taper pipe. He also found that for the best varying geometry of the pipe, the head loss per unit length of the pipe was constant.

Kline, Abbot and Fox⁽¹⁸⁾ employed a correlation method between the data of various geometries to get the optimum design of straight walled diffusers. They found that the variation of the coefficient of pressure recovery C_p with the angle of divergence is always greater than zero

at maximum pressure efficiency, η_p^* , where $\eta_p = \frac{C_p}{(1 - \frac{1}{A_R^2})}$ and $A_R = A_e/A_0$, A_0 and A_e are areas at the inlet and the exit sections respectively. They concluded that maximum η_p occurred at an angle lesser than that gave maximum C_p in straight walled diffusers. At optimum effectiveness for minimum loss it is only necessary to use a total angle of divergence of 7° and the length required to provide the necessary area ratio. The only precaution to be observed is that L/W_0 should not exceed about 25 to 30 if large fluctuations are to be avoided.

Waitman, Renoau and Kline⁽³⁹⁾ varied the length of the diffuser and said that very long diffuser was not desirable and gave $L/W_0 = 20$ to 25 for maximum pressure recovery. In long walled diffusers when $R_0 > 10^6$ intense secondary flows were created normal to the wall.

J.F. Norbury⁽²²⁾ said that the flow in a two-dimensional diffuser is not by any means two-dimensional, this term referring to the geometry rather than the fluid motion. In a diffuser having two plane and parallel walls and two divergent walls three-dimensional motion may arise in three ways:

- (a) As a result of boundary layer growth on the parallel walls.
- (b) As a result of secondary flows.
- (c) As an inherent property of an apparently two-dimensional boundary layer.

H. Tufts⁽³⁵⁾ conducted experiments in a unilaterally

expanding, two-dimensional, rectangular channel and predicted the optimum divergence for any required rate of gradual expansion. Among the methods used to improve pressure efficiency are (a) the increase of turbulence, (b) the deflection of kinetic energy into the separation area, and (c) the improved velocity distribution at the entrance to the expansion. So, it is concluded that the flow regime is changed due to the deflection of main current in the separation zone by the vanes and not by the insertion of a plate along the centre streamline as suggested by R. Burton.⁽⁵⁾

R.C. Bindor⁽⁴⁾ presented a method for calculating the efficiency of a diffuser for two-dimensional, steady, incompressible flow without separation. He used the following equation,

$$\eta \text{ (Efficiency)} = \frac{P_n - P_e}{\frac{\rho U_0^2}{2} \left[\alpha_e - \alpha_n \left(\frac{U_n}{U_0} \right)^2 \right]} \dots (2)$$

where U_0 = width of channel at exit section, α_n and α_e are constants to account for non-uniform velocity profiles at entry and exit sections of the diffuser respectively. The values of α_n and α_e are calculated from the velocity profiles.

Visual studies on flow models in boundary layer stall inception were carried out by Sandborn and Kline⁽³²⁾. They visualised that in a turbulent boundary layer the

separation did not occur two-dimensionally but often commenced with intermittent streaks of backflow very near to the solid boundary. When the adverse pressure gradients increase slightly they cause local intermittent separation. On further increase in these gradients a three-dimensional backflow near the wall occurs. If again these gradients increase then a complete breakdown of the boundary layer region occurs. Prandtl and Tietzens⁽²³⁾ had also reported that the two dimensionality of the flow is destroyed even when the ratio of the sides of the entrance rectangle is as small as 1:8, the flow ceases to be two-dimensional before it breaks away from the wall at a diverging angle of 8 to 10 degrees.

No study is available for the effect of exit conditions on two-dimensional diffusers.

(b) Axisymmetric Diffusers

(1) Effect of inlet conditions

Robertson and Ross⁽²⁸⁾ studied diffusers having total angles of 5° , $7\frac{1}{2}^\circ$ and 10° and 6 in. inlet diameter when preceded by 2 dia., 5 dia. and 9 dia. lengths of straight pipes. Within the range tested, the pressure efficiency was found to be a function of the product of diffuser angle (β) and effective entrance length (L_a / D_o), where L_a is the approach length. The energy efficiency (η_e) was found decreasing with increasing area-ratio, where

$$\eta_e = \left(P - P_o + \alpha \rho \frac{U^2}{2} \right) / \alpha_o \frac{\rho U_o^2}{2} \quad \dots (3)$$

where α and α_0 were the energy correction factors at a given section and the inlet section respectively. But found that η_e is practically independent of the angle and entrance conditions. Inlet Reynolds number was varied from 0.5×10^6 to 2.5×10^6 and found a small effect on the flow conditions. There is even less variation in the energy efficiency. Velocity profiles measured by them did not confirm well to the power law. The plots of η_p versus L_a/D_0 and β indicated a decrease in efficiency with increase in either of those parameters. Separation occurred for values of boundary layer form parameter, H greater than 2.4 and exponent of velocity distribution power law, n greater than 0.8. Neither of these form parameters can be correlated too well with geometric parameters near separation. If the product $(\frac{L_a}{D_0} \times \beta)$ is less than 60, separation should not occur for area ratio upto about 4.

A study was made, by Winternitz and Ramsay⁽³⁸⁾, of the effect of inlet conditions on the performance of conical diffusers with 4.1 area ratio and 5° and 10° total angles of expansion. The Reynolds number based on the inlet diameter was kept constant at 2.5×10^5 for all tests. The conditions at inlet were varied by using different approach lengths of diffuser inlet diameter, and by means of projecting annular screens of woven wire cloth. Both the methods were found effective in changing the velocity distributions. Energy efficiency and conversion

efficiency were found to depend on the diffuser angle β and the momentum thickness ratio at inlet θ_0/D_0 , irrespective of the nature of the velocity distribution, where θ_0 is the momentum thickness of the inlet boundary layer. Variation in the inlet shape parameter $H_0 (= \frac{\delta_0^*}{\theta_0})$ of the order of 20 % did not significantly affect the pressure recovery or the losses in the diffuser, where δ_0^* is the displacement thickness of the inlet boundary layer.

(ii) Effect of diffuser geometry and Reynolds Number

A.H. Gibson^(9,10,11) studied a number of straight tapered circular pipes of inlet dia. 1.5 inches and outlet dia. 3 inches having varied the total angle of divergence from 3° to 180° . He found that loss of head, expressed as a percentage of $(U_0 - U_e)^2 / 2g$ varies somewhat with mean diameter of the pipe, and with the area ratios, as well as with the angle of divergence β . For β values between 6° and 36° , the differences are comparatively small and the loss of head is given fairly accurately by,

$$\text{Loss} = 0.011 \beta^{1.22} \frac{(U_0 - U_e)^2}{2g} \text{ feet.} \quad \dots (4)$$

where β is measured in degrees. The minimum loss of head is attained with a value of β as 6° and maximum loss for $\beta = 65^\circ$. The value of β which makes the loss equal to 100 % varies from 40° to 60° . In 1910 he reported that the trumpet shaped pipe gave a larger loss of head than a corresponding straight pipe. But later in 1912, he said that the loss of head may be

reduced by making the passage trumpet-shaped according to the following formula,

$$\frac{1}{r^{5/4}} = \frac{1}{r_0^{5/4}} - \frac{X}{L} \left(\frac{1}{r_0^{5/4}} - \frac{1}{r_e^{5/4}} \right) \quad \dots (5)$$

where r , r_0 and r_e are radii of the conduit at a distance X , inlet and exit sections respectively. He further reported that a still greater saving may be effected by a design giving a gradual uniform enlargement in section from the initial section A_0 to one having an area A_1 and a sudden enlargement from A_1 to the final area A_e . By this method of construction the loss may be reduced to about 90 % (in rectangular) and to 96 % (in circular) of the minimum possible loss in a uniformly tapering pipe undergoing the full enlargement of section.

W.H.Archer⁽⁴³⁾ expressed the loss, in sudden expansions as,

$$\text{Loss} = \frac{1.098(U_0 - U_e)^{1.919}}{2g} \quad \dots (6)$$

where U_0 and U_e are average velocities at inlet and exit sections.

Kalinske⁽¹⁵⁾ in his paper presented data on mean velocity distribution, turbulence, and pressure changes for total angle of divergence 7.5° , 15° , 30° and 180° having 2.75 inches entrance dia. and 4.75 inches as exit diameter under fully established flow condition. It is observed that the total loss of energy is considerably

greater than the total energy of turbulence that is produced, thus indicating that a major portion of the energy is lost by direct conversion into heat at the regions of high, local shear in the fluid. He found that the maximum pressure is reached at distances beyond the start of the expansions which seem to increase with decrease in divergence angle. Also, the energy conversion occurs more gradually in sudden expansion than in 30° expansion. It is also noted that the efficiency of energy conversion in the 30° expansion is not much better than in the 180° (i.e. sudden) expansion. The turbulence characteristics and their effect on diffuser performance are summarised as under :-

- (i) $\bar{u}'^2 > \bar{v}'^2$, where u' and v' were the fluctuating velocity components in x and y directions respectively.
- (ii) \bar{u}'^2 and \bar{v}'^2 were the highest just below the sudden expansion.
- (iii) within the expansion the turbulence intensity was the highest near the boundary.
- (iv) turbulence in the 30° diffuser was of larger scale and of high diffusive power than that in the sudden expansion.
- (v) the ratio of $\sqrt{\bar{u}'^2}$ to the centre line velocity was the maximum in the 30° diffuser and was 0.5.
- (vi) the loss of energy mainly occurred in separation zone outside the high velocity free stream due to high shear.

(vii) the turbulence was only a byproduct in the energy conversion process.

Joel Warren⁽³⁷⁾ reported that the minimum percent head loss for recovery cones in venturimeters depends upon both the cone angle and ratio of the cone entrance dia. to exit diameter. Also, truncated cones of $L=1.37D_0$ and $L=1.88 D_0$ and $\beta = 13^\circ$ and 11° respectively, gave minimum percent head loss. In both instances, full length cones gave higher percent head loss. A.L.Jorissen⁽¹³⁾ stated that it was this phenomenon that prompted the German manufacturers of venturimeters to cutoff the diffusing section at a diameter lesser than the diameter of the pipe. Warren also indicated that for certain lengths of recovery cones including truncated cones there is a certain cone angle that will give minimum percent head loss.

Schubauer⁽³³⁾ compared certain statistical properties of turbulence observed in boundary layer and in fully developed pipe flow with zero or negligible pressure gradients. Attention is called to a region of high turbulent activity near the wall. The boundary layer was $3''$ thick and the radius of the pipe was $4.86''$. He showed that except for outer parts of boundary layer flows, the turbulence in pipes, channels and boundary layer is similar in many respects. The turbulence energy equation may be written in the simplified form,

$$P_r + D_d + C_c + W_d = 0 \quad \dots (7)$$

where P_r = Production of turbulence energy from the mean motion.

D_d = Diffusion of kinetic energy and potential energy across the flow.

C_c = Convection of turbulence energy by the mean motion.

and W_d = dissipation of turbulence energy.

Also, $P_r = \frac{\nu}{u_t^2} \overline{u'v'} \frac{dU}{dy}$ in which all terms can be easily known. Part of the mean flow energy is directly dissipated, the dimensionless direct-viscous-dissipation rate is given by

$$W_\mu = \frac{\nu^2}{u_t^4} \left(\frac{dU}{dy} \right)^2 \quad \dots (8)$$

The sum $P_r + W_\mu$ is evaluated to account for the loss of kinetic energy of mean flow. Part of this goes directly to heat through the action of viscosity and the remainder into the production of turbulence energy. Thus he established a relation between mean flow, and turbulence.

Measurements of turbulence intensity at five stations and shear at one station in the boundary layer on the inside of 7.5° conical diffuser are reported. The conclusions obtained are :

1. The turbulence, its rate of production, and its rate of dissipation in an adverse pressure gradient are generally in excess of similar quantities for zero-pressure gradient boundary layers.

2. The turbulence and its rate of production are far in excess of the zero pressure gradient case, even near the wall.

3. The longitudinal microscale of turbulence (λ_x) remains remarkably constant across and along the developing boundary layer.

M.C. Chaturvedi⁽⁶⁾ determined the characteristics and dynamics of flow for four abrupt expansions with total divergence angles of 30° , 60° , 90° and 180° at inlet Reynolds number equal to 2×10^5 with bellmouth entry. The presentation is made through the kinetic energy of the mean motion, kinetic energy of turbulence, pressure distribution, turbulence production, and turbulence shear in the form of their spatial distribution for all four expansion angles, by combining the experimental data with the analytical analysis. He also measured w' i.e. fluctuating velocity component in z-direction and concluded that $w' \approx v'$. He found that mean velocity of flow varied along the axial as well as radial directions, but mean pressure varied considerably only in the axial direction. He could not obtain a relation between the variation of velocity and variation of pressure and said that Bernoulli theorem can not be used for this study. But Chevray⁽¹²⁾, in his discussions, concluded that the requirements of Bernoulli theorem were satisfied, after analysing Chaturvedi's data for 180° expansion. He observed the stream line pattern for the 30° expansion well different from that of the

other expansions which were almost similar and differed slightly in magnitude. He obtained a momentum flux equation analytically and evaluated the various terms in it and found that experimental results varied within 2.5 % only. Though the change of momentum flux was constant in all the four diffusers, the rate of change in 30° expansion was strikingly different from that of the other three expansions.

He obtained an energy equation for the mean motion containing the terms of kinetic energy flux, work done by pressure, work done by Reynolds stresses and work done in producing turbulence. He omitted the normal stress terms and the product of $\overline{u'v'}$ and $\frac{\partial v}{\partial x}$, where v is the temporal mean velocity in y -direction. He showed that experimental data differed only by 5 percent. Rene Chovray⁽¹²⁾ in his discussion raise a question to the omission of the product term and said that the term was not that much small but was of the order of 20 percent and in some cases exceeding 100 percent. He also conducted independent head loss measurements in a water pipe assembly and found that the head loss was the same as that obtained in the air flow studies. The head loss was maximum at a divergence angle of 64° and was equal to $0.59 \frac{\rho U_0^2}{2}$ and if the angle is further increased, the loss decreased slightly and obtained a value $0.57 \frac{\rho U_0^2}{2}$ which was very close to the Borda value of $0.56 \frac{\rho U_0^2}{2}$. The value of angle i.e. 64°

is close to the results of Gibson for maximum head loss. According to Gibson the maximum head loss was 20 % while due to M.C. Chaturvedi it was only 5.3 % over the Borda value. Head loss obtained by Gibson is more because he performed the tests under fully established flow condition while M.C. Chaturvedi used a bellmouth entrance. A similar observation is made by Huang⁽¹²⁾.

M.C. Chaturvedi⁽⁶⁾ could not analyse the turbulence energy by means of the integrated turbulence energy equation obtained by analytical means. So he analysed the equation of motion in the axial direction and neglected the viscous stresses and other terms that were equal to zero and obtained,

$$U \frac{\partial u'}{\partial x} = -\frac{\partial u'}{\partial t} - \left[U \frac{\partial U}{\partial x} + u' \frac{\partial (U+u')}{\partial x} + v' \frac{\partial (U+u')}{\partial r} + \frac{1}{\rho} \frac{\partial (P+p')}{\partial x} \right] \dots (9)$$

He found that none of the terms within the bracket could be discarded as required by Taylor's approximation. He noted that cumulative dissipation lags behind the cumulative production. Also evident was the fact that the rates of production and dissipation achieved their maximum values very early and rapidly settle down to a comparatively much smaller rate when both were almost in equilibrium with each other. The smaller the angle of separation, the earlier was the onset of both these processes. However, it was seen that beyond the angle of 60°,

the earlier onset of diffusion had no effect either on the turbulence production or on the head loss. Also, rate of increase of head loss decreases with the increase in expansion ratio, the head loss tending to unity asymptotically. Kalinsko⁽¹⁴⁾ when plotted the data, obtained by various researchers, for different area ratio found that the efficiency of the diffuser decreased with increase in area ratio.

Turbulence characteristics of a diffuser as obtained by M.C. Chaturvedi may be summarised as under:-

- (i) The turbulence as it convected and diffused arrested its own formation and led to a uniform distribution of mean velocity.
- (ii) Turbulence produced its own decay having broken into smaller and smaller eddies.
- (iii) The production, convection, diffusion and dissipation rendered a unique distribution of turbulence energy over the entire region.

M.C. Chaturvedi observed that the large scale properties of motion are not affected by viscous action. Thus, beyond the effect of viscosity on the conditions of stability, it has no influence on the pattern of separation and the turbulence intensities.

He also noted that the most significant feature of the separation was the turbulence production, which caused the high energy loss. Chevray⁽¹²⁾ though agreed

with this high energy loss but said that since the transfer term was higher than the production term the energy loss from the mean motion was transferred to the eddy and that was the role played by separation.

M.C. Chaturvedi stated that because the dissipation of turbulence energy was also high, the kinetic energy of the turbulent motion remains comparatively small. He again made a note that although the flow field was intensely non-homogeneous and anisotropic at the beginning, conditions of homogeneity and isotropy were approached at a rapid rate.

Huang⁽¹²⁾ stated that M.C. Chaturvedi's results could not be generalised since he kept the Reynolds number constant and used the same inlet condition throughout. He conducted experiments on water-pipe assembly for different Reynolds numbers and for smooth and rough inlet conditions in addition to the bellmouth entry. He tested three more divergence angles viz. 50° , 15° and 7° and found that the head loss in case of only bellmouth entry depended on Reynolds number and decreased with increase in Reynolds number from 2×10^4 to 1.8×10^5 for $\beta < 50^\circ$ and said that it might be due to the significant changes produced in the flow pattern as R_0 varied. He further obtained the head loss to be independent of either R_0 or β for $\beta > 60^\circ$. He also observed that for the same divergence angle, the head loss was the least for bellmouth entrance and maximum for rough entrance. Also, variation in head loss for these

three types of entrances was negligible for $\beta > 60^\circ$ and significant for $\beta < 60^\circ$. So, he made a note that characteristics as presented by M.C. Chaturvedi would be much different in actual pipe expansions which were far from bell-mouth entry case.

(iii) Effect of exit conditions

Robertson and Holl⁽³⁰⁾ studied the effect of exit conditions on a 7.5° diffuser having inlet diameter as 6 inches. They provided the following exit conditions:

- 1) Free at 11.3 inches diameter,
 - 2) 23 inches long pipe of 7.38 inches diameter,
 - 3) 11.7 inches long pipe of 9.35 inches diameter,
- and 4) Free at 9.35 inches diameter.

They observed C_p , H , δ , and D_s to be practically constant in all the four cases, till the point of boundary changes, where $D_s =$ Darcy coefficient in the boundary layer velocity formula $(1 - \frac{u}{u_1}) = D_s (1 - \frac{y}{\delta})^{3/2}$, and $H = \frac{\delta^*}{\theta}$, u is the velocity at any point in the x -direction, $u_1 =$ velocity outside the boundary layer in x -direction, and $y =$ distance measured from the boundary surface within the boundary layer. Uram⁽²⁹⁾ in his discussion pointed out that the immediate changes in the shape parameters H and D_s at the point of boundary change was in conflict with the history concept of the outer region of the turbulent boundary layer in adverse pressure gradient.

(c) Square Diffusers

Very little information is available on square diffusers. A.H. Gibson^(9,10,11) tested some square expansions having angle of divergence $\beta = 5^\circ, 10^\circ, 20^\circ, 30^\circ$ and with side lengths 1.329 inches and 3.659 inches at the inlet and outlet respectively. He measured the pressure along one face and along one corner and found that there is no difference between the two pressures for small angle diffusers while for large angle diffusers they differ slightly and the corner pressure was more. The minimum loss of head was obtained for $\beta \approx 6^\circ$ and had a value of about 14.5 % . The loss of head in a pipe of square section was at the least 20 % greater than a circular pipe of the same length and same initial and final areas. Gibson tested one more pipe of constant cross-sectional area having one pair of diverging sides and the other pair of converging sides (i.e. from square to a rectangular section) to determine form effect. The length of the pipe was 9.94 inches, β for divergence $7^\circ 37'$ and β for convergence $3^\circ 50'$. He found that the head loss in that pipe was 48.4 % of the kinetic energy per pound of fluid in the pipe.

II. Turbulent Boundary Layer Growth and Separation under adverse pressure gradients

Robertson and Ross⁽²⁸⁾ observed during the study of diffusers that the product $\frac{L_a}{D_0} \times \beta$ should be less than 60 at $Re_0 = 1.5 \times 10^6$ for area ratio upto about 4 to avoid separation. In other words, the separation is not only

dependent on the inlet conditions and angle of diffuser, but is also a function of area ratio. They further reported that separation was observed for 7.5° and 10° diffusers for $\frac{L_a}{D_0} = 9$ and 5 respectively. Separation occurred for a value of H greater than 2.4 and n greater than 0.8 , where n is the exponent in the power law velocity distribution. Later on Winternitz and Ramsay⁽³⁸⁾ reduced the limit i.e. $\frac{L_a}{D_0} \times \beta < 50$ for no separation.

Robertson and Calehuff⁽²⁹⁾ also studied the boundary layer flows in adverse pressure gradients on a 7.5° conical diffuser having inlet diameter 5 inches and 11.25 inches at the exit. The mean velocity profiles were analysed to determine the displacement and momentum thickness according to the usual two dimensional relationship rather than three dimensional which should apply. The justification given by them was that for comparative purposes, the differences are irrelevant. The value of the shape parameter thus determined approached a value of 2.9 near separation.

Robertson and Fraser⁽³¹⁾ showed that the separation conditions depend on the initial momentum thickness, Reynolds number and a distance parameter involving the initial momentum thickness, the initial radius and the diffuser length. They assumed that separation occurred at $D_s = 1.3$ and obtained a relation between $\frac{U_s}{U_0} (= \sqrt{1 - C_p})$ and R_{θ_0} as a function of length parameter, $L_s^2 = (X/R_0)^2 \cdot R_0 / \theta_0$ graphically where $U_s =$ mean velocity at separation. They

also demonstrated a design method for an efficient conical diffuser for known values of R_{θ_0} and θ_0 / D_0 . For large values of L_*^2 , increase in Reynolds number had an adverse effect leading to earlier separation. Comparison with experimental information on diffuser separation indicated that the predictions were reliable, but conservative.

Clauser⁽⁷⁾ carried out an extensive experimental study of the problem of turbulent boundary layer separation in adverse pressure gradients. He observed that the experimental results obtained show little or no agreement with the methods yet available for prediction of separation. He further concluded that dependence on shape parameter, H , as a criterion for separation might give erroneous results as H not only expressed the effect of the adverse pressure gradient but also that of skin friction. He argued that a value of H equal to 2.2 and 2.6 could be obtained on rough surfaces in zero pressure gradient and without separation of flow. He further pointed out that the simple assumption of a constant eddy viscosity accurately predicted the behaviour of the outer 80 to 90 percent of turbulent layers. This outer eddy viscosity was proportional to $U\delta^*$, and when it was combined with an inner eddy viscosity proportional to u_*y , a complete and remarkably accurate picture of the turbulent velocity profile was obtained. The constants of proportionality were not affected by pressure gradients, Reynolds number, or roughness.

The tendency to separation can be delayed by the following methods, as suggested by different investigators.

- i) increasing the initial Reynolds number and slowing the rate of velocity deceleration.
- ii) increasing turbulence level of approach flow.
- iii) deflecting the main flow into the zone of separation, and
- iv) improving the inlet velocity distribution.

Previous Work Done at Roorkee University

S.P. Rai⁽²⁶⁾ studied boundary layer separation in two-dimensional linear and hyperbolic expansions. The fluming ratio was kept constant at 50 % and Froude number of the approach flow was varied in the range 0.65 to 0.80. He said that the experimental data have been found to agree closely with some of the theories. Ross and Robertson formula for the growth of momentum thickness, θ , was found to give very satisfactory result. He gave a simple formula, for the prediction of separation, according to which

$$C_p \left(x \frac{dC_p}{dx} \right)^{1/2} = 0.26 (R_x \times 10^{-6})^{1/10} ; C_p \leq 0.75$$

... (10)

The coefficient 0.26 is replaced by 0.35 for $C_p > 0.75$. This formula gave reliable results at Reynolds number, R_x , of the order of 2×10^6 . The hyperbolic transition given by R.S. Chaturvedi was found to be most efficient.

S.Kumar⁽²¹⁾ observed the effect of splitter walls in open channel expansions. Three transitions with different

flare designed by R.S. Chaturvedi, were studied, each with and without splitter walls. A straight transition was also tested and the length of splitter walls was also varied. He concluded that the transition length may be reduced 10 to 50 percent by the use of splitter walls. The reduction in the values of energy correction factor was of the order of 20 to 33 percent. It was also noted that advantage with respect to the head loss is more in shorter transitions and still more in straight line transition.

R.K.Jain⁽¹⁴⁾ described, in his thesis, theoretical and experimental studies of various expansion transitions in open channel with special reference to head loss. A method of designing expansion transition for minimum head loss was also recorded. The method consisted of optimizing the head loss integral and solving the resultant differential equations. The performance of the proposed transition was found to be superior over those proposed by R.S. Chaturvedi in both the splay 1:3 and 1:4. He also concluded that the efficiency improved with the reduction in splay and with decrease in discharge. Also, the phenomenon of separation was not observed with a flare less or equal to 1:4, in the proposed transition.

V.Pullaiah⁽²⁴⁾ studied the effect of boundary geometry and Reynolds number on the diffusers of constant area ratio of 4 and overall divergence angle of 32° . Three boundary geometries obtained by Potential Flow theory,

Gibson's formula and straight one were tested. Each one was tested for three Reynolds numbers ranging from 2.67×10^5 to 8.61×10^5 . He observed the flow asymmetry in both the directions perpendicular to the overall flow direction. The asymmetries were found to alternate from one wall to the opposite wall. The frequency of alternation decreased with the increasing Reynolds number. Separation was observed along the top face. The coefficient of head loss was the highest and the mean pressure recovery lowest in the straight diffuser while in the potential flow boundary diffuser the coefficient of head loss was the lowest and the mean pressure recovery highest. The head loss was found to increase with the Reynolds number for all the three geometries.

A similar study on conical diffusers, having an area ratio of 4, with total angle of divergence equal to 32° and 180° (abrupt expansion) was done by R.Khan⁽¹⁶⁾. He again tested three above said boundary geometries and varied the Reynolds number from 2.68×10^5 to 9.20×10^5 . The asymmetry in the flow was again observed for these diffusers, but coefficient of head loss was found to decrease with Reynolds number. The coefficient of head loss was found to be minimum for potential flow and Gibson's profiles, and wall pressure recovery was highest for potential flow model. As regards the growth of turbulent boundary layer and its separation, the potential

flow model was found to be quite satisfactory. Growth of turbulent boundary layer was very rapid in large adverse pressure gradients, and the value of the shape parameter at separation point, as found for the potential flow and Gibson's models, for highest Reynolds number (9.20×10^5) was 2.80 and 2.40 respectively.

The following conclusions can be drawn from the above review.

(i) Performance of a diffuser depends upon the divergence angle, area ratio, boundary shape, turbulence level and inlet conditions.

(ii) At smaller Reynolds numbers, the diffuser performance is affected by Reynolds number.

(iii) Optimum efficiency of a diffuser is observed at an angle of divergence between 6° to 8° .

(iv) If the angle of divergence exceeds 40° , then an abrupt expansion should be preferred.

(v) A compound shape or a trumpet shape improves the performance of a diffuser for the same length as straight diffusers.

(vi) Separation in a turbulent boundary layer flow does not occur at a fixed point and also in a two-dimensional manner.

(vii) Still accurate methods are not available for

the prediction of separation and growth of the turbulent boundary layer in an adverse pressure gradient.

(viii) Occurrence of separation increases the losses in a diffuser.

CHAPTER III

EXPERIMENTAL PROCEDURE

1. Apparatus

The apparatus consisted of an inlet followed by a diffuser and then, by a uniform square duct on the same horizontal axis as shown in fig. (1). Two types of inlet and diffusers, one circular and other square were used. The inlets were compound elliptical transitions which converged from the plane vertical walls at one end to the size of the inlet cross-section of the diffusers at the other end. For both circular and square diffusers, three boundary geometries, as shown in figs. (3 and 4) were tested. Circular one had an inlet diameter of 15 cms. and outlet diameter of 30 cms. and square one varied in cross section from 15 cm. x 15 cm. at the inlet to 30 cm. x 30 cm. at the outlet. In both cases an overall divergence angle of 16° was observed. The duct was 370 cms long and 50 cm. x 50 cm. in cross-section. The inlets and the diffusers were 18.0 cm. and 54.0 cm. long respectively. The circular inlet and diffusers were made of wood and the desired boundary geometry was obtained on the lathe with the help of templates. These were smoothed by hard sand paper and painting. After that a soft sand paper was used for smoothing. The square inlet and diffusers were made of M.S. sheet.

Each side of the diffusers was pressed to the desired form with the help of a templates and the four sides were joined along the corners by welding. They were smoothed with the help of sand paper. The square duct was made of hard-boards 6.25 mm. thick on three sides and lucite sheet on one side. A window was also provided to approach the diffuser outlet end joined to the duct. A constant speed centrifugal blower coupled to a 7.5 h.p. motor at the end of the duct gave the necessary air flow in the diffusers and the air was exhausted through a vertical square duct. The rate of flow was regulated by means of a butterfly control valve on the exhaust section. There were nine openings provided for the valve. The whole of the duct and diffusers were mounted on trestles.

2. Measurement Technique

Average values of total head and static head were measured in the direction of overall motion of the fluid (air). The total head was measured with a total head tube and static head, by a static pressure tube separately. The difference between these two heads gave the velocity head. Measurement of mean value of total head created some difficulty in the highly turbulent flow. These total head and static head tubes were made from a stainless steel tube of 1.8 mm. diameter (external). A total head tube, made from hypodermic tube of 1.5 mm. diameter flattened at the end to 0.7 mm overall thickness was used for measurements

within the boundary layer. The static head tube was sealed at the end by soldering and finished to a shape of hemisphere and four pressure holes were made around the tube at a distance of 6 diameters from the sealed end. Piezometric openings along the centre line in case of circular and along the centre line and the corner both in square diffusers at the top were provided at close intervals to measure the wall pressures. Three piezometric openings were also provided in both inlets along the centre line at the top.

A bridge was mounted on the diffuser along the diffuser axis, carrying a moveable gauge which could be moved up and down by means of the rack and pinion arrangement provided on the gauge. A vernier was also provided at the gauge having a least count of 0.1 mm. A brass tube was attached to the bottom of gauge which could be joined to another brass tube having the probe parallel to the flow. Holes were made in the diffusers for the vertical movement of the probe. The position of the probe could be located with the vernier on the gauge. The bottom of that brass tube having the probe was connected by means of plastic tube to a limb on the multiple tube manometer with a mirror base. The spirit was used in the manometer. Another vernier having 0.1 mm. as the least count was provided at the manometer. The piezometric heads were taken, on a vertical water manometer.

S. Procedure

The whole set-up was checked for any suction of air before starting the motor. Holes, if any were sealed with the help of either moulding clay or tape. Two brass tubes one fitted with the static pressure probe and the other with the total pressure probe were fitted alternately to the gauge on the bridge and mean values of static and total pressure heads were observed. Values are taken for full section at inlet and outlet centre line of all the six diffusers and also at the right hand corner at inlet and outlet in case of square diffusers. Along the length of all the six diffusers these heads were measured only within the bottom boundary layer along the centre line. Threads were attached along the centre line of diffusers to visualize the flow pattern and asymmetry. All measurements were made with the probe pointing in the upstream direction. However, in the regions of back flow the total head tube was reversed to obtain the negative velocities. All the measurements were taken for three valve openings which corresponded to three Reynolds numbers. Temperature was also recorded during the measurements.

CHAPTER IV

DESIGN OF MODEL GEOMETRY

Three different boundary geometries for both axisymmetric and square diffusers are tested for their hydraulic performance in this thesis. The same inlet flow conditions are ensured in the six models by adopting the Kirchhoff free-stream surface approximated by two ellipses as given by Eqs. 11 and 12 and shown in Fig. 2.

1. Inlet Profile

This inlet was found⁽²⁵⁾ to give a smooth entry of flow into the conduit and it was found to give a constant velocity distribution across the section except in the boundary layer flow. The ellipses are given by

$$\left(\frac{X}{D}\right)^2 + \left(\frac{Y}{0.32 D}\right)^2 = 1 \quad \dots \quad (11)$$

$$\left(\frac{X}{D}\right)^2 + \left(\frac{Y}{0.16 D}\right)^2 = 1 \quad \dots \quad (12)$$

Here, D = lateral dimension of inlet at uniform section and x and y are the coordinates as shown in Fig. 2.

2. Axisymmetric Diffusers

(1) Potential Flow Geometry

It is a general practice to streamline the sluice inlets according to the potential-flow theory. As fully developed turbulent flow in a conduit approximates the irrotational flow, it is felt that a geometry based upon the shape of the bounding streamlines should give a trouble-free design. Utilizing this concept the potential flow geometry was obtained as follows:

The flow of an incompressible fluid can be represented by Laplace equation in 3-dimensions as

$$\frac{\partial^2 \phi}{\partial x^2} + \frac{\partial^2 \phi}{\partial y^2} + \frac{\partial^2 \phi}{\partial z^2} = 0 \quad \dots (13)$$

where ϕ is a potential function.

Let the solution of this equation is,

$$\phi = \frac{1}{2}(ax^2 + by^2 + cz^2) \quad \dots (14)$$

since $\nabla^2 \phi = a+b+c$, we get a solution of equation $\nabla^2 \phi = 0$ when $a+b+c = 0$.

This equation may be satisfied in several ways, such as $c = a$, $b = -2a$, or $b = -a$, $c = 0$ etc.

Considering $b = c$, $a = -2c$ as the solution, we get,

$$\phi = \frac{c}{2}(2x^2 + y^2 + z^2) \quad \dots (15)$$

The velocity components then will be,

$$u = \frac{\partial \phi}{\partial x} = -2cx, \quad v = \frac{\partial \phi}{\partial y} = cy, \quad w = \frac{\partial \phi}{\partial z} = cz$$

Hence, for the stream line we have,

$$-\frac{dx}{2x} = \frac{dy}{y} = \frac{dz}{z} \quad \dots (16)$$

Considering in xy -plane only, the equation of streamlines will be,

$$-\frac{dx}{2x} = \frac{dy}{y}$$

or $-\frac{1}{2} \log x = \log c + \log y$ or $x^{1/2}y = \text{constant}$.

or $xy^2 = \text{constant} \quad \dots (17)$

This satisfies the partial differential equation of the Stokes stream function. So, the projection of streamlines on the xy-plane is a family of cubic hyperbolas with x and y-axes as asymptotes. In the present case y varies from 7.5 to 15 cm. in a distance of 54 cm. We get $y = 7.5$ cm. for $x = 72$ cm. So, the governing equation will be

$$xy^2 = 4050 \quad \dots (18)$$

The coordinates of diffuser geometry are given in Appendix I and shown in Fig.3.

(ii) Gibson's Profile

From his experiments, Gibson concluded that trumpet shaped boundaries gave lower values of head loss as compared to straight boundaries, other parameters being same. It was also concluded that the passages in which head loss per unit length was constant were most efficient. For circular pipes the boundary geometry can be obtained by the following equation,

$$\frac{1}{r^{5/4}} = \frac{1}{r_o^{5/4}} - \frac{x}{L} \left(\frac{1}{r_o^{5/4}} - \frac{1}{r_e^{5/4}} \right) \quad \dots (19)$$

where, r , r_o and r_e are the radii of diffuser at any distance x , at inlet and exit sections. In the present study $r_o = 7.5$ cm., $r_e = 15$ cm. and $L = 54$ cm.

$$\text{So, } \frac{1}{r^{5/4}} = \frac{1}{(7.5)^{5/4}} - \frac{x}{54.0} \left(\frac{1}{(7.5)^{5/4}} - \frac{1}{(15)^{5/4}} \right) \quad \dots (20)$$

$$\text{or } \frac{1}{r^{5/4}} = 0.0806 - 0.000867 x \quad \dots (21)$$

The coordinates are given in the Appendix I and plotted in Fig.3.

(iii) Straight Profile

A straight conical diffuser having 7.5 cm. and 15 cm. as the inlet and exit radii and length equal to 54.0 cm. was also tested. The coordinates are given in Appendix I and plotted in Fig.3.

2. Square Diffusers

(i) Potential Flow Geometry

A potential flow solution for the two dimensional diffuser is sought as follows.

The two dimensional flow pattern of confined seepage below an impervious floor of length $2b$ under a head, h is considered as shown in fig.4. The equation of the equipotential lines is given by,

$$\frac{x^2}{(b \cos \phi_n)^2} - \frac{y^2}{(b \sin \phi_n)^2} = 1 \quad \dots (22)$$

which gives conformal hyperbolas of constant ϕ lines where ϕ = potential function and $\phi_n = \phi\pi/kh$, and k = coefficient of permeability. An equipotential line of $\phi = 57.5\%$ is considered. So, $\phi_n = 0.575\pi = 103.5^\circ$, and the equation reduces to

$$\frac{x^2}{(b \cos 103.5^\circ)^2} - \frac{y^2}{(b \sin 103.5^\circ)^2} = 1 \quad \dots (23)$$

$$\text{or } \frac{x^2}{(0.2334b)^2} - \frac{y}{(0.9724)^2} = 1 \quad \dots (24)$$

The equipotential line of $\phi = 42.5\%$ yields a similar equation which defines the image of constant equipotential line $\phi = 57.5\%$ about the axis of symmetry. The present diffuser is proposed to consist of bounding surface a'c' and a''c'', shown in fig. (4), defined by constant $\phi = 57.5\%$ and 42.5% lines on the two sides of the axis of symmetry.

Interchanging the coordinates and adopting area ratio 4, equation for the diffuser geometry is

$$\left(\frac{x}{2.08w_0} \right)^2 - \left(\frac{y}{0.5 w_0} \right)^2 = -1 \quad \dots (25)$$

It is proposed to have a width of 15 cm. at inlet and 30 cm. at the exit section to give an area ratio 4.

$$\text{At, } x = 0, \quad y = 0.5 w_0 = 0.5 \times 15 = 7.5 \text{ cm.}$$

$$\text{At, } x = L, \quad y = w_0 = 15 \text{ cm.}$$

$$\text{So, } L = 2.08 \times 1.732 w_0 = 3.6 w_0 = 54 \text{ cm.}$$

The overall total angle of divergence,

$$\tan^{-1}(\beta) = 2 \times \frac{0.5}{3.6} = 0.278$$

$$\text{or } \beta = 16^\circ.$$

Coordinates for diffuser geometry are given by

$$\left(\frac{y}{7.5} \right)^2 - \left(\frac{x}{31.2} \right)^2 = 1 \quad \dots (26)$$

and are tabulated in Appendix II and plotted in Fig.3.

(ii) Gibson Geometry

Similar to axisymmetric diffusers Gibson gave an equation for rectangular pipe boundary which was as follows,

$$\frac{1}{(0.5W)^{1/4}} = \frac{1}{(0.5W_0)^{1/4}} - \frac{K}{L} \left\{ \frac{1}{(0.5W_0)^{1/4}} - \frac{1}{(0.5W_e)^{1/4}} \right\} \dots (27)$$

where W = width of the diffuser at a distance x from the inlet and W_e is the diffuser width at exit section. The same overall dimensions are adopted as for potential flow theory. For coordinates See Appendix II and Fig.3.

(iii) Straight Geometry

A square diffuser of straight boundaries on all four sides and of the same overall dimensions has also been tested.

CHAPTER -V

PRESENTATION OF RESULTS

The experimental data and the results are presented in dimensionless forms. The quantities at the inlet section of the diffuser are used for making them dimensionless because the flow at inlet section is uniform, as also no separation and asymmetry are present there.

1. Wall Pressure Distributions

As the motion of the threads attached along the centre line of the diffusers indicated flow asymmetry, it has been considered desirable to find the pressure recovery along the top centre line in all the six diffusers and also along a corner of the square diffusers. Accordingly the pressure recovery obtained from the piezometer readings have been made dimensionless in terms of the inlet dynamic pressure and presented graphically against the dimensionless distance along the surface as $(P-P_0) / \frac{\rho U_0^2}{2}$ versus S/D_0 for axisymmetric and versus S/W_0 for square diffusers, shown in figs. 17 to 19 where P is the pressure at any section at a distance S along the surface from inlet section. P_0 is the pressure at the inlet and U_0 the mean velocity at inlet section of the diffusers. As the flow proceeds downstream of the diffuser the pressure in the flow field increases. This

may also help in rough judgement of the location of separation zone, in which the pressures become constant.

2. Velocity Profiles in Boundary Layer

The total and static heads were measured within the boundary layer. The growth of the turbulent boundary layer in the diffuser is shown by the dimensionless velocity defect $(1 - u/U)$ versus the dimensionless distance from the boundary i.e. y/D_0 in axisymmetric diffusers and y/W_0 in square diffusers in figs. 23 to 40.

3. Pressure and Velocity Profiles at inlet and outlet sections

Pressure head is measured along the centre line at inlet and outlet. The variation was very little at these sections. So the pressure profiles are not presented. Velocity profiles are obtained at the inlet and exit sections in the centre and also at the right corner in case of square diffusers and are shown in fig. 8 to 16.

4. Calculation of Energy Correction factor

Energy correction factors are obtained at inlet and exit sections of the diffusers by graphical integration of the following expressions for all the three Reynolds numbers and for all the six diffuser geometrics.

Energy correction factor at any section is given by,

$$\alpha = \frac{1}{A} \int_A \left(\frac{v}{V} \right)^3 dA \quad \dots (28)$$

where A is the area of the section, V is the mean velocity

and v = velocity within the strip area, dA . Eq. 28 can be simplified for axisymmetric and two-dimensional flows. Since the flow at the entrance section was uniform in all the cases giving a constant velocity except near the boundary, the values of α at this section were conveniently found using

$$\alpha = \frac{2}{R^2} \int_0^R \left(\frac{v}{V}\right)^3 r dr \quad \dots \quad (29)$$

for axisymmetric geometry and

$$\alpha = \frac{1}{Y} \int_0^Y \left(\frac{v}{V}\right)^3 dy \quad \dots \quad (30)$$

for the square geometry. However, at the exit section of the diffusers the velocity distributions were found to be asymmetrical (Fig. 22) in all the six models, and hence the values of α at this section were obtained by contour plotting of the isolines of $(v/V)^3$ and integrating over the corresponding flow section according to Eq. 28. The values of α for all the six models and for three Reynolds numbers were given in Table 1.

5. Energy-Loss Coefficient

Having obtained the velocities, pressures and energy correction factors at the entrance and the exit sections, one can readily compute the energy loss using the Bernoulli equation. Application of this equation implies one-dimensional flow analysis, a good approximation which should be sufficiently accurate for the purpose of evaluating the relative performance of the six models. The Bernoulli equation in terms of energy per unit mass per second can be written as

$$P_0 + \alpha_0 \frac{U_0^2}{2} = P_e + \alpha_e \frac{U_e^2}{2} + \Delta E \quad \dots \quad (31)$$

Here, ΔE = Total energy loss and subscript e means exit section.

$$\text{or } \Delta E = (P_o - P_e) + \frac{\rho}{2} (\alpha_o U_o^2 - \alpha_e U_e^2) \quad \dots (32)$$

Dividing this by convertible kinetic energy, the coefficient of energy loss C_L is given by

$$C_L = \frac{\Delta E}{\frac{\rho U_o^2}{2}} = \frac{P_o - P_e}{\frac{\rho U_o^2}{2}} + \alpha_o - \alpha_e \left(\frac{U_e}{U_o} \right)^2 \quad \dots (33)$$

$$\text{or } C_L = \alpha_o - \left\{ \frac{P_e - P_o}{\rho U_o^2 / 2} + \alpha_e \left(\frac{U_e}{U_o} \right)^2 \right\} \quad \dots (34)$$

To calculate the values of C_L values of energy correction factor and the mean pressure are obtained at inlet and outlet of the diffusers. The variation of coefficient of energy loss with Reynolds number for all the diffuser geometries has been plotted in fig. 20 and 21 and are given in table 2. Energy loss as the percentage of $\frac{(U_o - U_e)^2}{2g}$ is also plotted against the divergence angle β for all the geometries. Gibson's curve of percentage head loss versus β is also shown for comparison in fig. 6 and 7. The values of energy loss coefficient in all cases, ignoring the kinetic energy correction factor were also computed and shown in tables.

CHAPTER VI

DISCUSSION OF RESULTS

The object of this study is to compare the diffuser performance of the proposed potential flow geometry with the other two geometries, namely, the Gibson and the straight-line geometries as applied to the circular and square diffusers essentially from three stand points:

- (1) pressure recovery,
- (2) flow asymmetry,
- (3) energy loss

in the diffuser section. Depending upon its situation in a flow system a diffuser may have to satisfy one or more of the above functions. As for example when it is adopted as a draft tube it has to satisfy the former two functions only while it is required to give minimum energy loss when the diffuser is used as an outlet into a reservoir for a pump-discharge line. These cases occur in the pumped storage plants and the conventional water-power plants. Similar instances can be cited from engineering practice in venturi-meters, diffuser cones in wind and water tunnels and ventilation engineering. The performance of the six models is compared from the above three functional utilities.

1. Wall Pressure Distributions

Figure 17 indicates that the pressure increase in the axisymmetric diffusers is very gradual. The potential flow geometry gives the maximum pressure recovery while the straight-line geometry is found to give the lowest recovery of pressure. The Gibson model is, however superior to the latter, but the pressure recovery is 15

percent less than in the potential flow model as it can be seen in Fig.17. For square diffusers the pressure rises in the diffuser section rather steeply in the initial portion of the diffuser upto $S/w_0 = 1$ (Fig. 18). Thereafter its increase is very mild for all the three boundary geometries. Among the three square models, the Gibson model is the best closely followed by the potential flow model with 9 percent less recovery than the Gibson model. The straight-line model once again gives the lowest pressure recovery.

For the convenience of comparison the pressure recovery coefficients of the six models are listed below:

Model	Axisymmetric	Square
Potential flow	0.72	0.41
Gibson	0.61	0.45
Straight-line	0.34	0.18

It can be seen from Fig. 19 that in the square models the wall pressures along the corners are somewhat higher than the centre-line pressures. This observation was first reported by Gibson^(9,10,11) as long back as 1910 and also by Pullaiah⁽²⁴⁾ in 1969. This can be explained as a consequence of the secondary currents which build up at the sharp corners and rapidly grow in the diffuser with the distance in the flow direction. The secondary flow at the corner occurs due to undue thickening of the boundary layer at the corner relative to the centre-line. It results in a transverse flow directed towards the corner along the diagonal and away from the corner along either adjacent side

forming a pair of closed spiral cells.

2. Flow Patterns in the Diffuser

The velocity traverses at the entrance section to the diffuser are found to be uniform across the section except in the boundary layer region (see Figs. 8 to 10 for axisymmetric models and Figs. 12 to 14 for square models). Such ideal entrance flow conditions were obtained in all the models because the inlet was designed according to Kirchhoff's free-streamline theory. It is well known that the established turbulent flow in a duct gives uniform velocity distributions well approximating the velocity distributions obtained in the models at the entrance section. Thus the results of this experimental study should be useful for practical application as the entry conditions representing the fully established turbulent flow are satisfactorily simulated in all the six models.

It is evident from the velocity traverses in Fig. 11 that the flow at the exit section of the diffuser is nearly uniform in the case of the straight line geometry of the circular models while in the case of the Gibson model the flow is found to be very asymmetrical. However, there is no separation or any tendency to separation in any of the three circular models. Surprisingly enough, it is the straight-line geometry among the square models which gives the most erratic velocity distribution and even a small zone of separation on one side (Fig. 15). The high velocity flow streams past the opposite side. The potential flow model is surely the best choice from the stand point of the symmetry of the exit flow. The Gibson model can be ranked between the above two models. The corner velocity profiles of the three square

models (Fig. 16) show the same trend as described above. These trends can be seen to be the same for all the three Reynolds numbers.

Here it may be pointed out that M.C. Chaturvedi⁽⁶⁾ did not take into account the possibility of flow asymmetry in his detailed study of flow characteristics in conical diffusers. He measured the velocities, pressures, turbulence and other quantities along a radius and in the direction of flow. In actuality this is not the case. Pullaiah⁽²⁴⁾ and Khan⁽¹⁶⁾ also noticed asymmetry in flow in square and circular diffusers respectively for the angle of divergence equal to 32° . At this angle of divergence flow alternated from one side to the opposite wall and the period of alternation increased with the increasing Reynolds number. In the present study, asymmetry of varying degree in the exit flow is observed for 16° conical and square diffusers. The flow asymmetry was duly taken into account in calculating the energy loss by computing the kinetic energy correction factors. However, it may be noted that the separation of flow occurred in a very small zone only in one model that is, straight line geometry square model. There were no alternation of flow from one side to the other side in any one of the six models.

3. Energy-loss in the Diffuser Section

The energy loss was computed using the one-dimensional Bernoulli equation, Eq. 32. The variation in the coefficient of the energy loss, (Eq. 34) was studied with the Reynolds number for each geometry. The results are shown in Table 2 for circular and square diffusers. As the values of α were not sufficiently accurate, it was considered fair to compare the efficiency of the

six models on the basis that $\alpha = 1.0$. For the value of the highest Reynolds number the energy-loss coefficients are shown below:

Model	Axisymmetric	Square
Potential flow	0.37	0.57
Gibson	0.31	0.48
Straight-line	0.33	0.51

It is evident that there is no appreciable variation in the energy-loss coefficient with the geometry of the diffuser transition while there is a clear and definite improvement with axisymmetric diffusers as compared with the square diffusers. The energy-loss coefficient of the square diffusers is 54.5 percent higher than that of the axisymmetric diffusers. The loss in the case of the square diffusers is more than in the axisymmetric diffusers due to the effect of the four sharp corners where secondary circulation grows at the expense of the mean flow energy. From the stand point of the geometry of the transition, any geometry can be selected for the transition, but if a choice has to be made between the square and the circular diffusers, it is surely the circular one which gives the minimum energy-loss.

The Reynolds number range that can be obtained in the experimental set-up is unfortunately very small and it can only give a qualitative conclusion on the dependence of C_L on R . It is shown for circular diffusers in Fig. 20 and one can notice that the value of the energy loss coefficient is not dependent on the Reynolds number for all the three geometries. For the square

diffusers also such an invariance in Q_L with R can be seen in Fig. 21, although there is some experimental error and scatter of data. In both the Figs. 20 and 21 the results were based on the computed values of the kinetic energy correction factor, α .

The results of this study for 16° -diffusers and those of other investigators were shown on the Gibson curve, percentage head loss ($= (U_0 - U_e)^2 / 2g$) versus the divergence angle, β in degrees. Values obtained by Khan⁽¹⁶⁾ and M.C. Chaturvedi⁽⁶⁾ for $\beta = 32^\circ$ are also shown on the same curve, Fig. 6, for circular diffusers for comparison. Gibson's values were also shown for comparison in Fig. 20. There is a satisfactory agreement in the results of the various investigators and the present study. A similar comparison for square diffusers had been made in Figs. 7 and 21 and the data of Gibson^(9,10,11) and Pullaiah⁽²⁴⁾ were included here. The comparison is satisfactory for straight-line geometry and for other geometries the observed values are below Gibson curve. This can be expected because Gibson tested only the straight line geometry.

4. Boundary-layer Velocity Profiles in the Diffuser Section

Few measurements of the velocity profiles in the developing turbulent boundary layer under the effect of an adverse pressure gradient are available in literature. Figures 23 to 31 give dimensionless velocity distributions for three Reynolds numbers in the range 3.6×10^5 to 7.4×10^5 for the three circular diffusers. It is observed that the velocity profiles are less full and the boundary layer thickness larger for the Gibson geometry than for the other two geometries. This observation is consistent with the observed flow patterns at exit discussed in

section 2 of this chapter. Figures 32 to 40 represent similar boundary-layer data for the three square diffusers and for three Reynolds numbers in the range 3.2×10^5 to 6.4×10^5 . The data are found to indicate a systematic development of the turbulent boundary layer consistent with the distance and the Reynolds number in the case of all the three geometries of the square diffusers.

It would be interesting to analyse this boundary layer data in terms of the universal log law and defect law of the turbulent boundary layer on a smooth surface under the effect of adverse pressure gradient.

CHAPTER VII

CONCLUSIONS

The hydraulic performance of six 16° -angle diffuser models having circular and square cross-sections and incorporated with three boundary geometries is studied at three Reynolds numbers. The following conclusions can be drawn from this study:

1. From the stand-point of pressure recovery the potential flow geometry (proposed in this thesis) is superior to Gibson and straight-line geometries among the circular diffusers. The Gibson or potential flow geometry is found to be better than the straight-line geometry in the case of square diffusers. Between the square and circular diffusers, the circular models give much higher pressure recovery (varying from 35% to 90%) than in the case of square models.
2. The flow pattern at the exit end of the diffuser is found to be relatively better for the straight-line geometry among circular models and for the potential-flow geometry among the square diffusers. The gradation is indicated in the summary table given at the end of this Chapter. The grades A and B compare between the circular and the square models.
3. From the point of energy loss the geometry of the diffuser transition shows little variation in the values of the loss coefficients. However, the square models give considerably higher energy loss (as much as 55% increase) compared to the circular diffusers.

4. Within the range of the Reynolds numbers tested, here the energy-loss coefficient is found to be independent of the Reynolds number.

5. When the results of the present study are compared with Gibson's data, it is found that they compare satisfactorily in the case of circular diffusers. While in the case of square diffusers only the straight-line geometry fits well with Gibson's data. It is because Gibson considered only a straight-line geometry.

In the following Table a comparative statement which summarizes the conclusions 1 to 3 is given for ready reference.

Summary of Results

	Model	Pressure Recovery	Flow pattern at exit	Energy loss coeff.
Circular	Potential flow	0.72	II-A	0.37
	Gibson	0.61	III-A	0.31
	Straight-line	0.34	I-B(Best)	0.33
Square	Potential flow	0.41	I-A(Best)	0.57
	Gibson	0.45	II-B	0.48
	Straight-line	0.18	III-B	0.51

A programme for further research work on diffuser flows is indicated on the next page.

Programme for Further Work

Analysis of boundary layer data using the boundary layer momentum analysis, which could not be done due to lack of time, should be done. Also, measurements of turbulence quantities and the spatial distributions of energy production, energy transfer and diffusion quantities, with the help of hot wire anemometer, are required. Asymmetry in separated flows seems to be inherent with the phenomenon of turbulent boundary layer separation and a study of stability of flow in adverse pressure gradient flows is essential to explain it.

A rigorous study is required for smaller divergence angles to know the effect of Reynolds number and the occurrence of separation. A wide range of Reynolds number should be included to know its effect on the coefficient of energy loss accurately. In case of non-circular diffusers the available literature is not adequate and there is a need for more work especially for small divergence angles.

BIBLIOGRAPHY

1. ABBOT, D.E., and KLINE, S.J.,
'Experimental Investigation of Subsonic Turbulent Flow over Single and Double, Backward Facing Steps', Journal of Basic Engineering, Trans. ASME, Series D, Vol.84, September 1962, p.317-326.
2. ARCHER, W.H.,
'Experimental determination of loss of Head due to Sudden Enlargements in Circular Pipes', T-ASCE 1913, p.999.
3. BLACK, T.J.,
'A Simplified Form of auxiliary equation for use in the calculation of Turbulent boundary layers', Journal of Royal Aeronautical Society, Vol.62, 1958, p.215-218.
4. BINDER, R.C.,
Calculation of Diffuser Efficiency for Two-dimensional Flow', Journal of Applied Mechanics, Trans. ASME, Vol.14, No.3, September 1947, p.A-213.
5. BURTON, R.,
'Discussion of the influence of confining surfaces upon the boundary layer in a channel', Journal of Aeronautical Sciences, Vol.24, 1957, p.149.
6. CHATURVEDI, M.G.,
'Flow characteristics of Axisymmetric Expansions', Journal of the Hydraulics Division, Proc. ASCE, Vol.89, No.HY3, May 1963, p.61-92.
7. CLAUSER, F.H.,
'The Turbulent Boundary Layers', Advances in Applied Mechanics, 1956, Vol.IV, Academic Press Inc., New York, p.2-51.
8. CARMODY, T.,
'Discussion to Flow Characteristics of Axisymmetric Expansions by M.C.Chaturvedi', Journal of Hydraulics Division, Proc. ASCE, September 1963, p.173.

9. GIBSON, A.H.,
'On the Flow of Water through Pipes and passages having Converging Boundaries', Proc. Royal Society of London, Series A, Vol.83, May 1910, p.366-378.
10. GIBSON, A.H.,
'On the Resistance to Flow of Water through Pipes or passages having Divergent Boundaries', Trans. Royal Society EDIN, 1911, Vol.48, Part I (No.5), p.97-116.
11. GIBSON, A.H.,
'The Conversion of Kinetic to Pressure Energy in the Flow of Water through Passages having Divergent Boundaries', Engineering, Vol.93, June 1912, p.205-206.
12. HUANG, T.T., and CHEVRAY, H.,
'Discussions to Flow Characteristics of Axisymmetric Expansions by M.C. Chaturvedi', Journal of the Hydraulics Division, Proc. ASCE, January 1964, p.277-282.
13. JOBISSEN, A.L.,
'Discharge Measurements by Venturi Tubes', Trans. ASME, Vol.73, May 1951, p.403-411.
14. JAIN, R.K.,
'A Study of Expansion Transition in Open Channels', M.E. Thesis, University of Roorkee, 1968.
15. KALINSKE, A.A.,
'Conversion of Kinetic to Potential Energy in Flow Expansions', Trans. ASCE, Vol.111, 1946, p.355-390.
16. KHAN, R.,
'Hydraulic Performance of Conical Diffusers', M.E. Thesis, University of Roorkee, Roorkee, 1969.
17. KLINE, S.J.,
'On the Nature of Stall, ' Journal of Basic Engineering, Trans. ASME, Vol.81, September 1959, p.305-320.
18. KLINE, S.J., ABBOT, D.E., and FOX, R.W.,
'Optimum Design of Straight Walled Diffusers', Journal of Basic Engineering, Trans. ASME, Vol.81, September 1959, p.321-331.

19. KLINE, S.J.,
'Some New Conceptions of the Mechanism of Stall in Turbulent Boundary Layers,' Journal of Aeronautical Sciences, Vol.24, 1957, p.470.
20. KLINE, S.J., MOORE, C.A. and COCHBAN, D.L.,
'Wide Angle Diffusers of High Performance and Diffuser Flow Mechanisms', Journal of Aeronautical Sciences, Vol.24, 1957, p.469.
21. KUMAR, S.,
'Efficiency of Splitter walls in Open Channels Expansions', M.E.Thesis, University of Roorkee, Roorkee, 1967.
22. NORBURY, J.F.,
'Some Measurements of Boundary Layer Growth in a Two-dimensional Diffusers', Journal of Basic Engineering, Trans. ASME, Vol.81, 1959, p.285-296.
23. PRANDTL, L., and TIETJENS, O.G.,
'Applied Hydro and Aeromechanics,' Dover Publications Inc. New York, p.85.
24. PULLAIAH, V.,
'Study of Diffusers for Submerged Pipe Outlets', M.E. Thesis, University of Roorkee, Roorkee, 1969.
25. BAO, P.V.,
'Boundary Layer Development at Curved Conduit Entrances', Journal of Hydraulics Division, Proc. ASCE, Vol.94, No.HY1, January 1968, p.195-217.
26. RAI, S.P.,
'Boundary Layer Separation in two-dimensional Expansions' M.E.Thesis, University of Roorkee, Roorkee, 1966.
27. ROUSE, H.,
'Engineering Hydraulics', John Wiley and Sons, Inc., New York, p.114.
28. ROBERTSON, J.M. and ROSS, D.,
'Effect of Entrance Conditions on Diffuser Flow,' Proc. ASCE, Vol.78, Separate No.141, July 1952.

29. ROBERTSON, J.M. and CALEHUFF, G.L.,
'Turbulence in a Diffuser Boundary Layer', Journal of Hydraulics Division, Proc. ASCE, October 1957, Paper 1393.
30. ROBERTSON, J.M., and HOLL, J.W.,
'Effect of Adverse Pressure Gradients on Turbulent Boundary Layers in Axisymmetric Conduits', and Discussions by H.R. FRASER and E.M. URAM, Journal of Applied Mechanics, Trans. ASME, Vol.79, 1957, p.191.
31. ROBERTSON, J.M., and FRASER, H.R.,
'Separation Prediction for Conical Diffusers', Journal of Basic Engineering, Trans. ASME, Vol.82, March 1960, p.201-209.
32. SANDBORN, V.A. and KLINE, S.J.,
'Flow Models in Boundary Layers Stall Inception', Journal of Basic Engineering, Trans. ASME, Vol.83, September 1961, p.317-327.
33. SCHUBAUER, G.B.,
'Turbulent Process as observed in Boundary Layer, and Pipe', Journal of Applied Physics, Vol.25, Jan. 1954, p.188-196.
34. SPENCE, D.A.,
'The Development of Turbulent Boundary Layers', Journal of Aeronautical Sciences, Vol.23, 1956, p.3.
35. TULIS, H.,
'Flow Expansions and Pressure Recovery in Fluids', Trans. ASCE, Vol.121, 1956, p.65-84.
36. URAM, E.M.,
'The Growth of an Axisymmetric Turbulent Boundary Layer in an Adverse Pressure Gradient', Proc. of the Second U.S. National Congress of Applied Mechanics, ASME, 1954,
37. WARREN, J.,
'A Study of Head Loss in Venturimeter Diffuser, Sections', Trans. ASME, Vol.73, May 1951, p.399-402.

38. WINTERNITZ, F.A.L., and RAMSAY, W.J.,
'Effects of Inlet Boundary Layer on Pressure Recovery,
Energy Conversion and Losses in Conical Diffusers',
Journal of Royal Aeronautical Society, Vol.61, February,
1957, p.116-124.
39. WAITMAN, B.A., RENU, L.R. and KLINE, S.J.,
'Effects of Inlet Conditions on Performance of Two-
dimensional Subsonic Diffusers', Journal of Basic Engg.
Trans. ASME, September 1961, p.349-360.

TABLE -1

KINETIC ENERGY CORRECTION FACTOR, α

Values of α at the exit sections for different Reynolds numbers are as follows,

(1) 16° Conical Diffusers

Potential Flow Model		Gibson Model		Straight Model	
Reynolds Number	α	R_o	α	R_o	α
3.83×10^5	3.56	3.58×10^5	3.45	3.89×10^5	4.165
6.30×10^5	3.22	6.30×10^5	2.405	6.52×10^5	3.32
6.82×10^5	3.825	7.20×10^5	2.935	7.38×10^5	3.675

(2) 16° Square Diffusers

Potential Flow Model		Gibson Model		Straight Model	
R_o	α	R_o	α	R_o	α
3.23×10^5	9.230	3.24×10^5	6.996	3.30×10^5	6.00
5.73×10^5	9.310	5.82×10^5	6.52	5.72×10^5	6.007
6.28×10^5	10.473	6.40×10^5	5.618	6.09×10^5	6.160

TABLE -2

Coefficient of Energy Loss, $C_L = \frac{\Delta E}{\rho U_0^2 / 2}$

16° Conical Diffusers

Straight Model			Gibson Model			Potential Flow Model		
α	C_L	C_L $\alpha=1.0$	R_0	C_L	C_L $\alpha=1$	R_0	C_L	C_L $\alpha=1.0$
9×10^5	0.2125	0.3805	3.58×10^5	0.217	0.3713	3.83×10^5	0.193	0.3340
2×10^5	0.218	0.3375	6.30×10^5	0.276	0.3462	6.30×10^5	0.218	0.3617
3×10^5	0.167	0.3285	7.20×10^5	0.2015	0.3137	6.82×10^5	0.176	0.3735

Gibson's value of C_L is equal to 0.1695 for $R_0 = 5.82 \times 10^4$

16° Square Diffusers

Straight Model			Gibson Model			Potential Flow Model		
α	C_L	C_L $\alpha=1.0$	R_0	C_L	C_L $\alpha=1.0$	R_0	C_L	C_L $\alpha=1.0$
0×10^5	0.167	0.4045	3.24×10^5	0.10	0.4645	3.23×10^5	0.021	0.4792
2×10^5	0.303	0.5405	5.82×10^5	0.164	0.4958	5.73×10^5	0.047	0.512
9×10^5	0.274	0.5115	6.40×10^5	0.227	0.4846	6.28×10^5	0.020	0.5682

Gibson's value of C_L is equal to 0.365 for $R_0 = 6.175 \times 10^4$

APPENDIX I

The coordinates of three boundary geometries for axisymmetric diffusers.

x from inlet of diffuser cms.	Radius at a distance x from the start of diffuser		
	Potential flow Geometry (cms)	Gibson's Profile (cms)	Straight Profile cms.
0 (Start)	7.50	7.50	7.50
5	7.78	7.84	8.195
10	8.09	8.22	8.890
15	8.44	8.63	9.585
20	8.83	9.11	10.28
25	9.30	9.68	10.975
30	9.82	10.30	11.67
35	10.45	10.90	12.36
40	11.25	11.78	13.06
45	12.25	12.72	13.75
50	13.58	13.90	14.45
54 (End)	15.00	15.00	15.00

APPENDIX II

The coordinates of three boundary geometries for square diffusers.

x from inlet of diffuser (cms)	y at a distance x from the start of diffuser		
	Potential flow profile (cms)	Gibson Profile (cms)	Straight bound- ary (cms)
0(start)	7.50	7.50	7.50
5	7.60	7.94	8.195
10	7.87	8.43	8.89
15	8.32	9.00	9.585
20	8.90	9.60	10.28
25	9.60	10.20	10.975
30	10.40	10.85	11.67
35	11.27	11.53	12.36
40	12.18	12.40	13.06
45	13.15	13.25	13.75
50	14.17	14.22	14.45
54 (End)	15.00	15.00	15.00

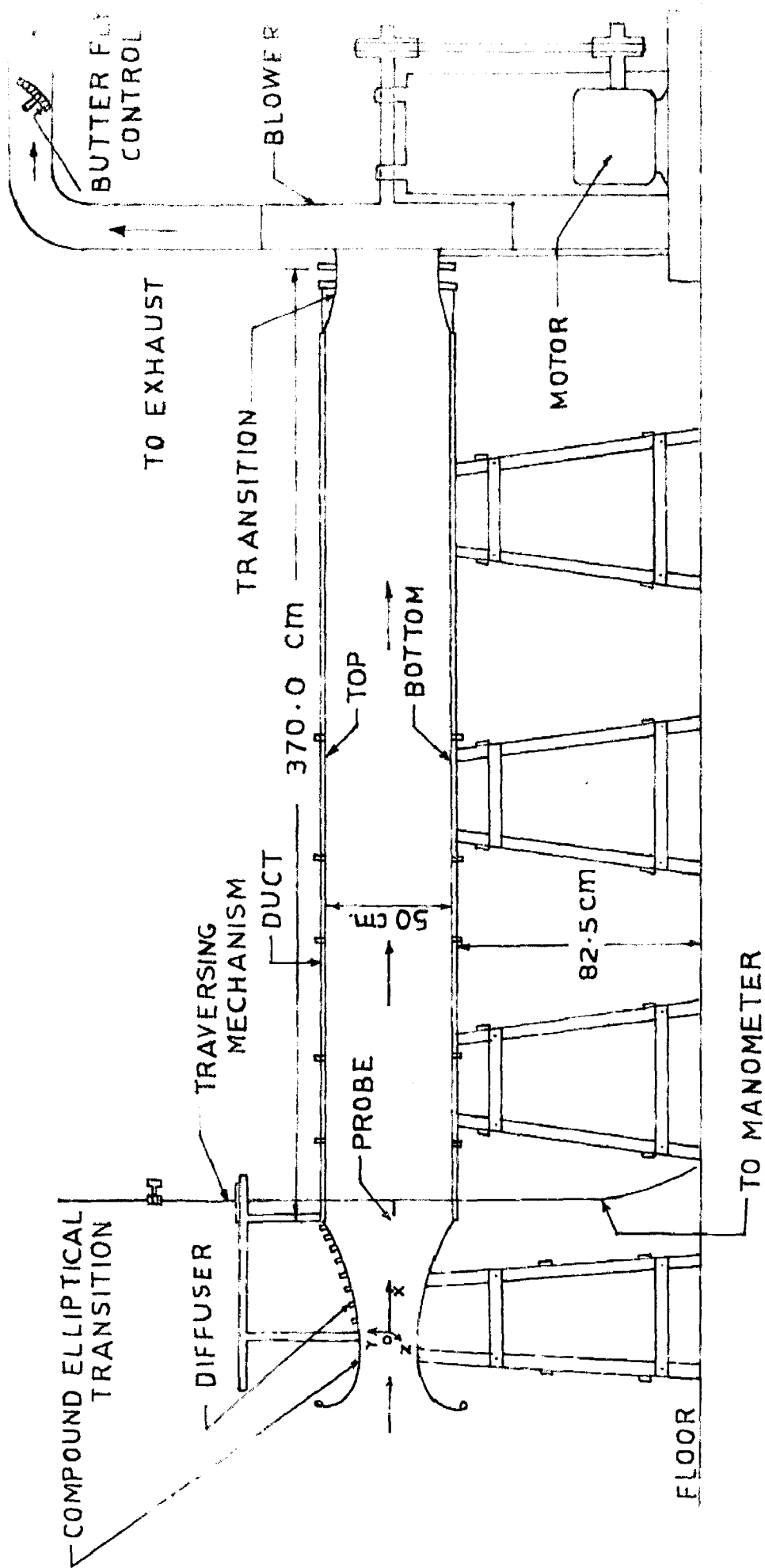


FIG.1- SKETCH OF THE EXPERIMENTAL SET-UP

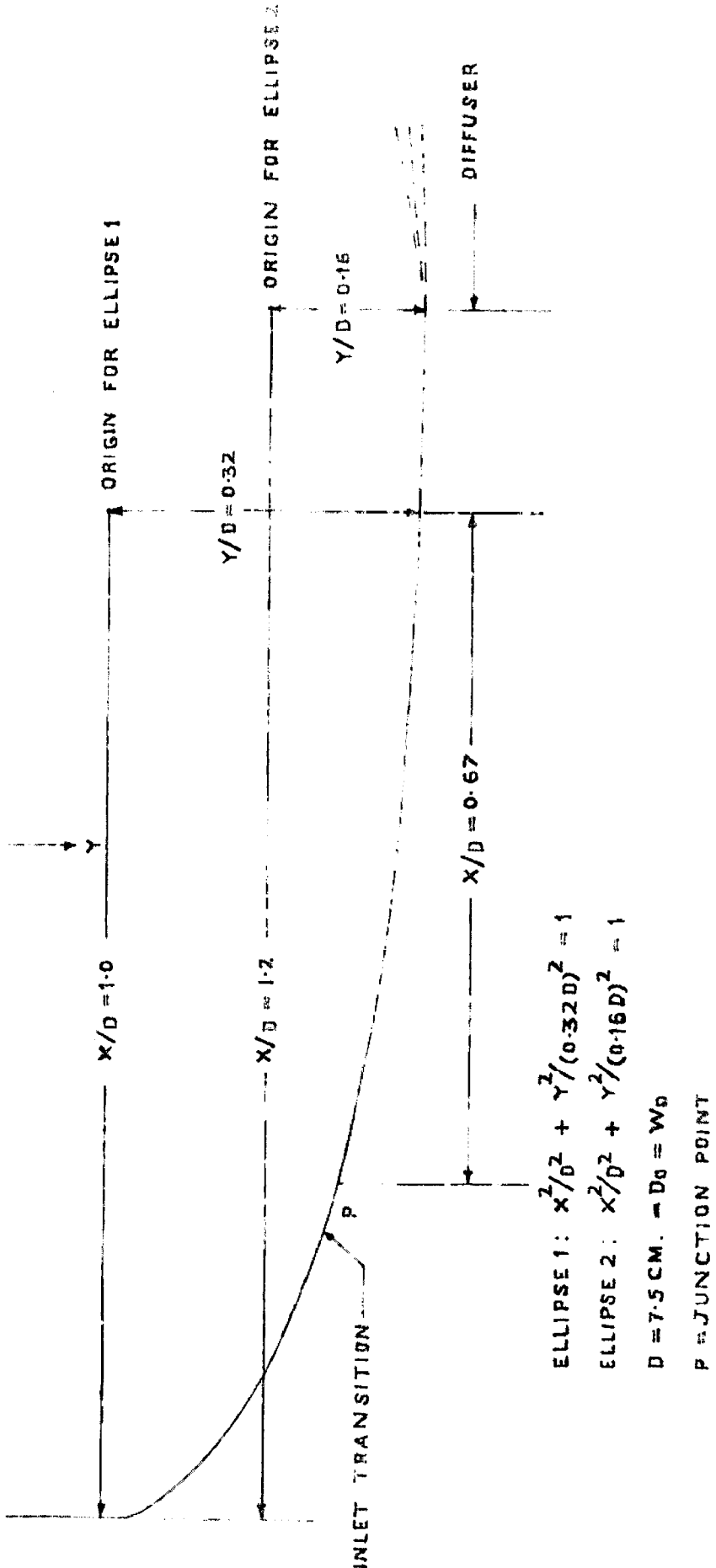
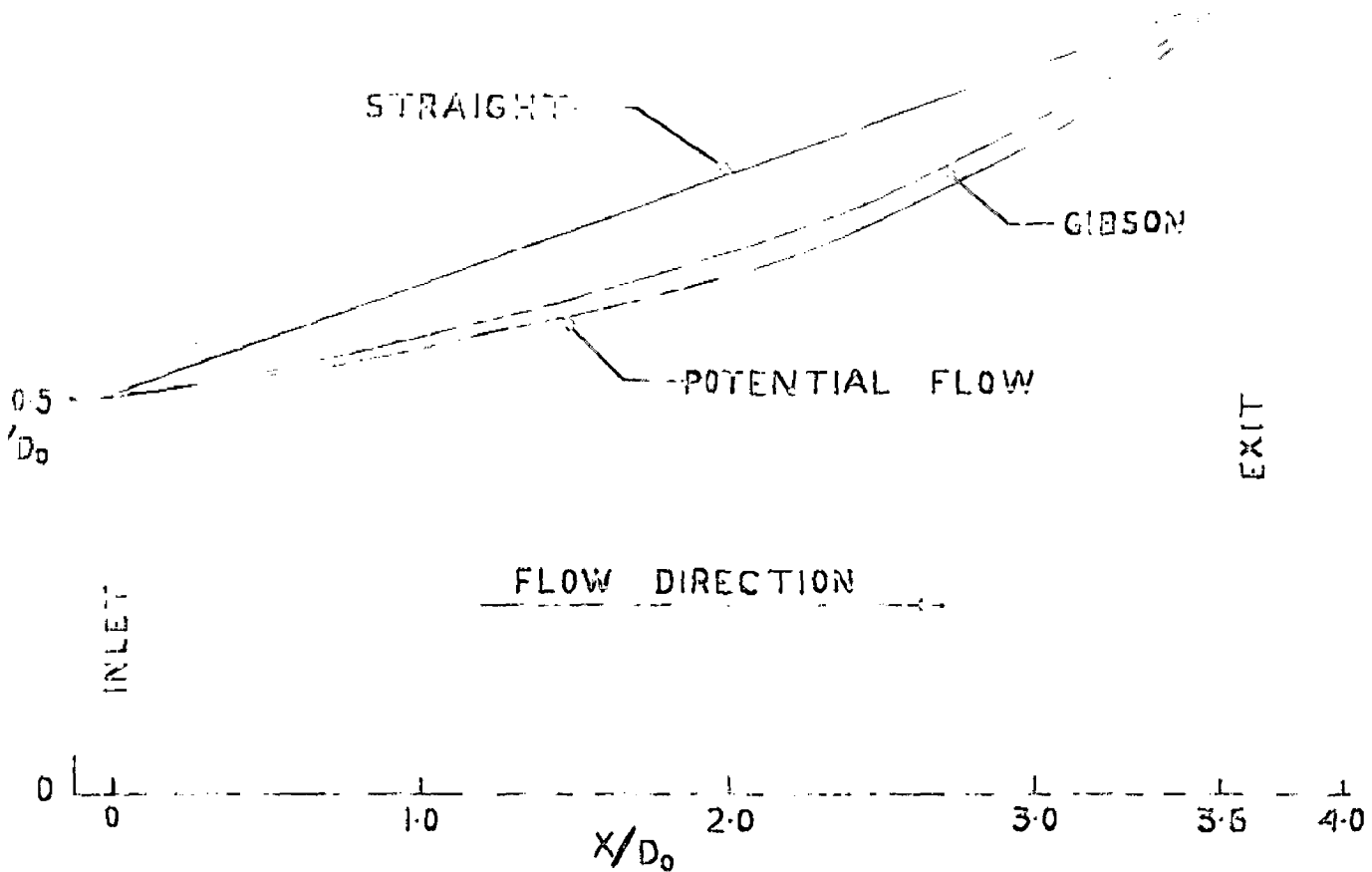
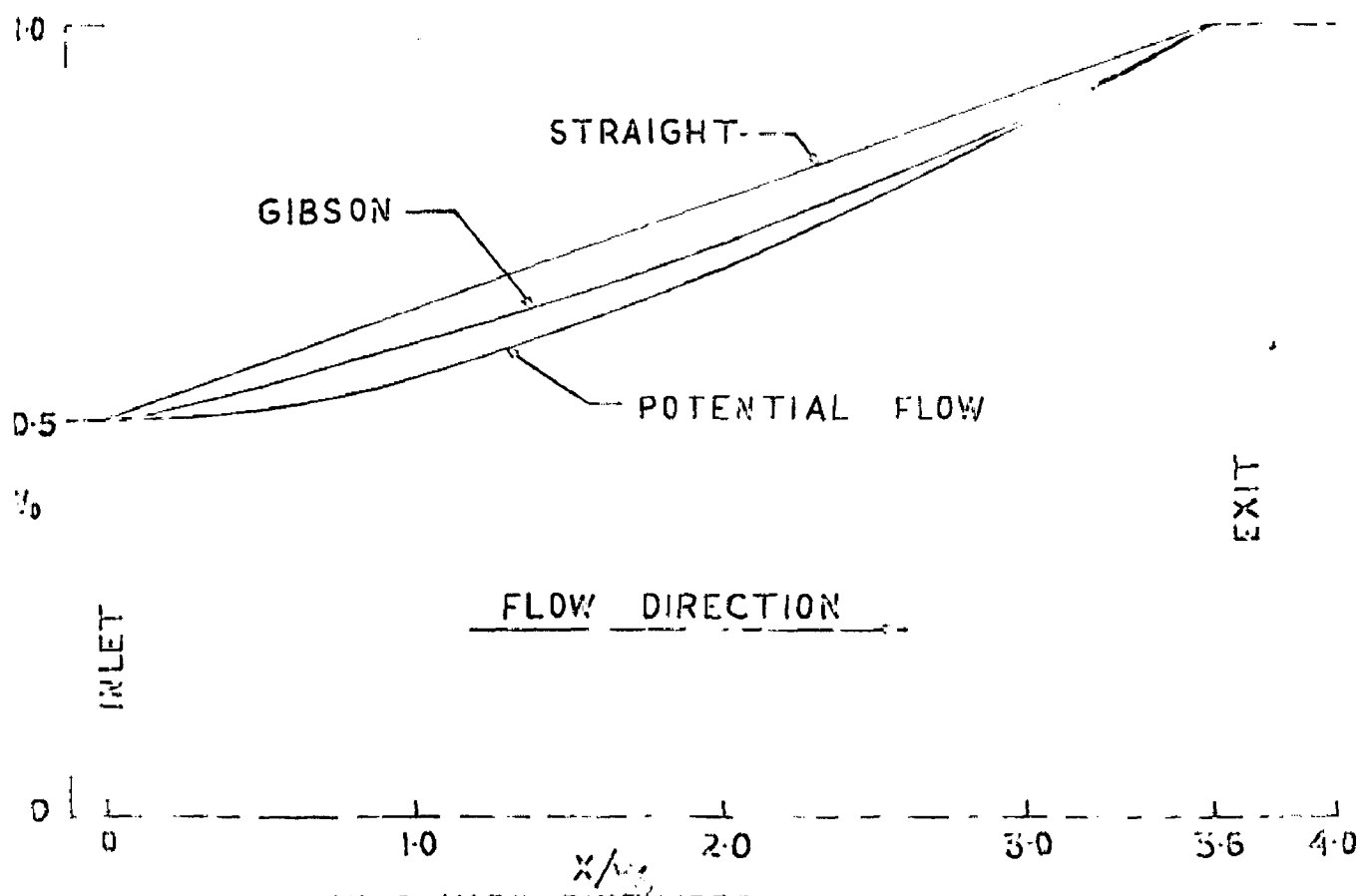


FIG. 2 - COMPOUND ELLIPTIC TRANSITION FOR THE INLET



(A) AXISYMMETRIC DIFFUSERS



(B) SQUARE DIFFUSERS

FIG.3- BOUNDARY GEOMETRIES

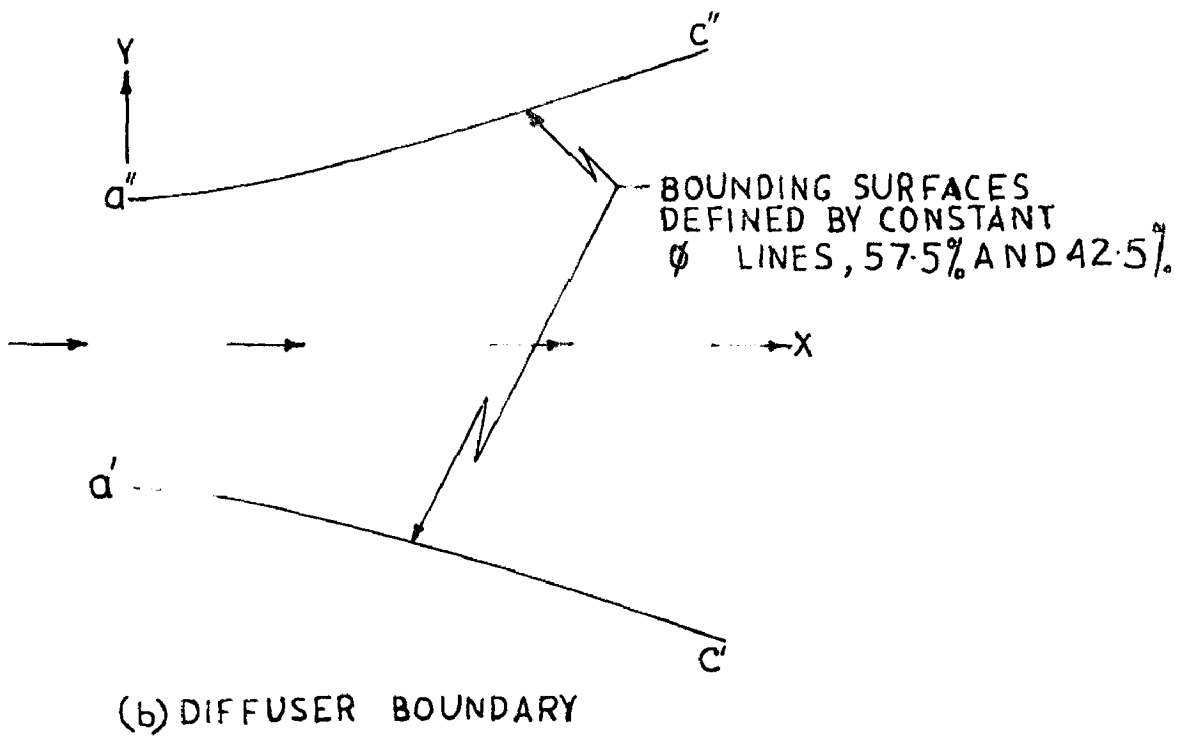
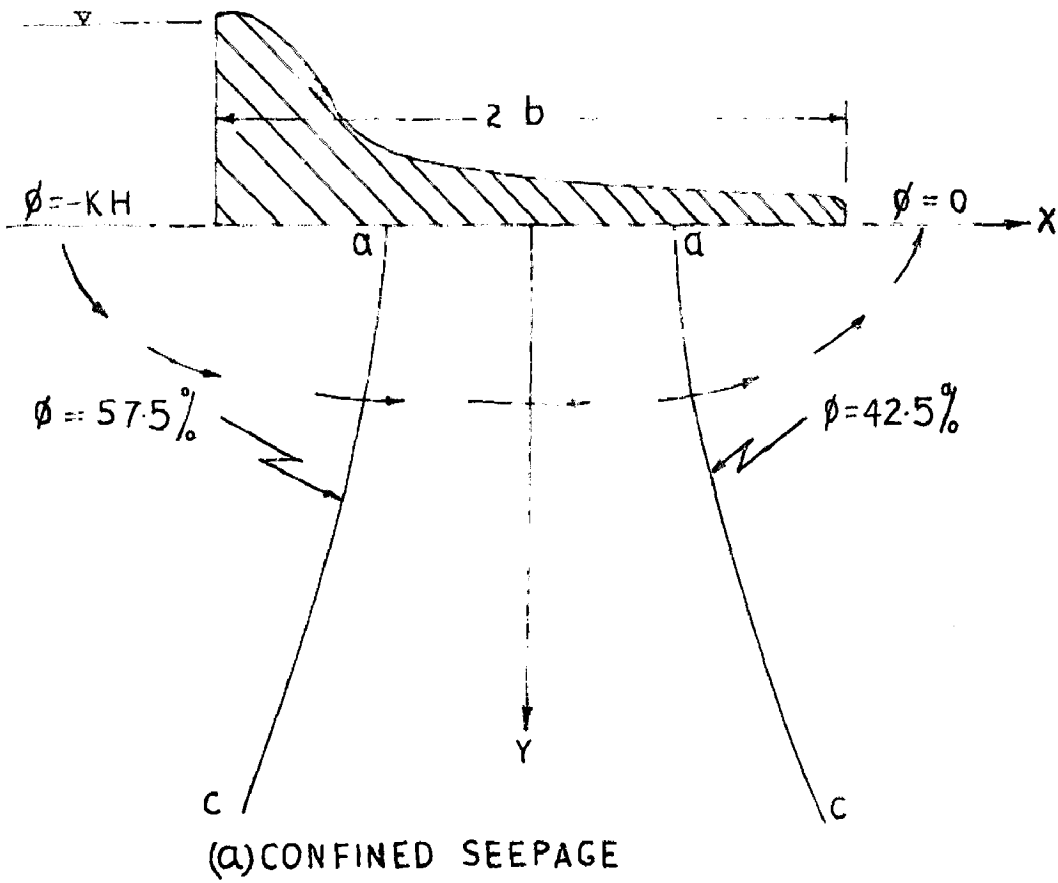
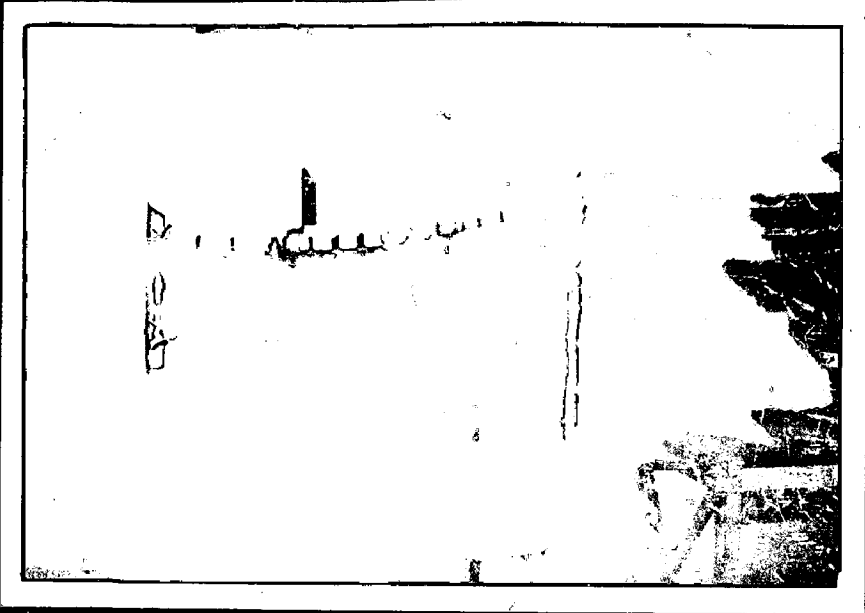


FIG 4 - POTENTIAL FLOW SOLUTION



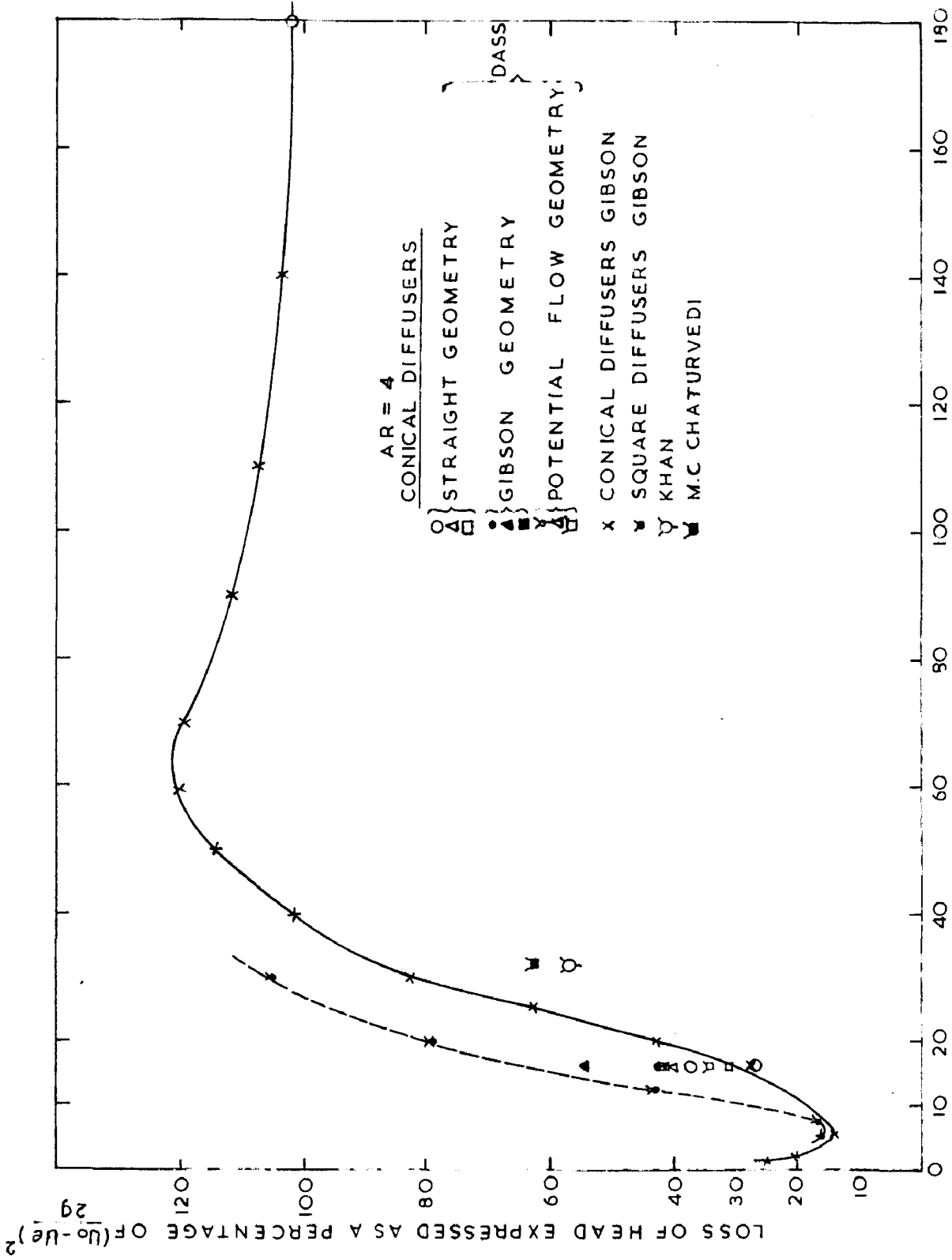


FIG 6 HEAD LOSS IN STRAIGHT TAFFERD FIFES BY GIBSON

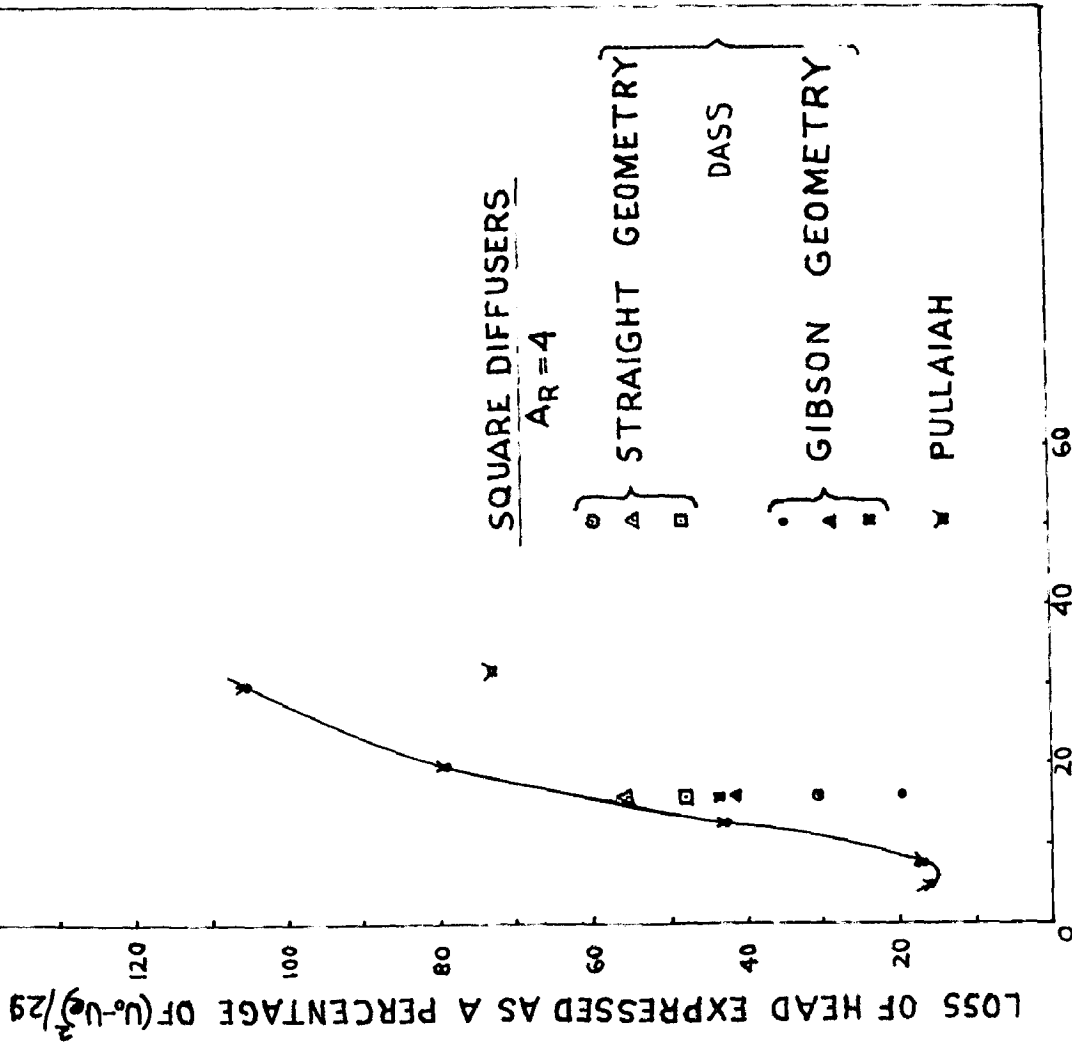


FIG. 7 - HEAD LOSS $V^2 \beta$ CURVE BY GIBSON

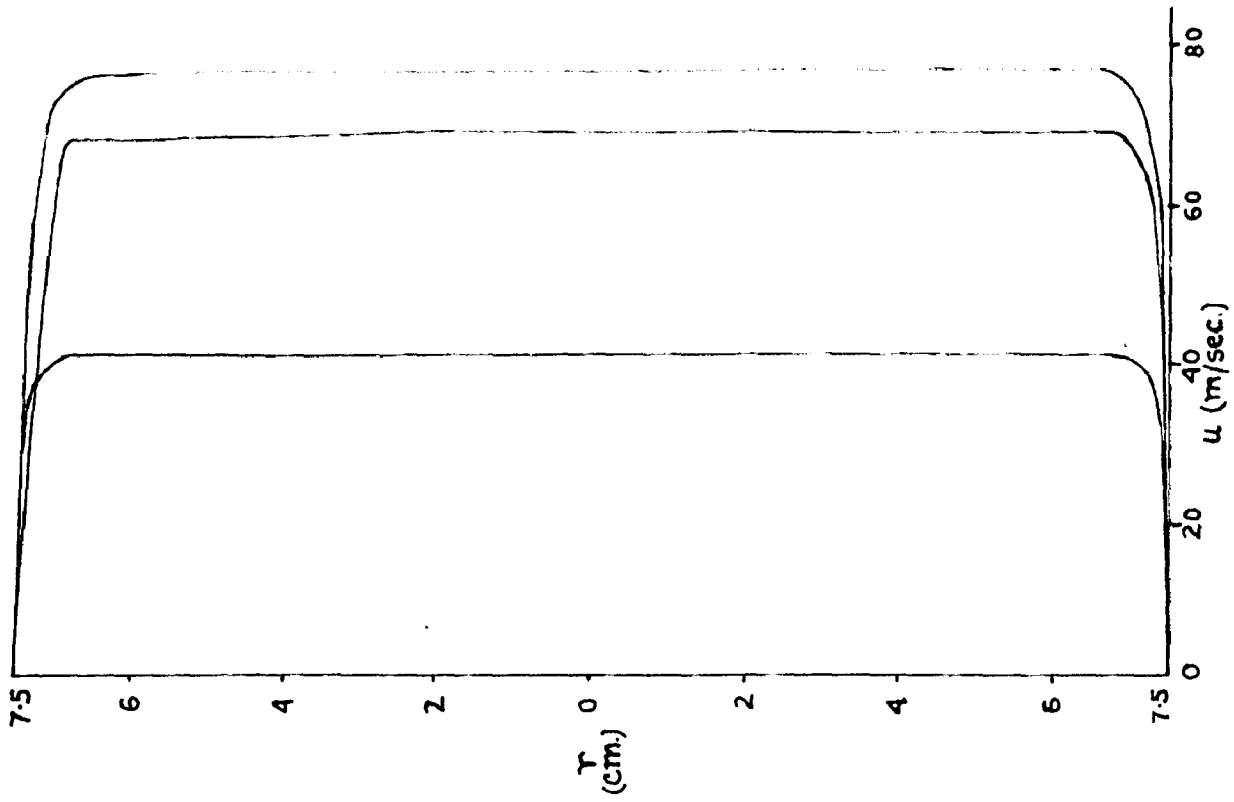


FIG. 8 - STRAIGHT BOUNDARY CONICAL (INLET VELOCITY PROFILES)

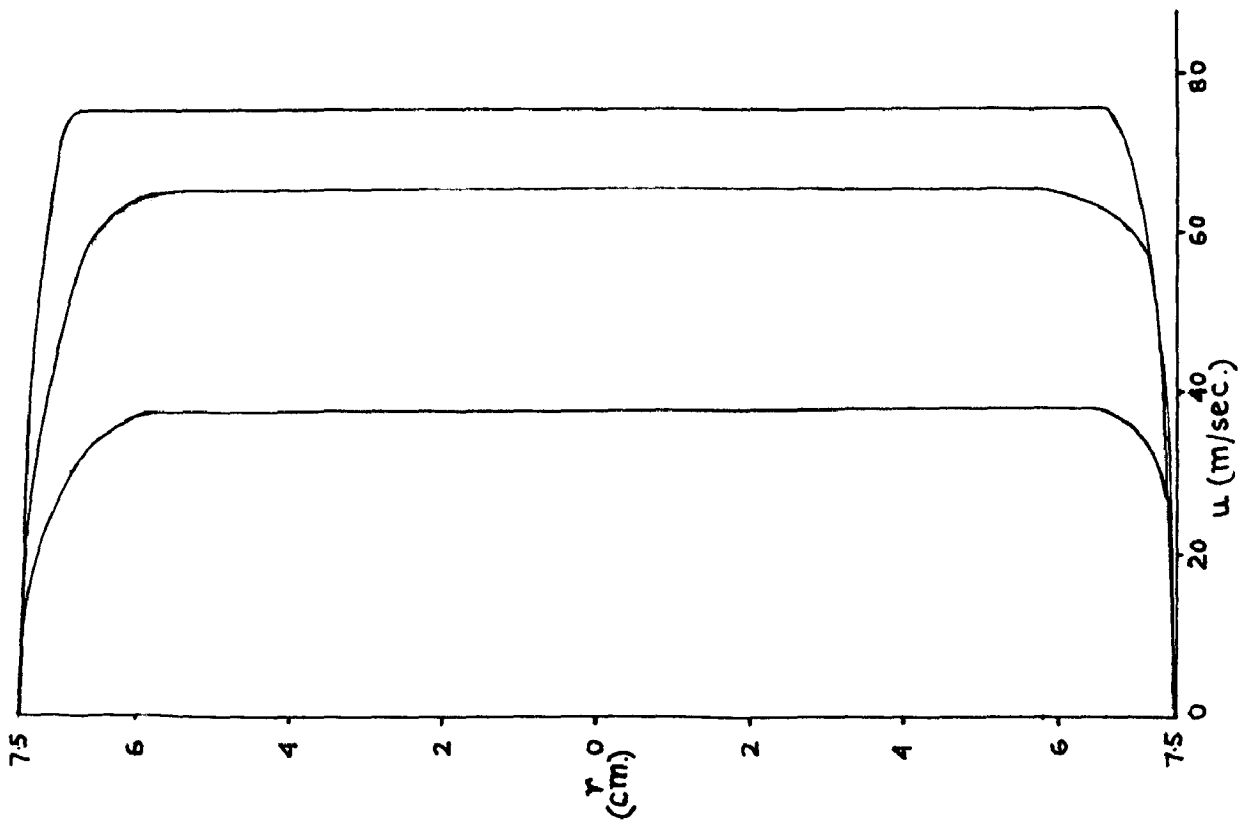


FIG.9- GIBSON'S GEOMETRY CONICAL (INLET VELOCITY PROFILES)

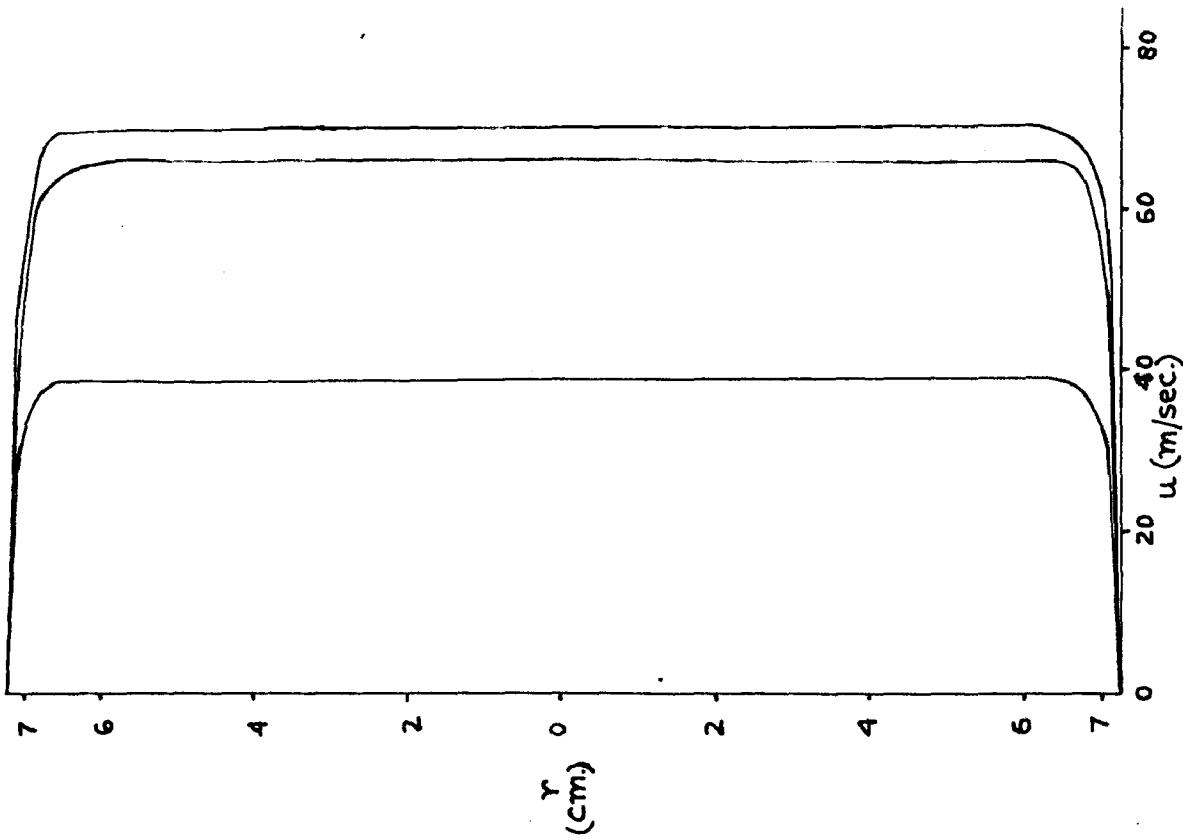
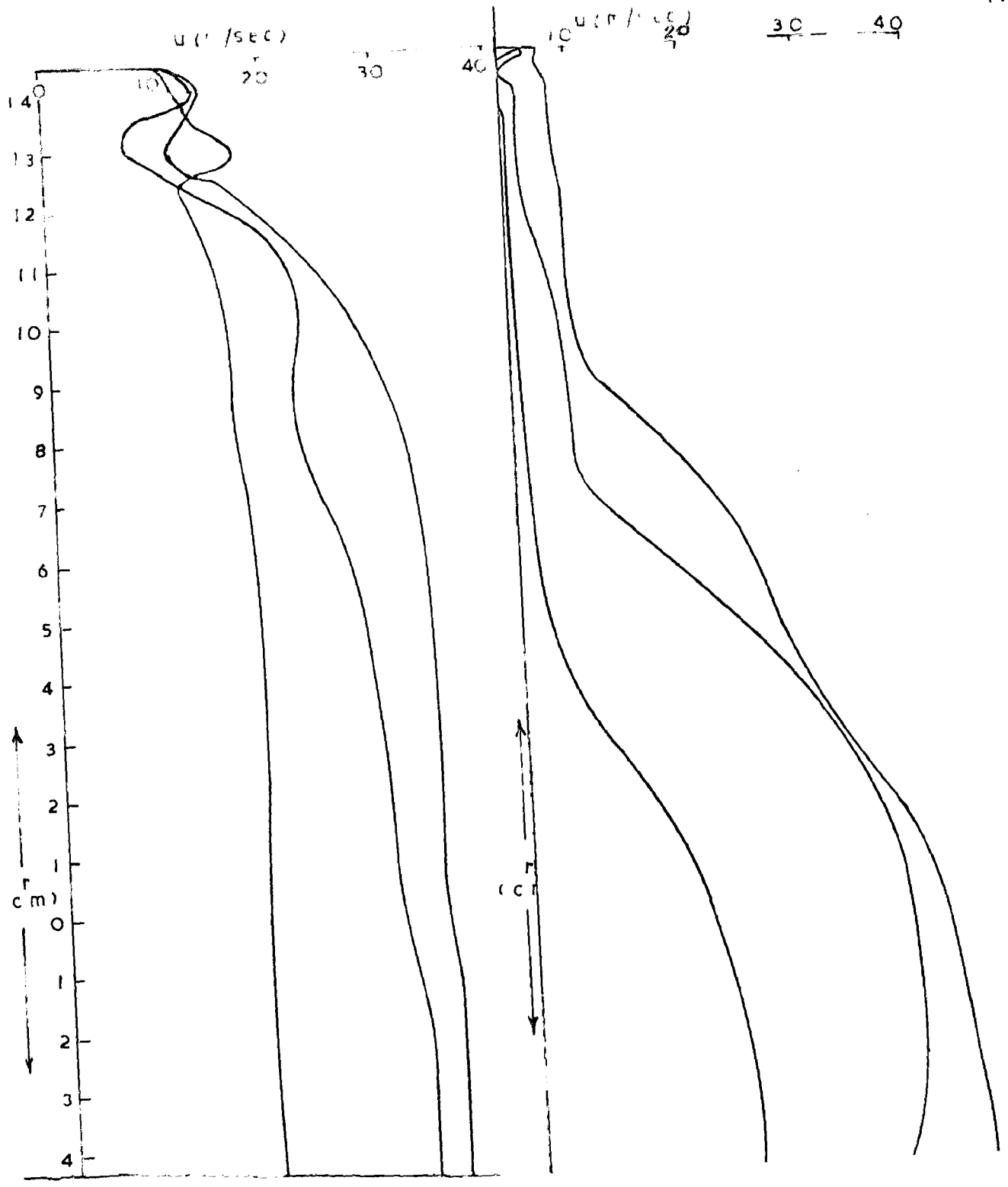
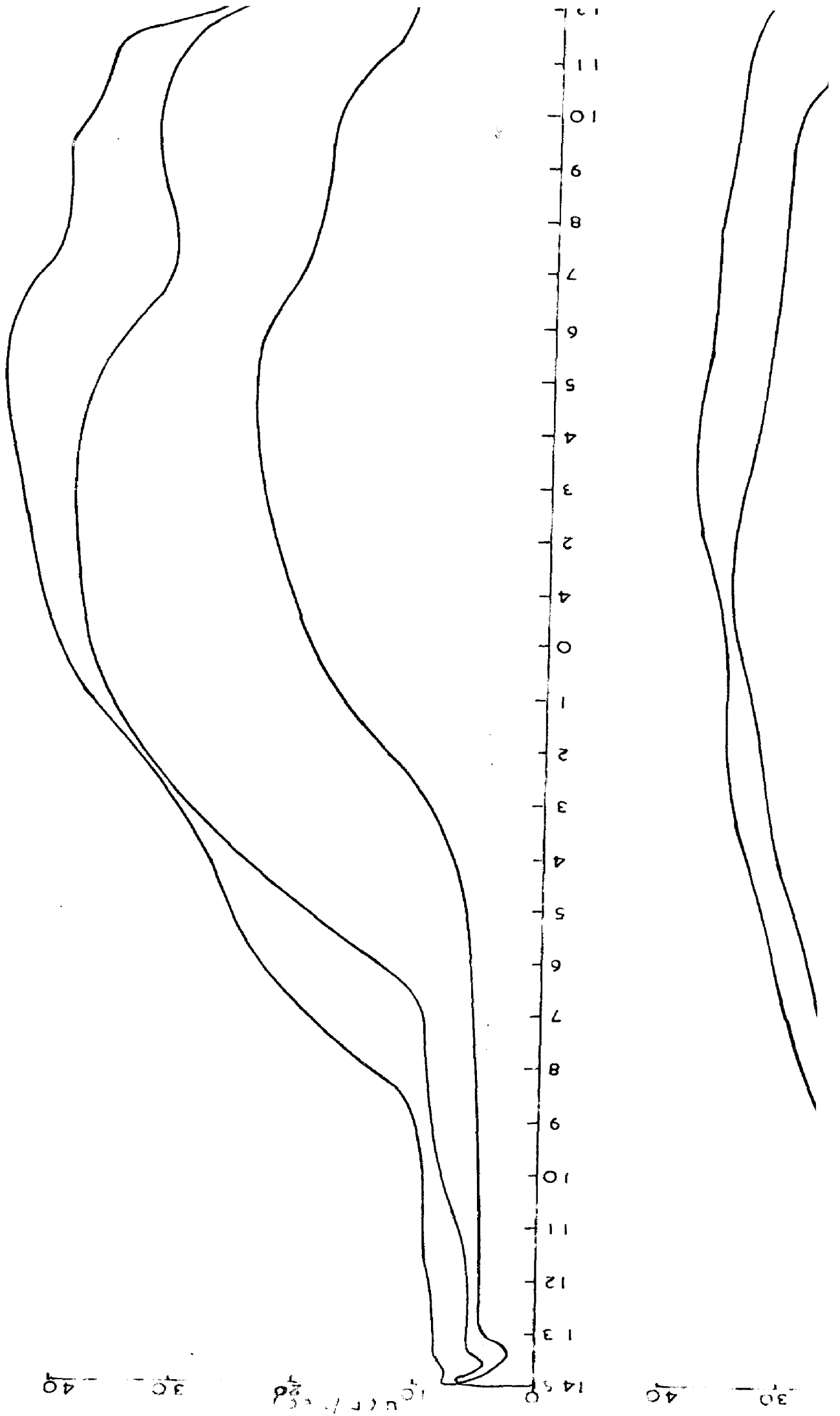


FIG.10- POTENTIAL FLOW GEOMETRY CONIC





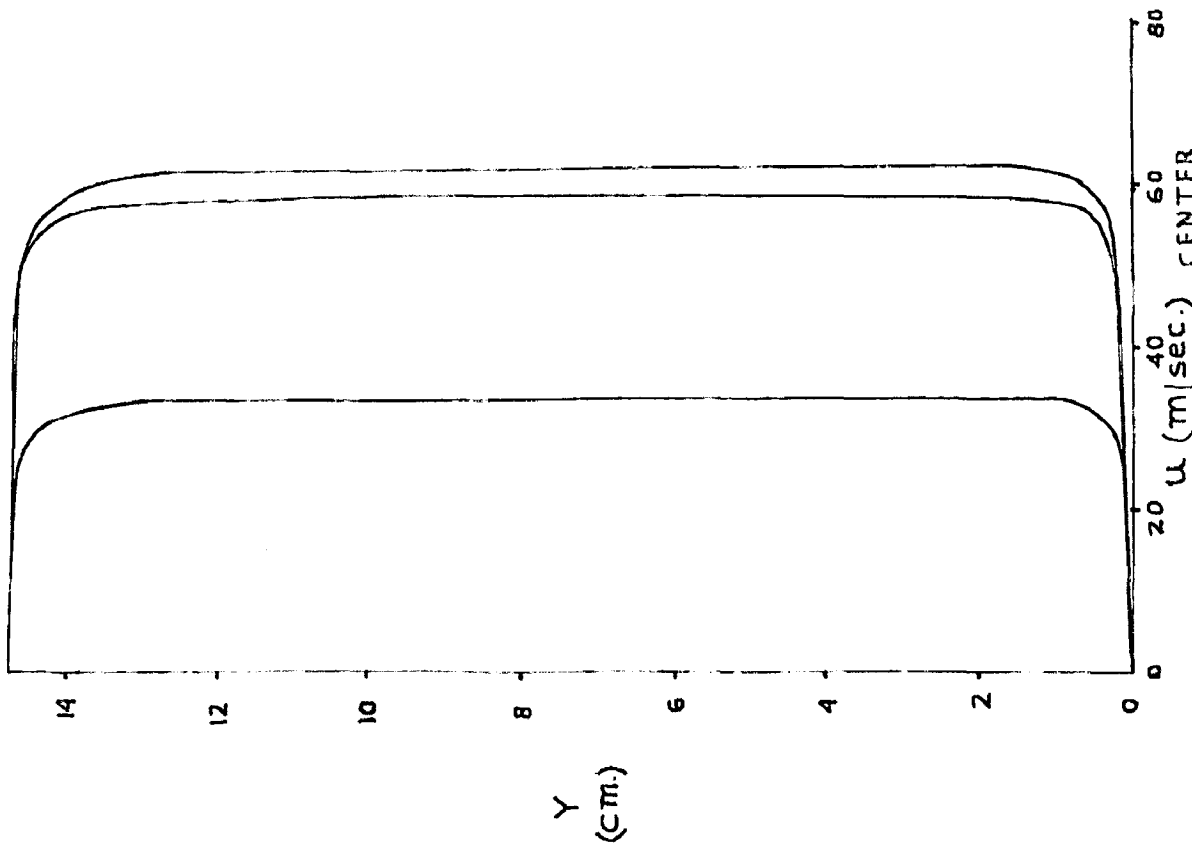
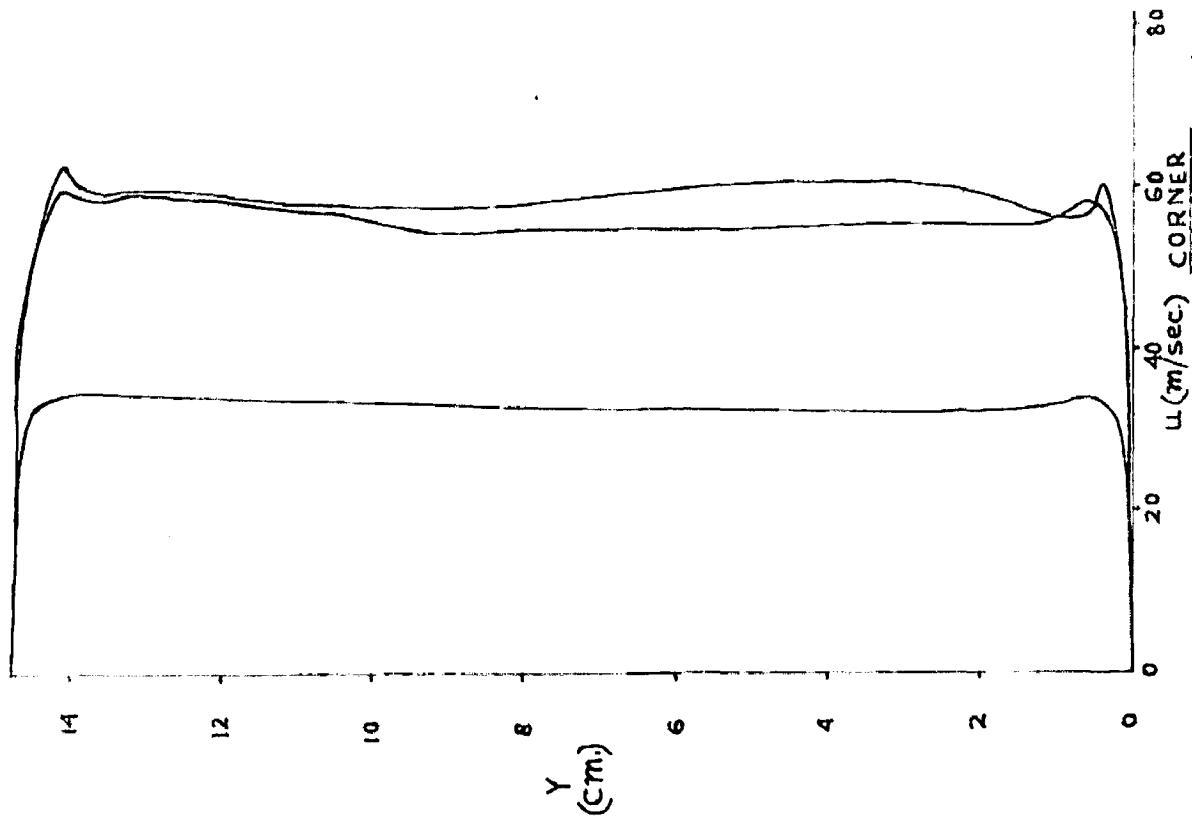


FIG.12- INLET VELOCITY PROFILES (STRAIGHT GEOMETRY SQUARE)

FIG.12- INLET VELOCITY PROFILES (CORNER GEOMETRY SQUARE)

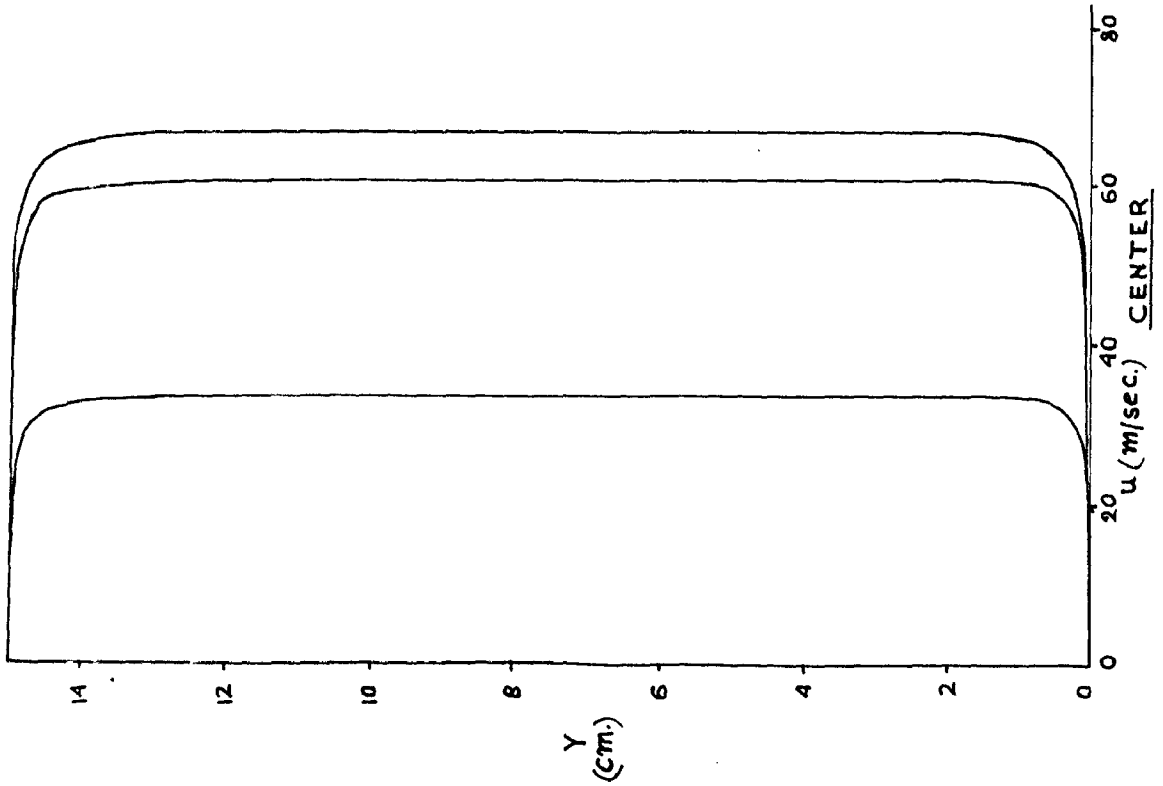
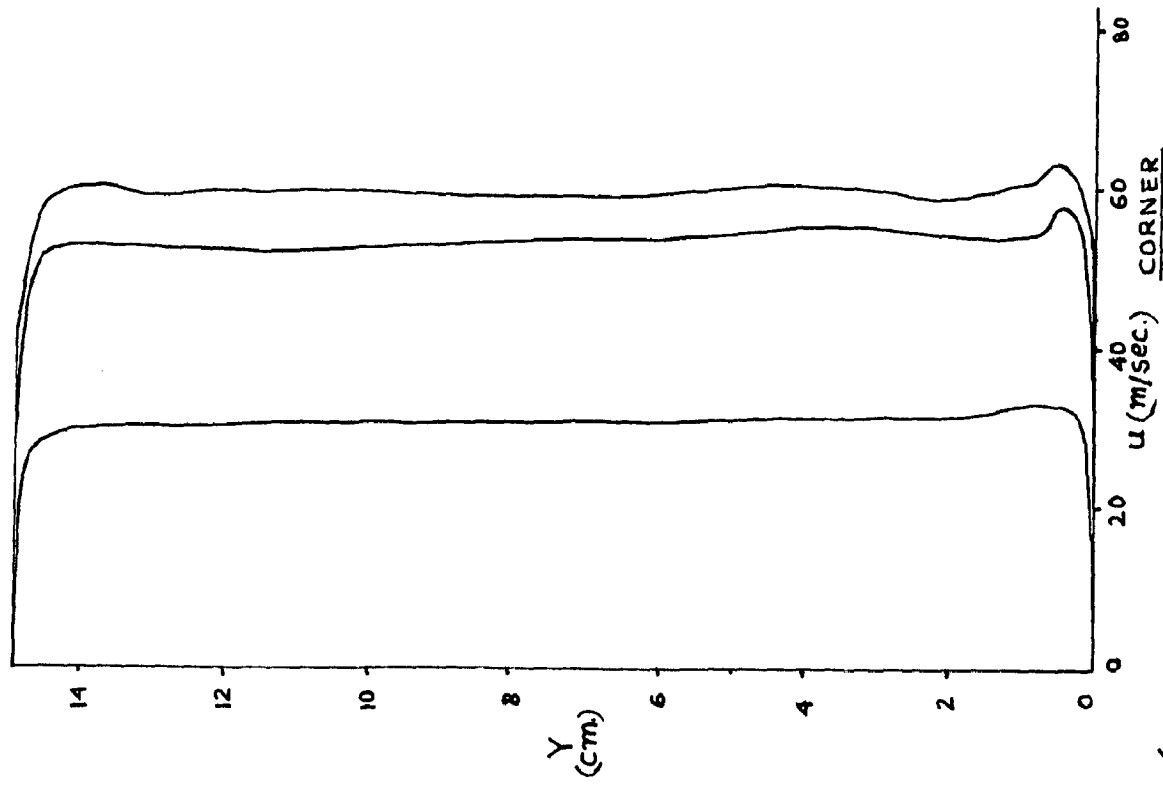


FIG. 13 - INLET VELOCITY PROFILES (GIBSON'S GEOMETRY SQUARE)

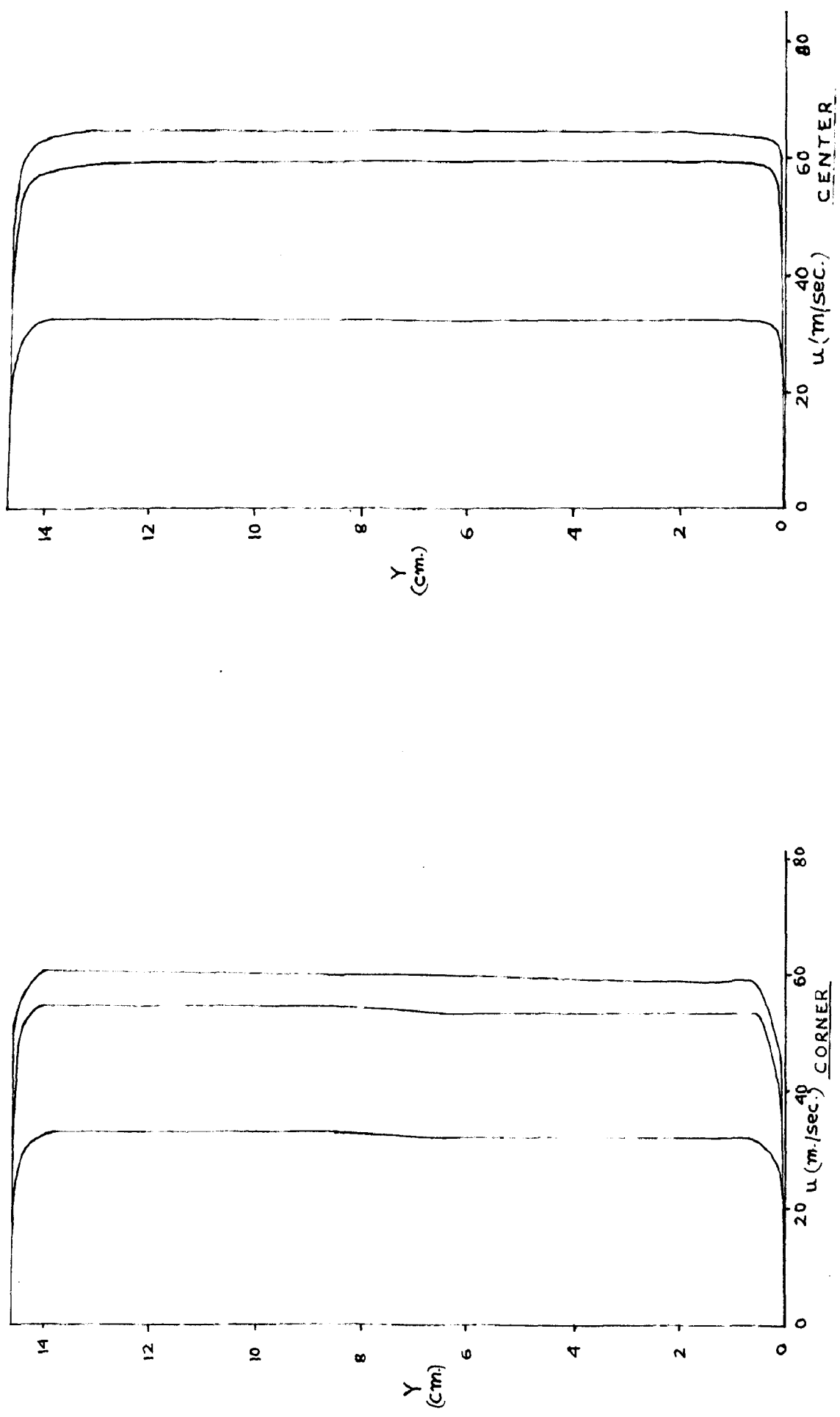
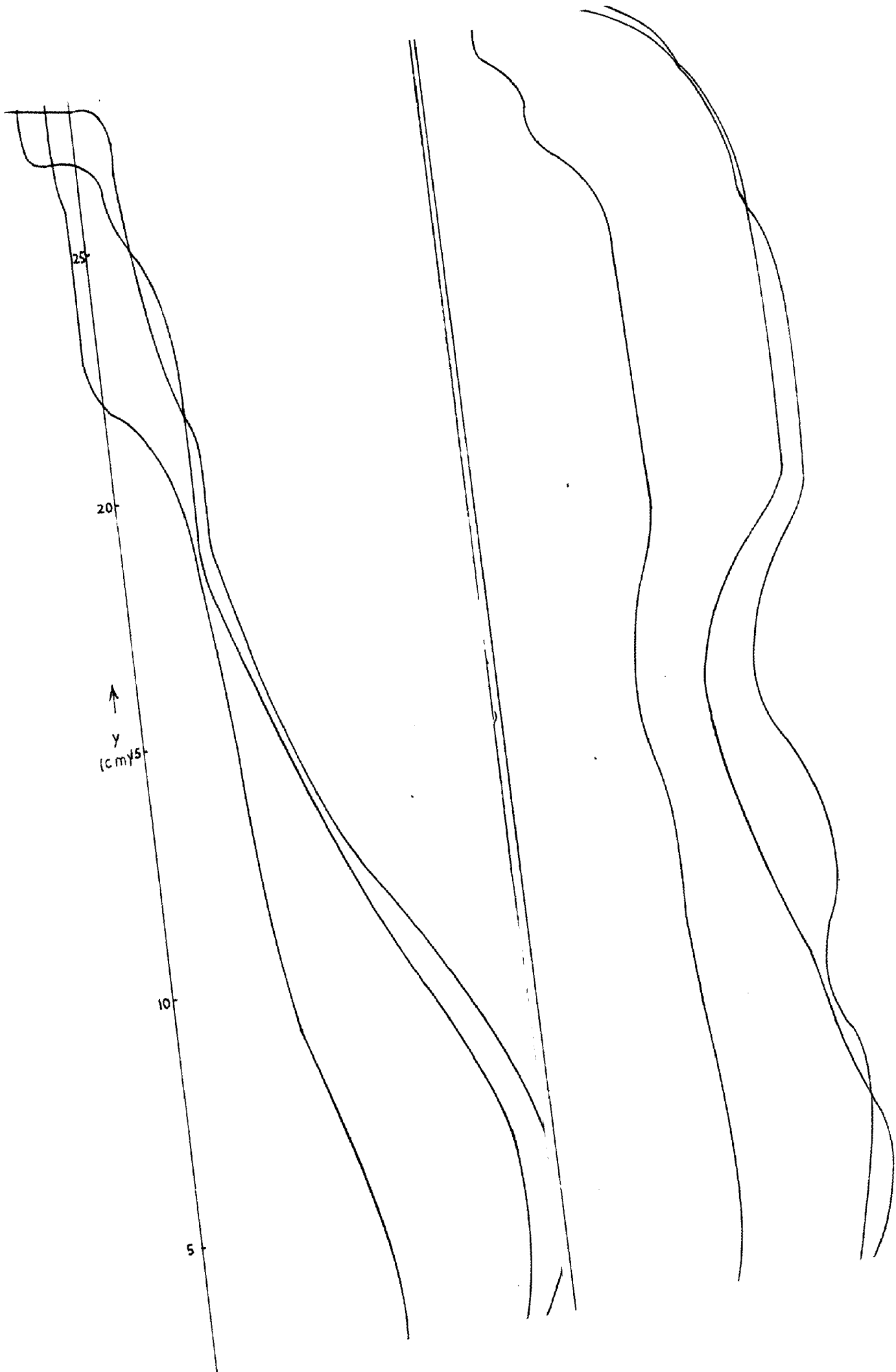


FIG.14 - INLET VELOCITY PROFILES (POTENTIAL FLOW GEOMETRY SQUARE



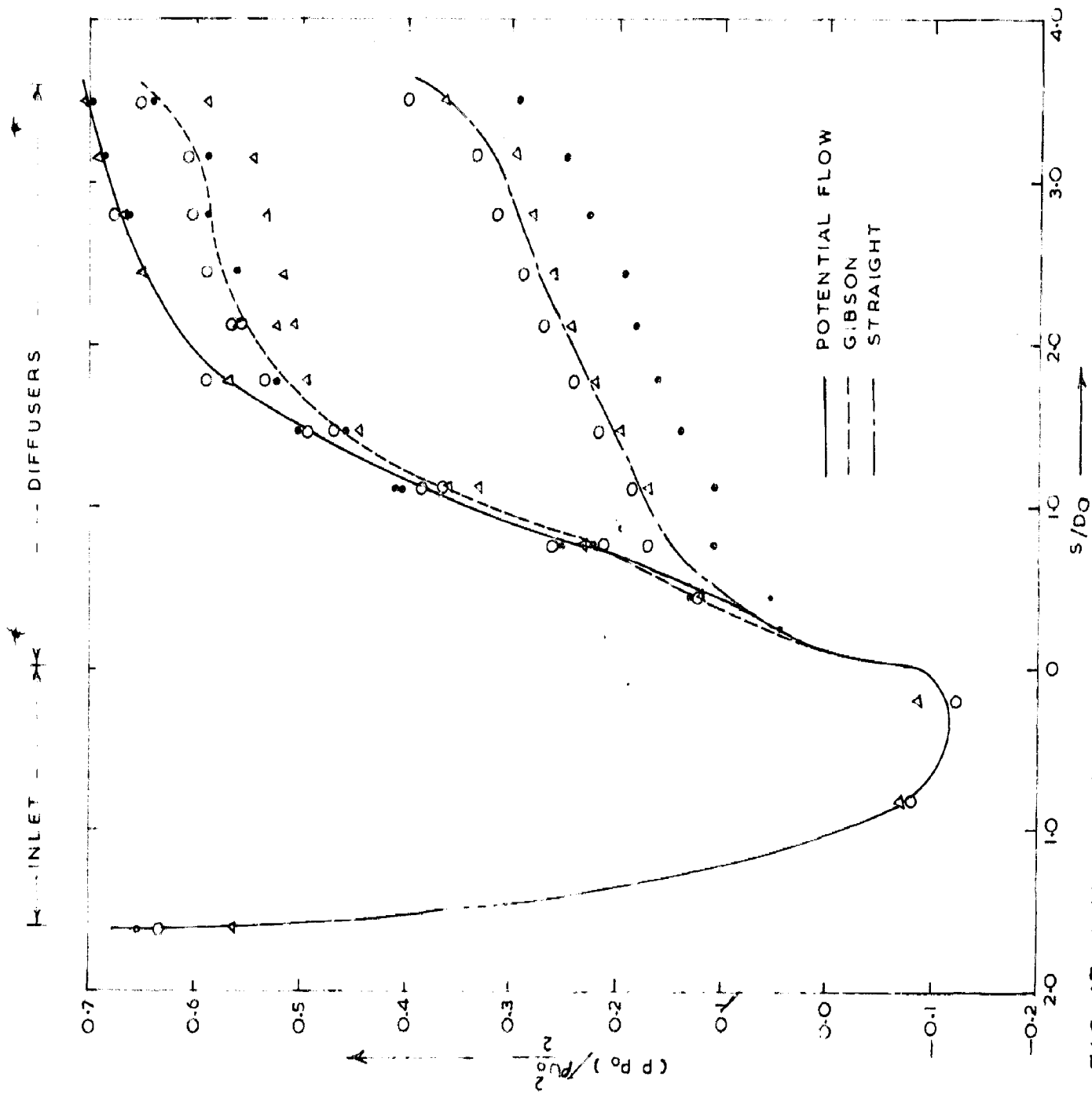


FIG. 17 WALL PRESSURES WITHIN CONICAL DIFFUSERS (TOP CENTER LINE)

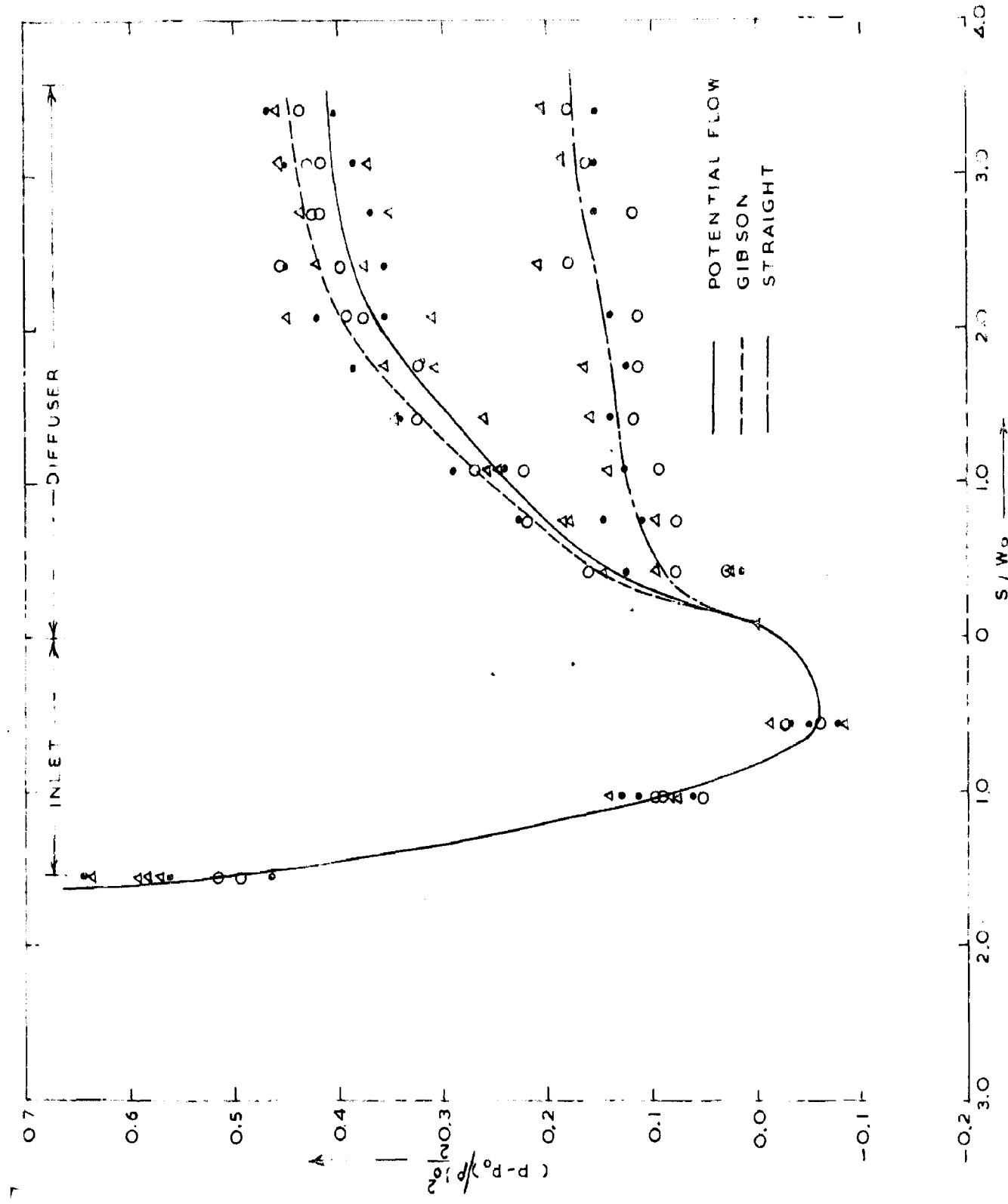


FIG 18 WALL PRESSURES WITHIN SQUARE DIFFUSERS (TOP CENTER)

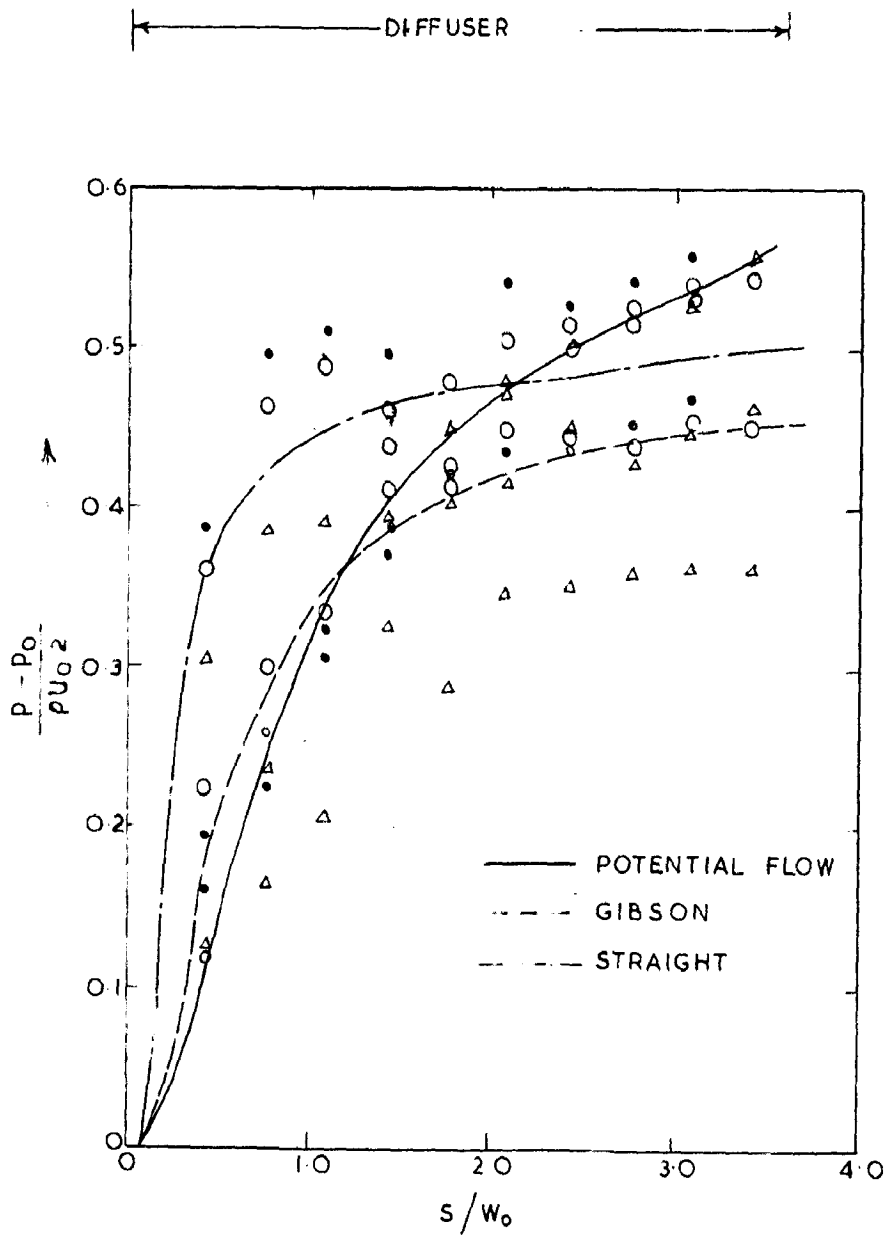
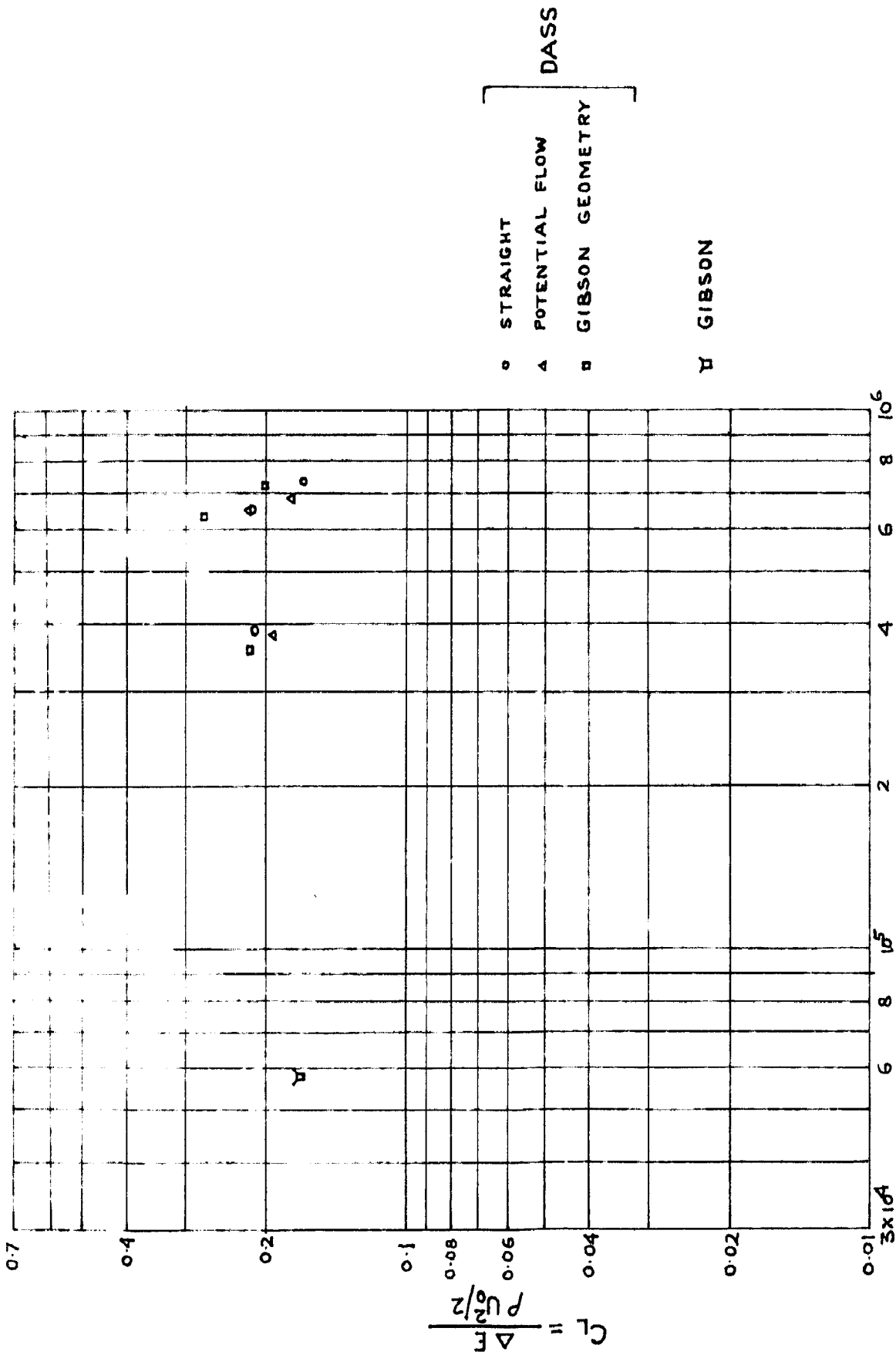
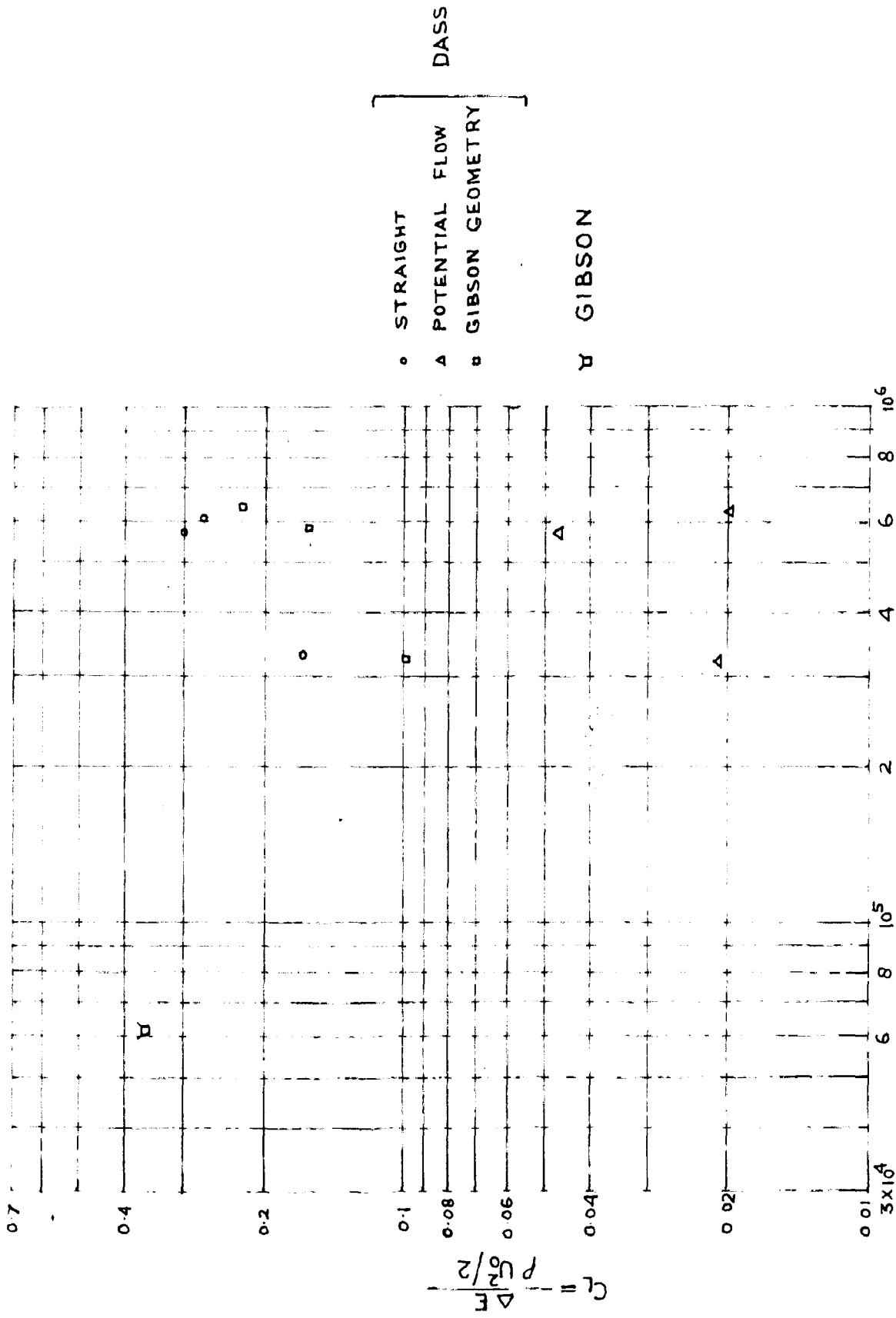


FIG 19 WALL PRESSURES WITHIN SQUARE DIFFUSERS
(TOP RIGHT CORNER)



REYNOLDS NO. $R_0 = \frac{U_0 D_0}{\nu}$
 FIG. 20 - VARIATION OF C_L WITH R_0 (CONICAL DIFFUSERS)



REYNOLDS NO. $R_0 = \frac{U_0 W_0}{2\nu}$

FIG.21 - VARIATION OF C_L WITH R_0 (SQUARE DIFFUSERS)

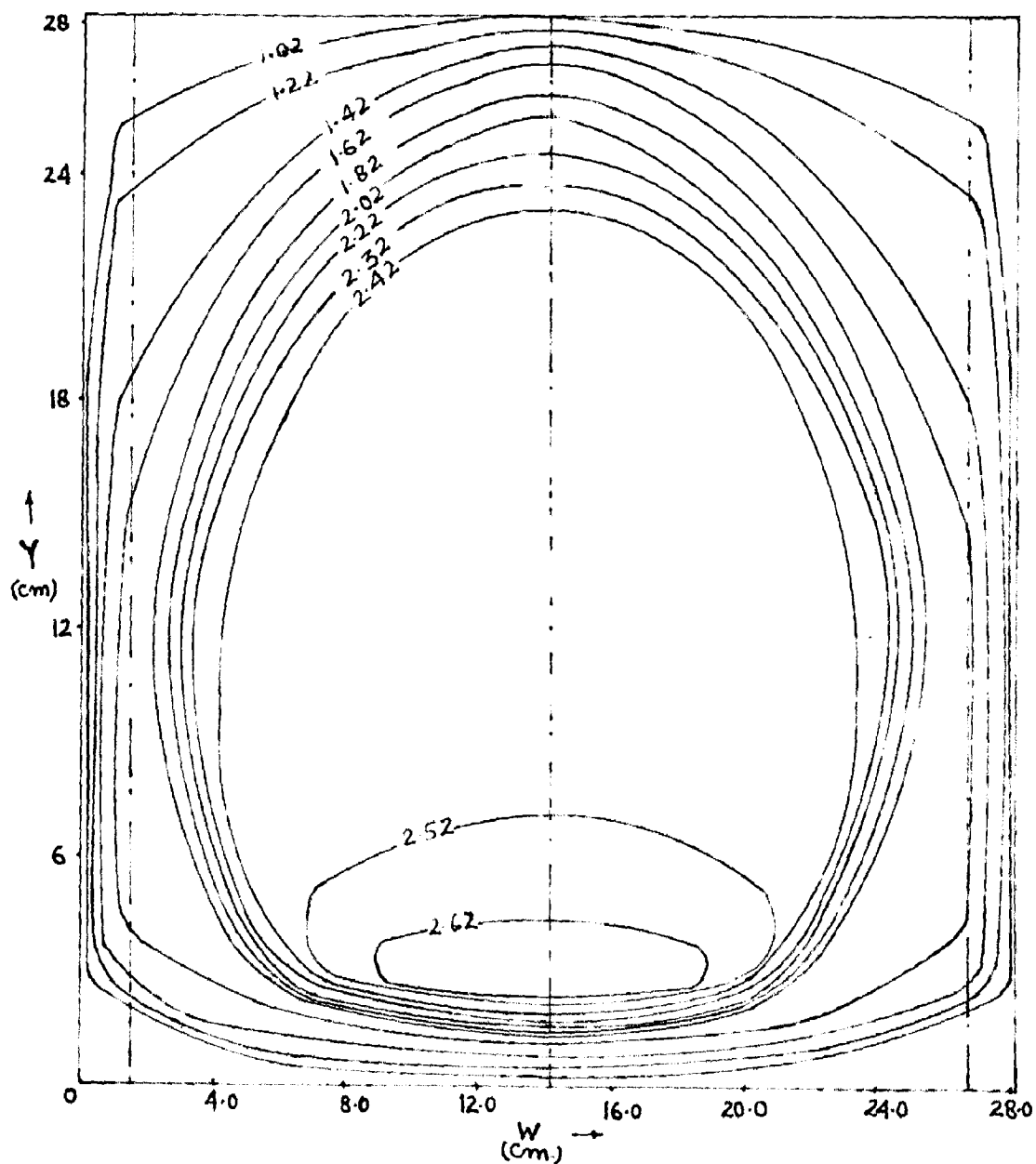


FIG.22- CONTOURS OF $\left(\frac{U}{U_e}\right)$ AT EXIT SECTION
FOR POTENTIAL FLOW GEOMETRY (SQUARE)

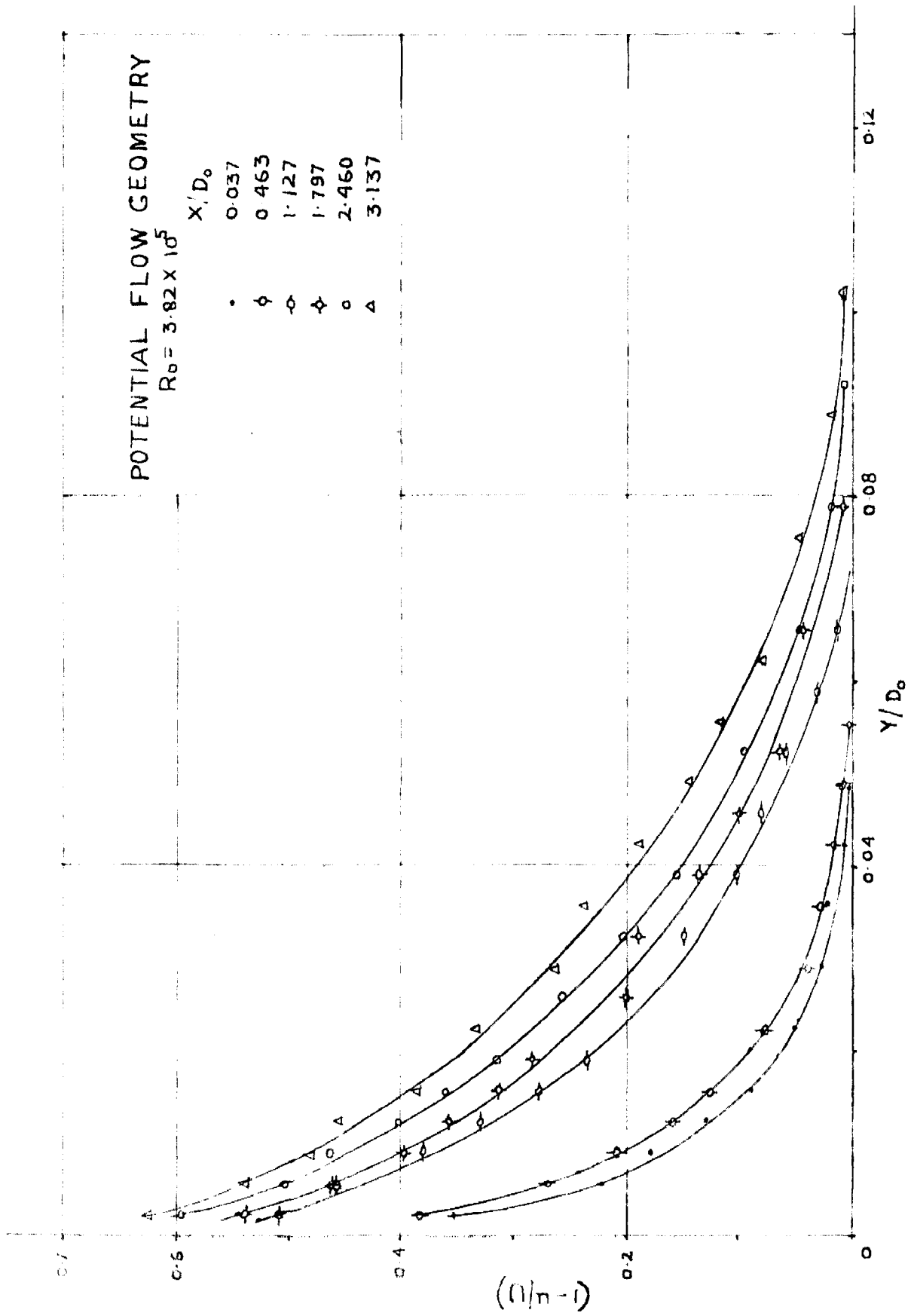


FIG. 23 - Boundary layer velocity profiles (Conical Diffusers)

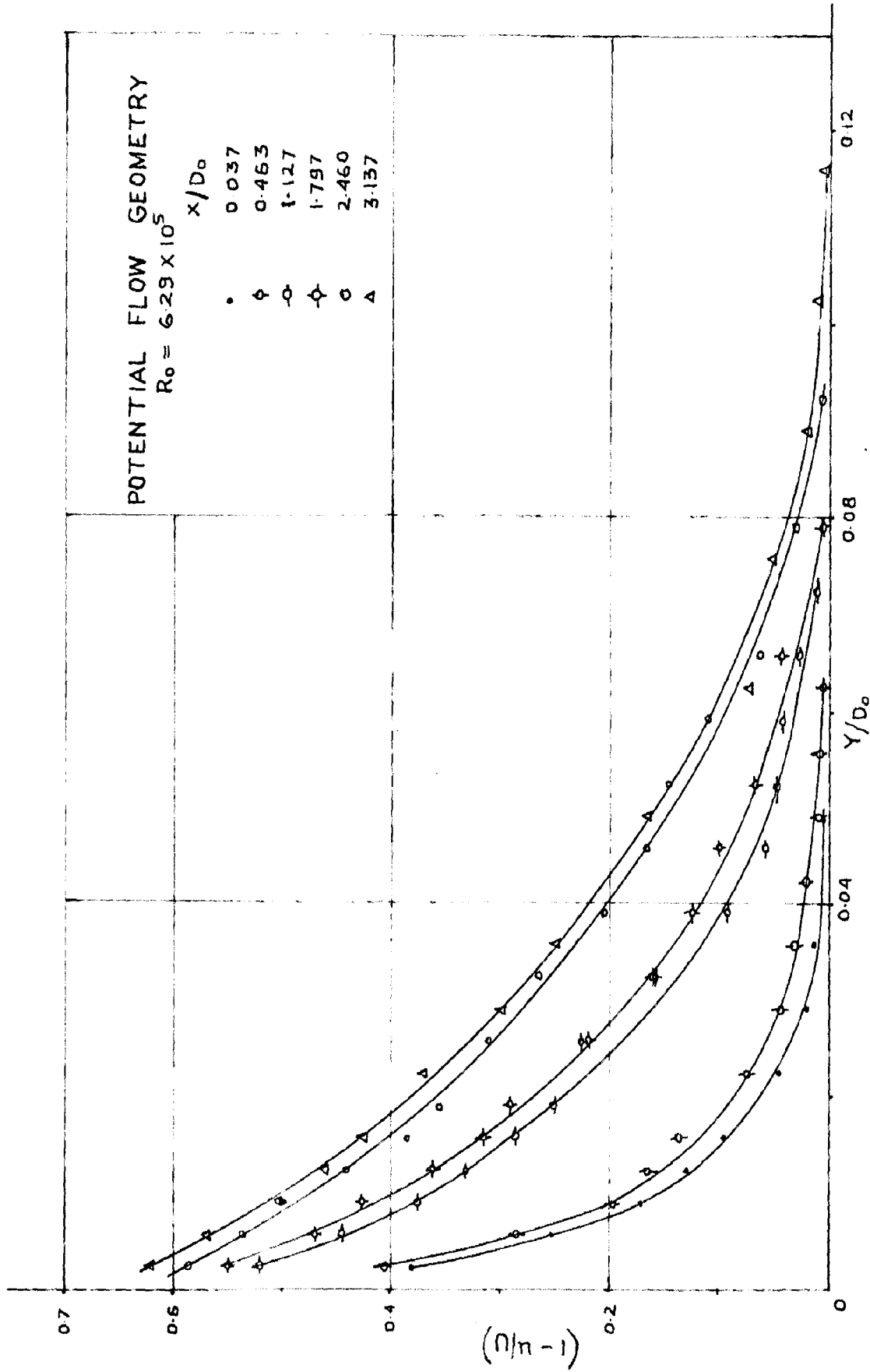


FIG.24 - Boundary Layer Velocity Profiles (Conical Diffusers)

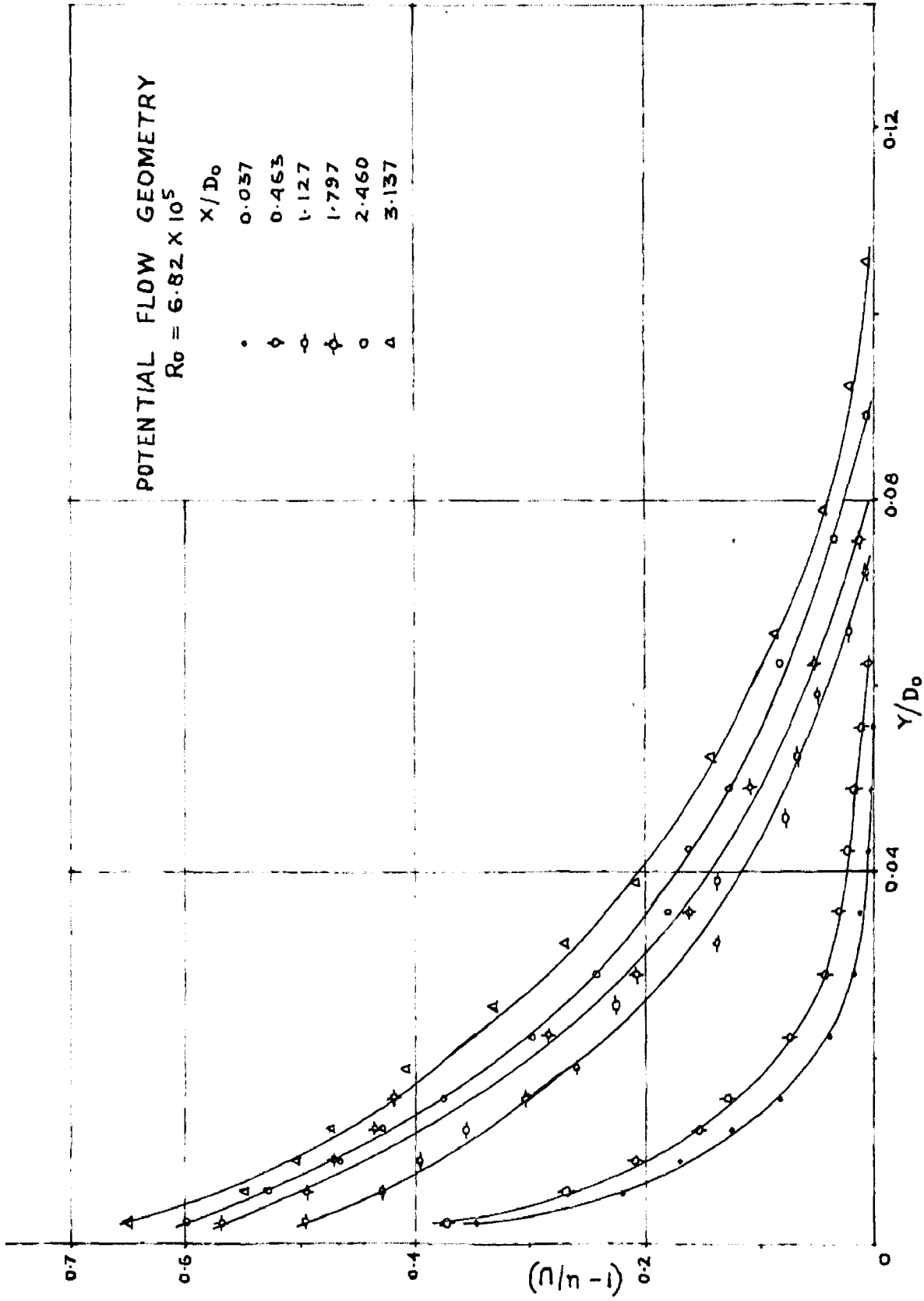


FIG.25- Boundary Layer Velocity profiles (Conical Diffusers)

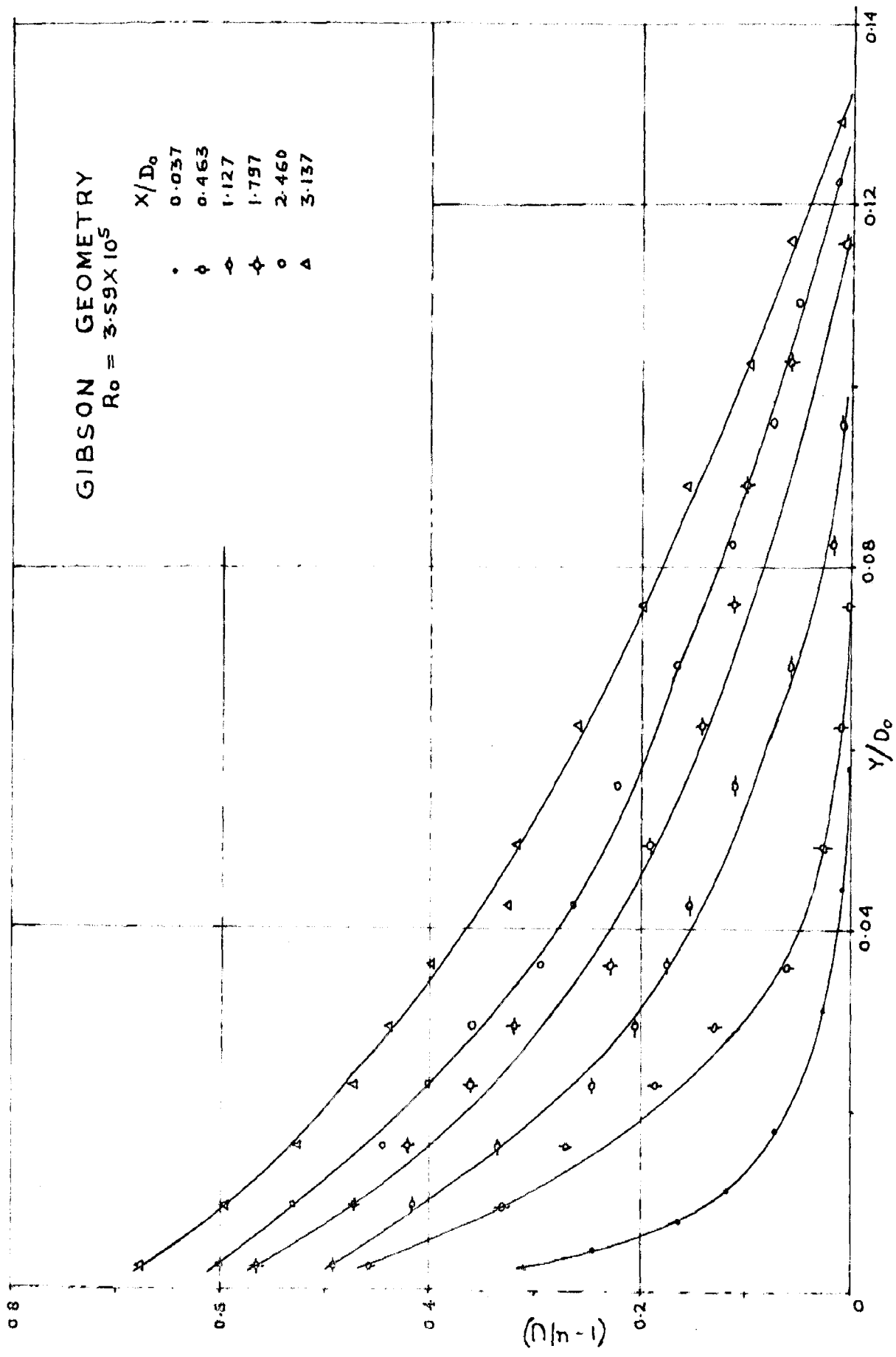


FIG. 2.6 - Boundary Layer Velocity Profiles (Conical Diffusers)

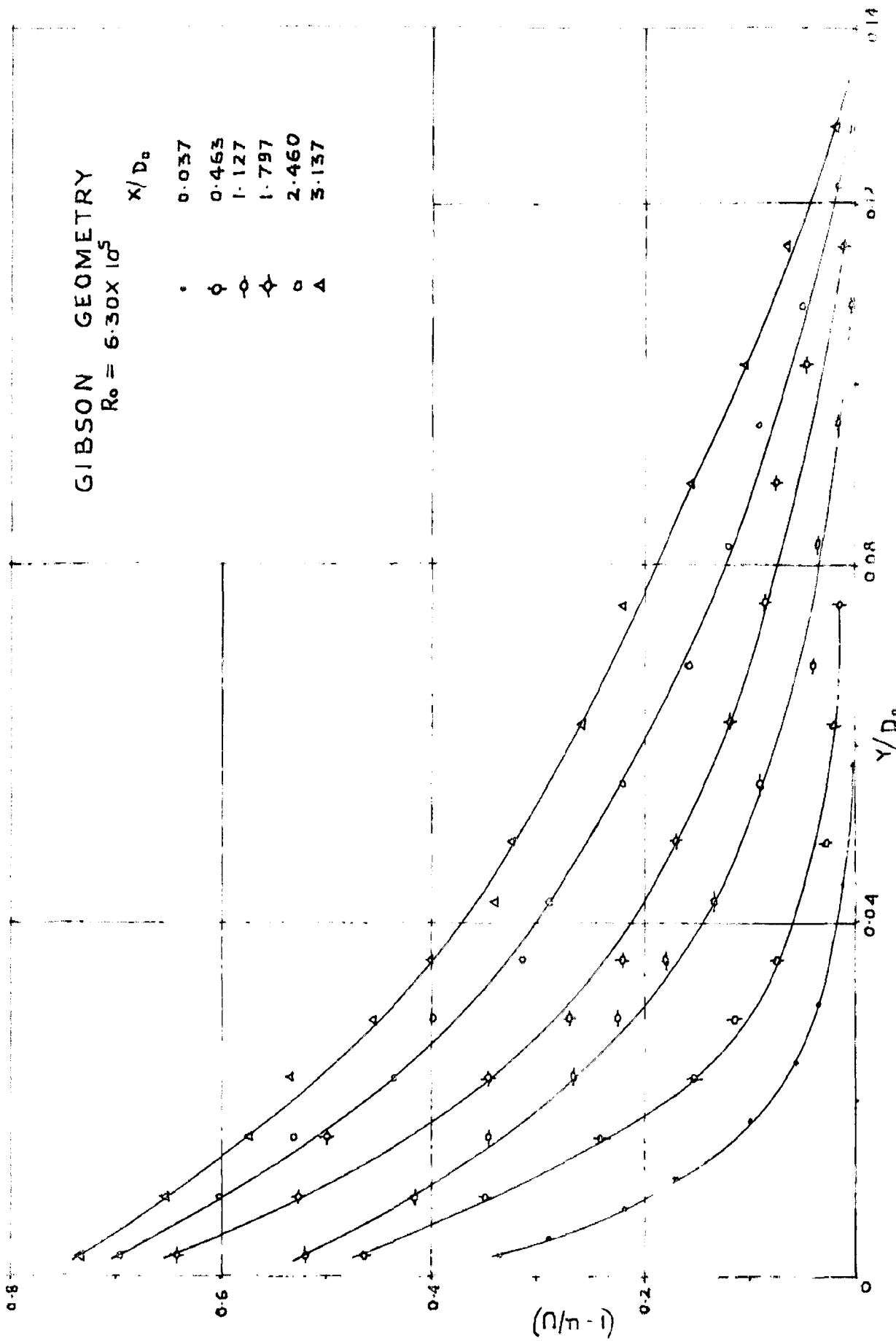


FIG. 27 - Boundary Layer Velocity Profiles (Conical Diffusers)

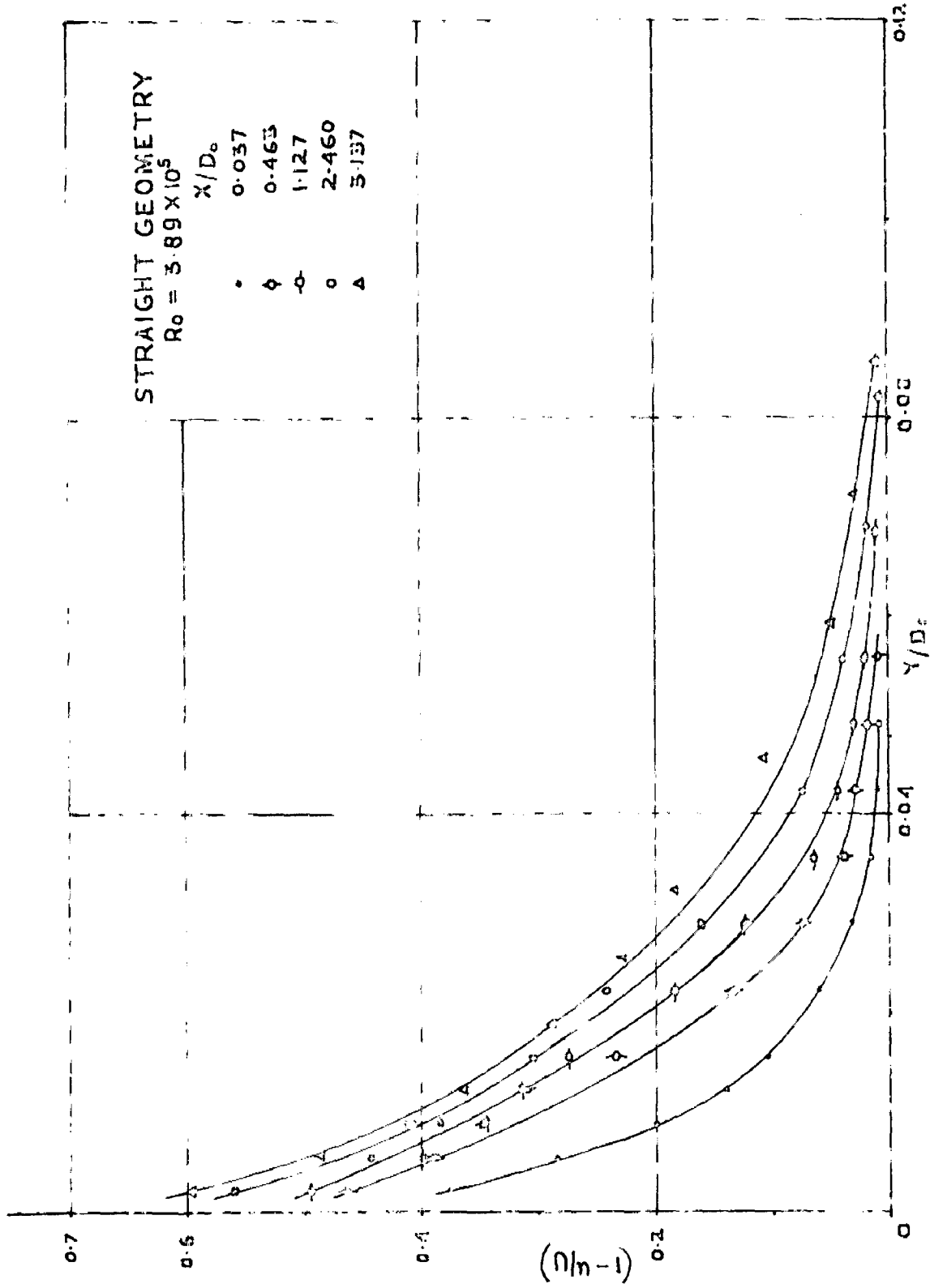


FIG. 29 - Boundary Layer Velocity Profiles (Conical Diffusers)

POTENTIAL FLOW
GEOMETRY
 $R_0 = 6.28 \times 10^5$
 X/W_0
• 0.00
◊ 0.83
◊ 1.50
✦ 2.17
◊ 2.83
△ 3.33

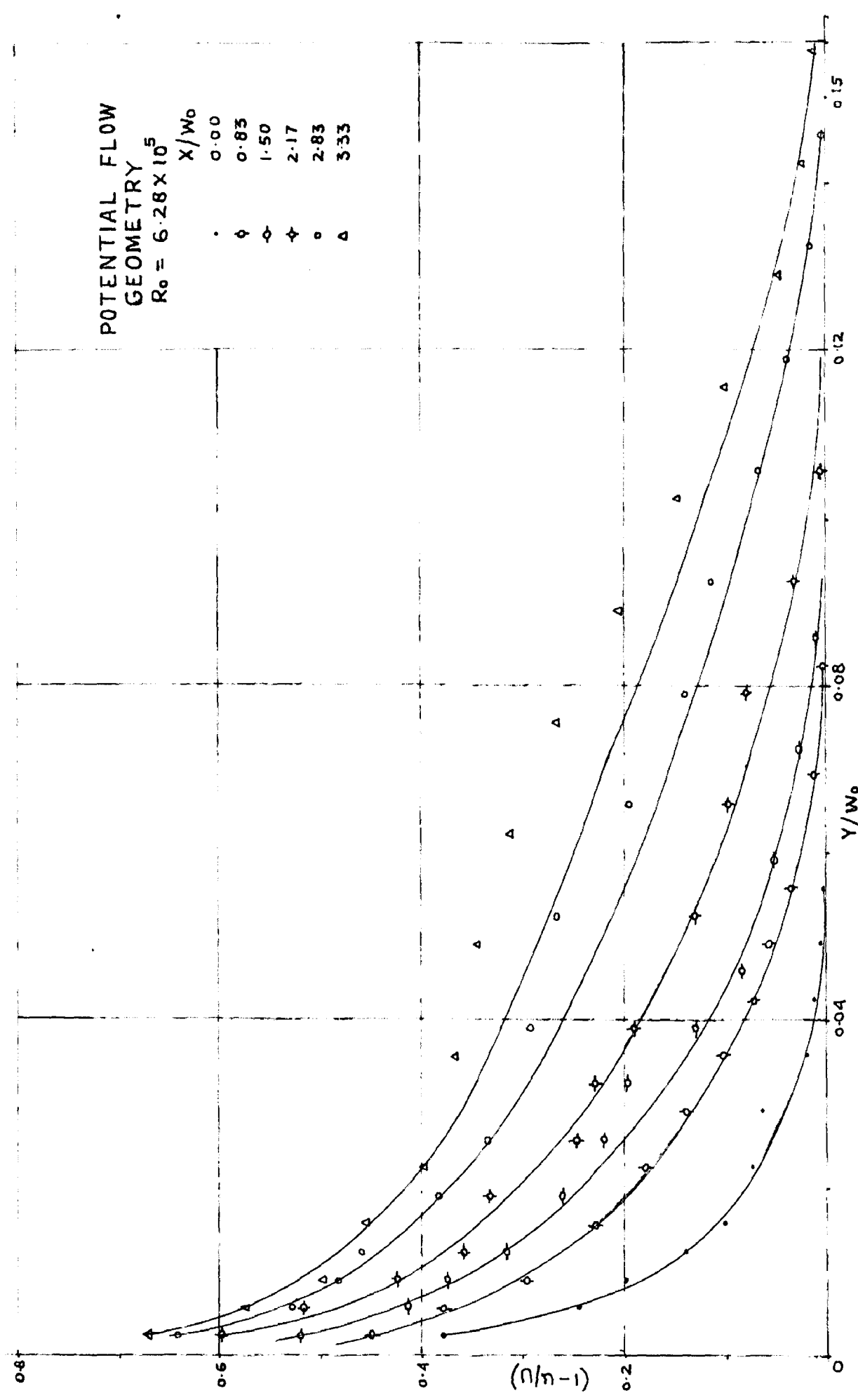


FIG.34 - Boundary layer velocity profiles (square diffusers)

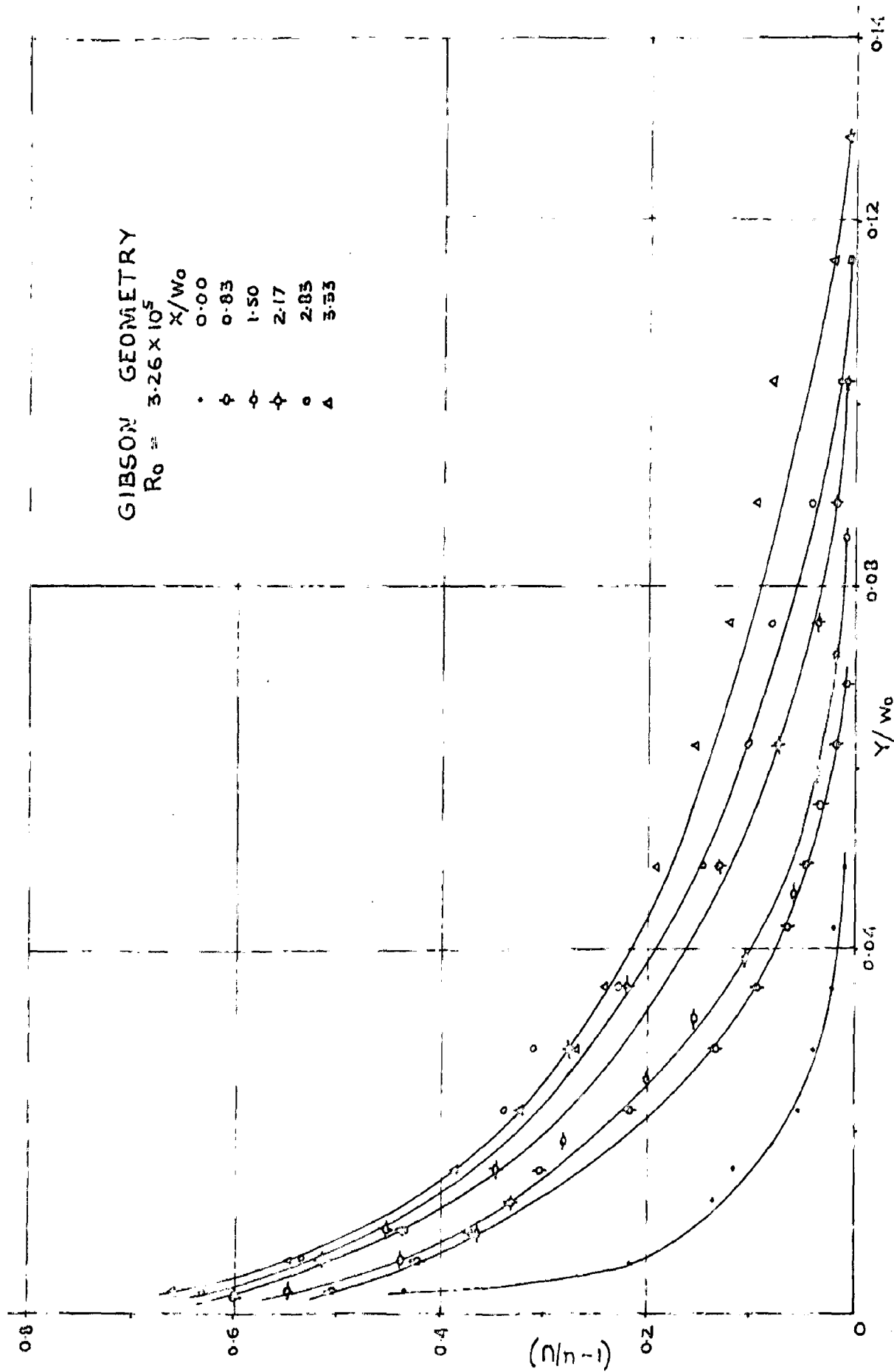


FIG. 35 - Boundary Layer Velocity Profiles (Square Diffusers)

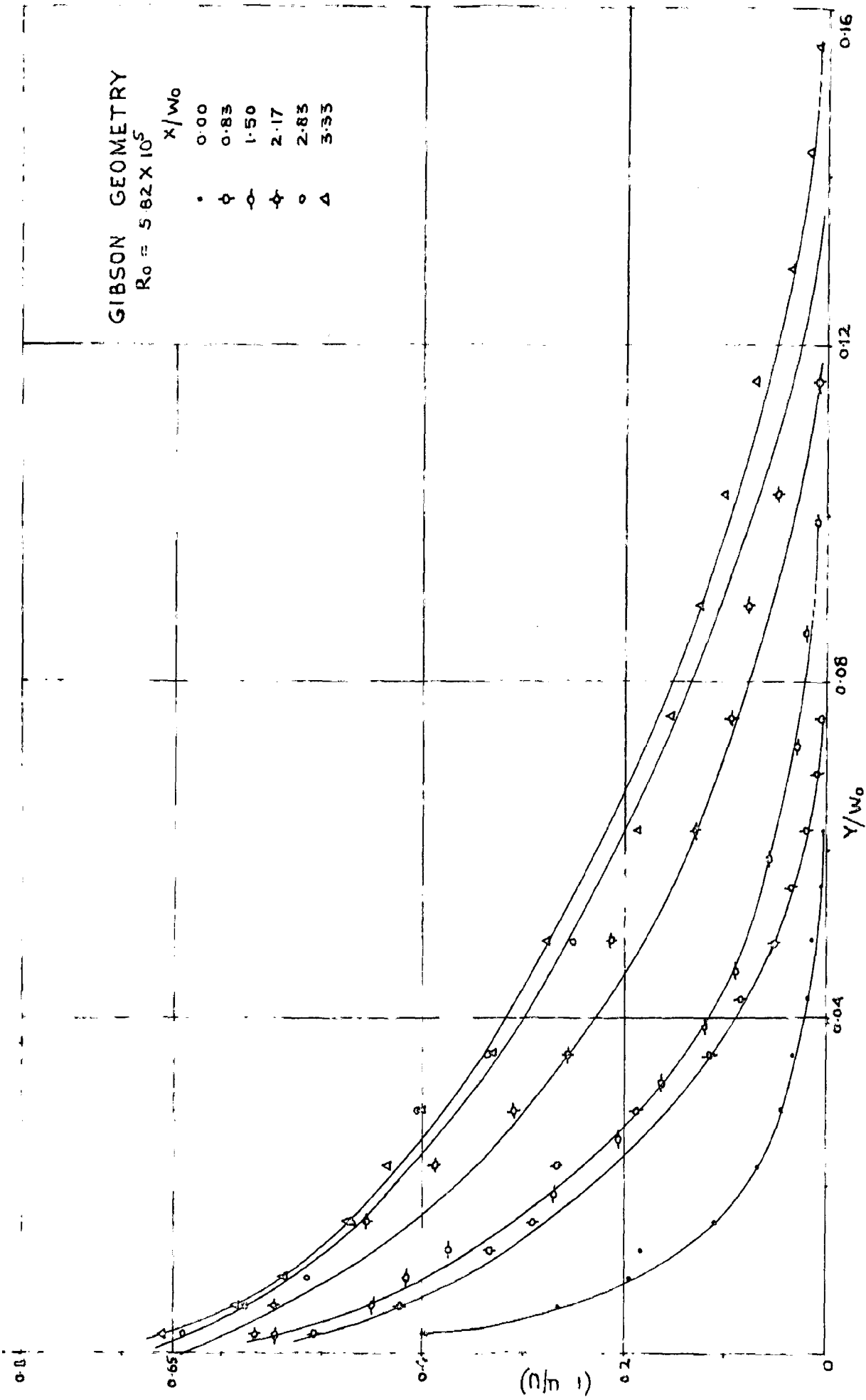


FIG 56 - Boundary layer velocity profiles (square diffusers)

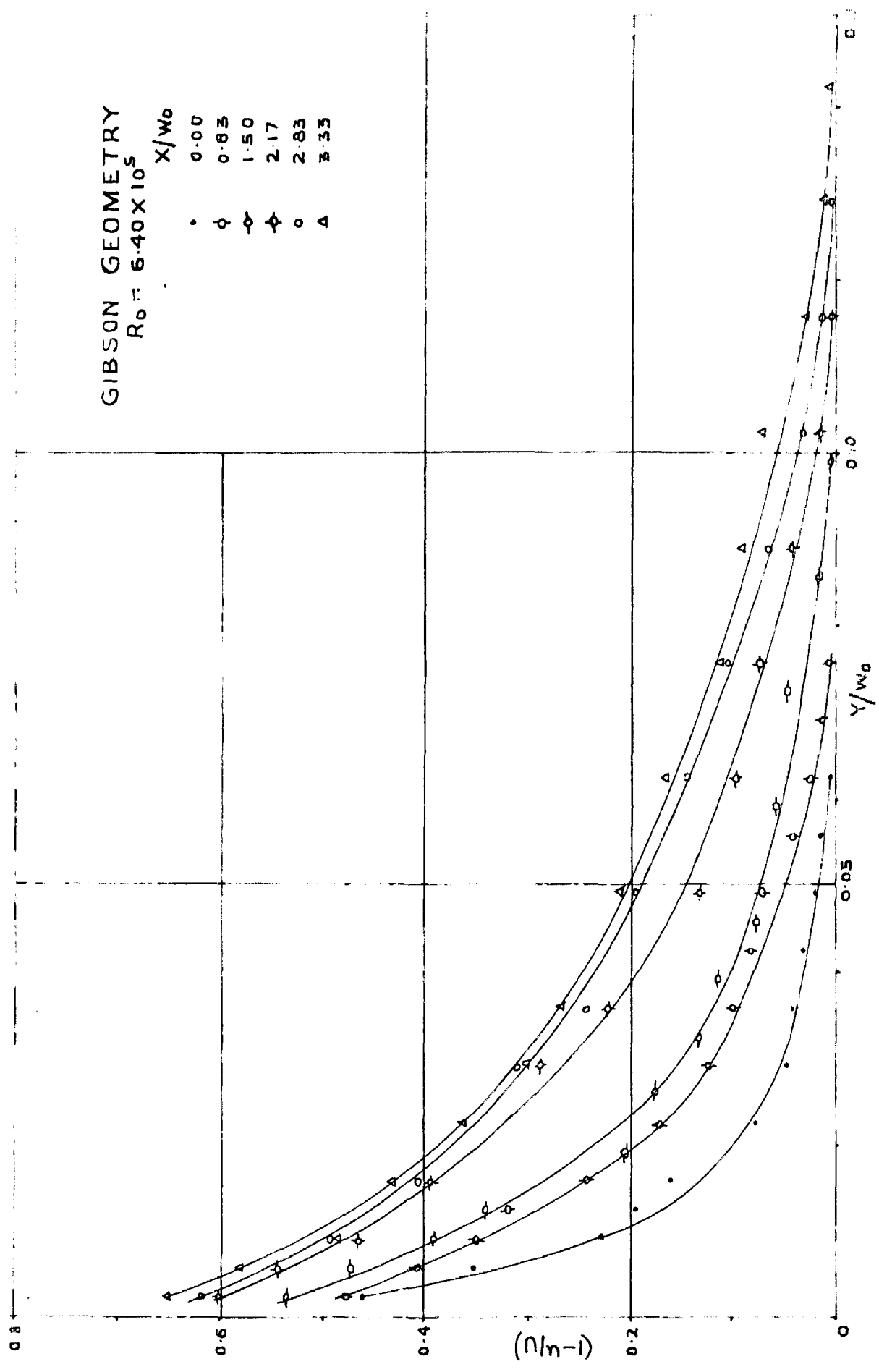


FIG.37- Boundary Layer velocity profiles (square diffusers)

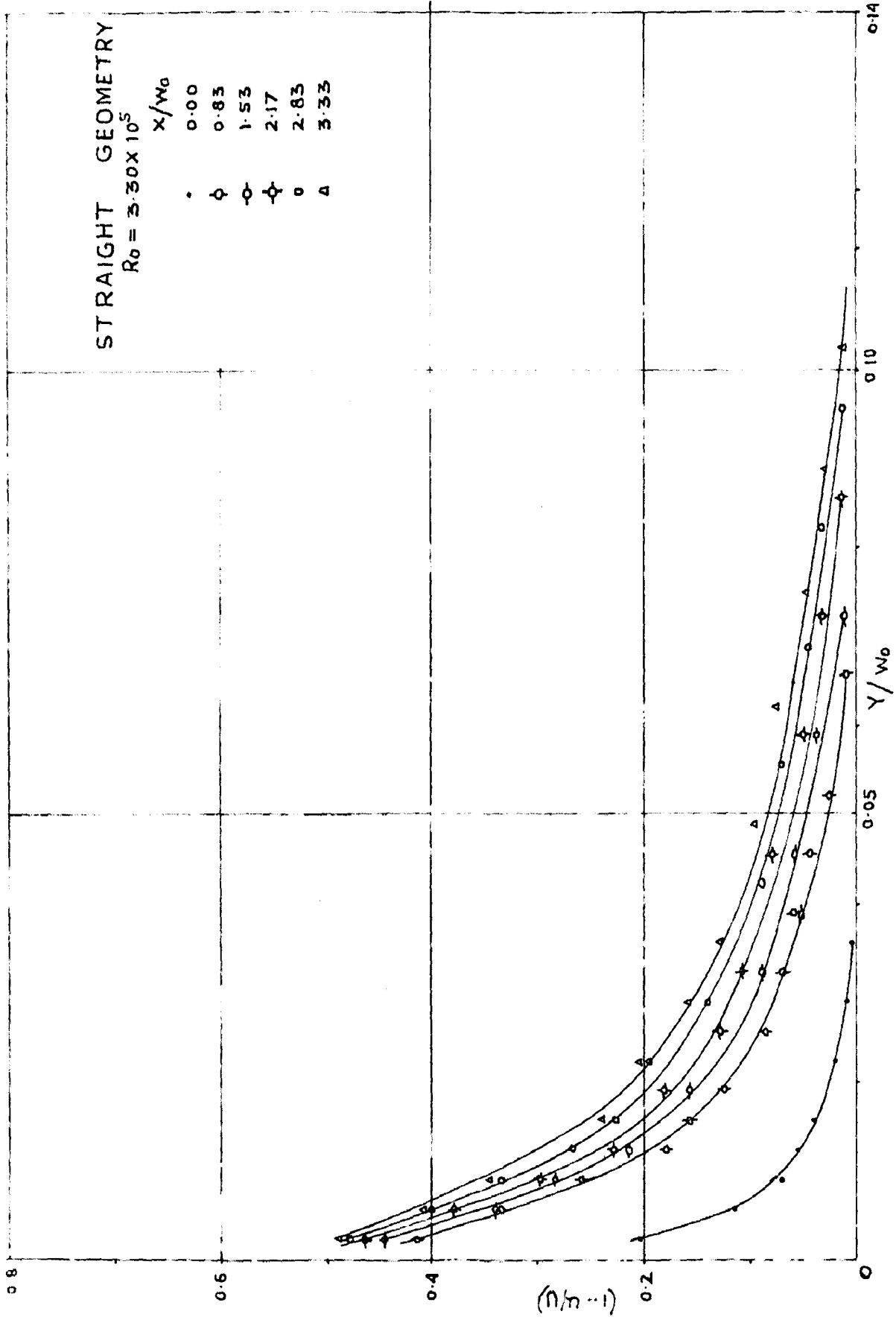


FIG.38 - Boundary Layer Velocity Profiles (square Diffusers)

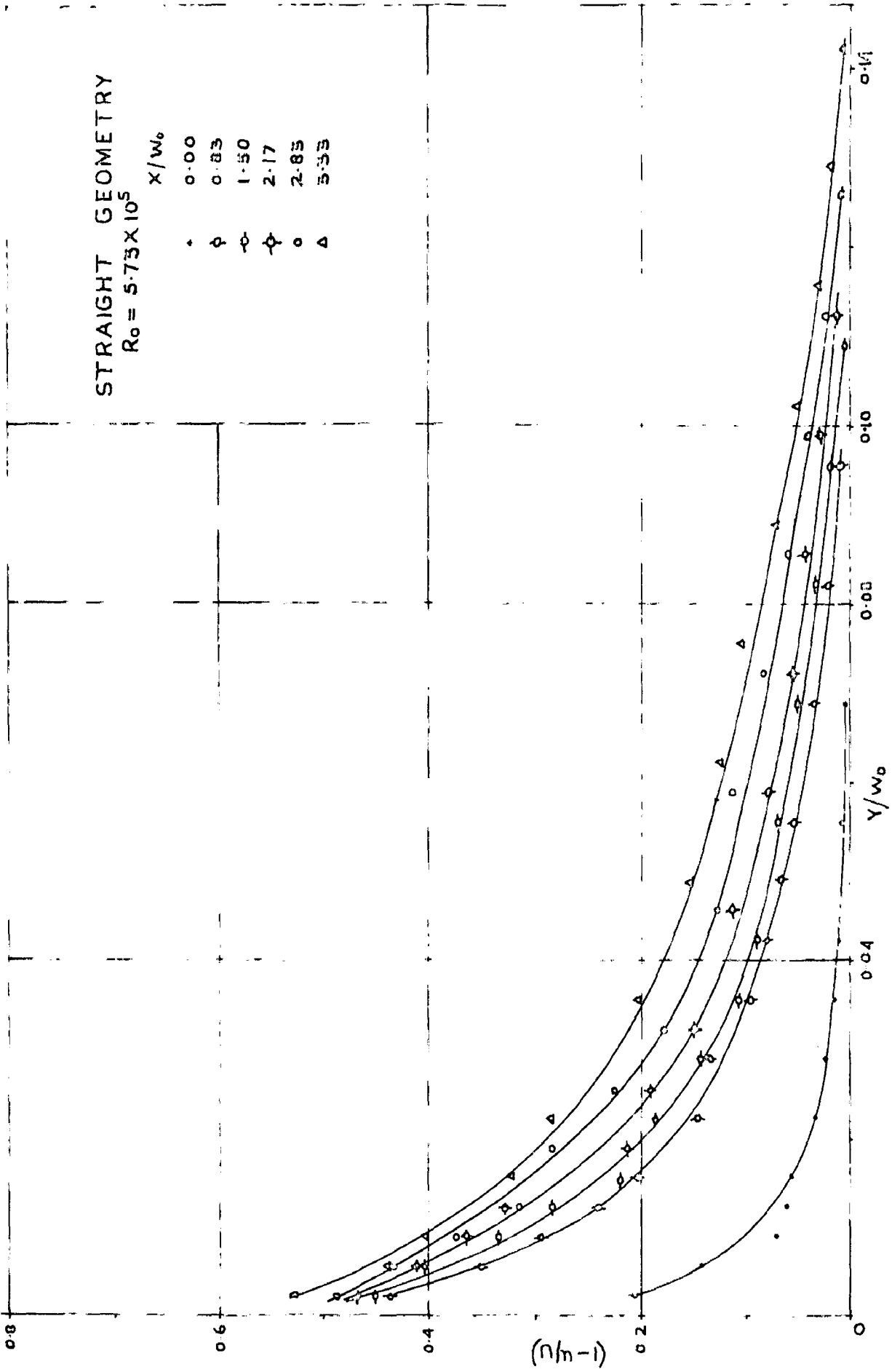


FIG.39 - Boundary Layer velocity Profiles (square Diffusers)

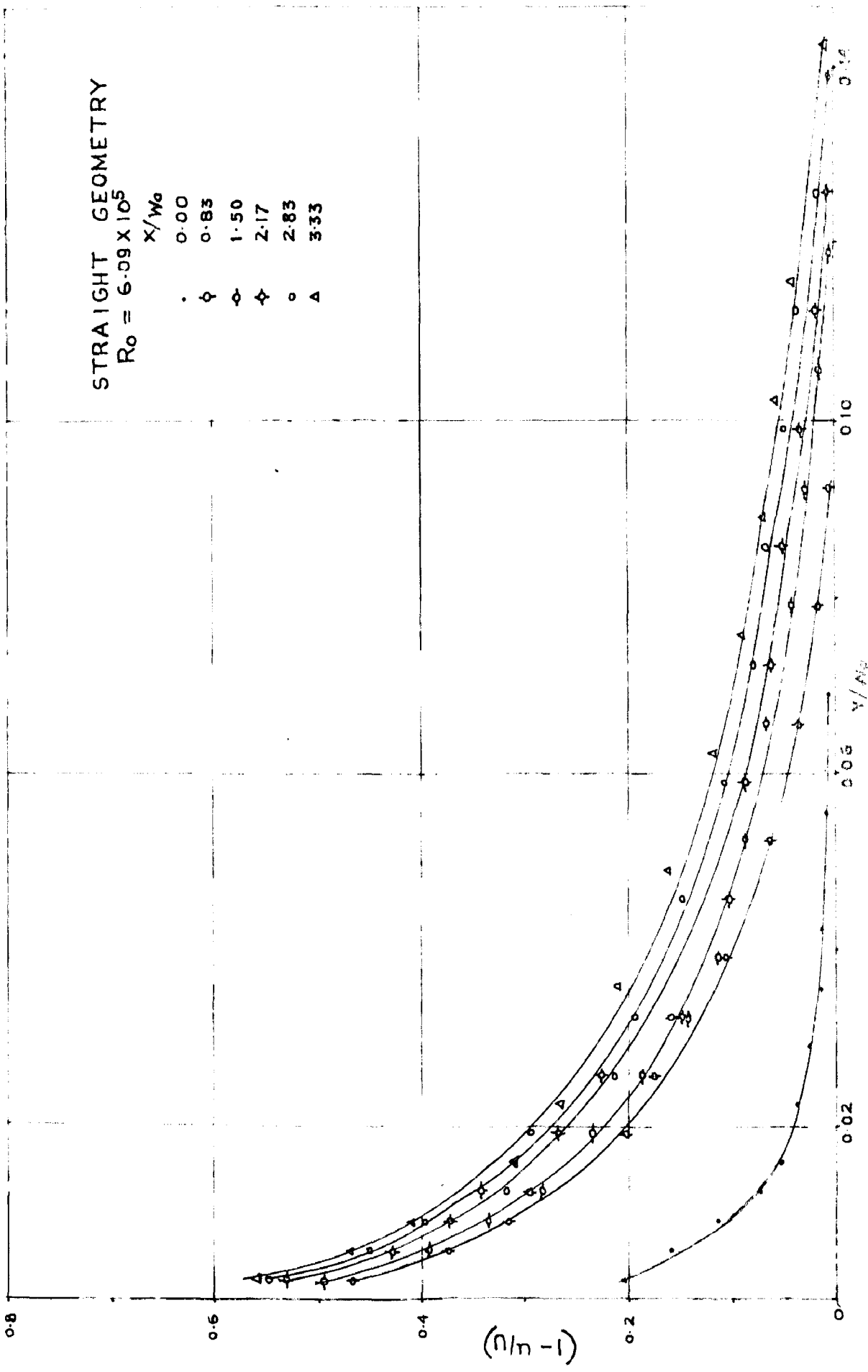


FIG 40 - Boundary layer velocity Profiles (Square Diffusers)